

TECHNISCHE UNIVERSITÄT MÜNCHEN
Physik Department

Max-Planck-Institut für Astrophysik

**Stationary, Axisymmetric
Neutron Stars
with Meridional Circulation
in General Relativity**

Reiner Birkel

Vollständiger Abdruck der von der Fakultät für Physik der Technischen Universität München zur Erlangung des akademischen Grades eines

Doktors der Naturwissenschaften (Dr. rer. nat.)

genehmigten Dissertation.

Vorsitzender: Univ.-Prof. Dr. L. Oberauer
Prüfer der Dissertation:

1. Priv.-Doz. Dr. E. Müller
2. Univ.-Prof. Dr. M. Ratz

Die Dissertation wurde am 01.12.2009 bei der Technischen Universität München eingereicht und durch die Fakultät für Physik am 12.01.2010 angenommen.

Contents

1. Introduction	7
1.1. The beginning	7
1.2. Neutron stars	7
1.3. Modelling	9
1.4. Current state	10
1.5. Investigation goals	11
1.6. Outline	11
2. Theory	13
2.1. Notations and conventions	13
2.2. Fields and equations	14
2.3. Symmetries	15
2.4. Foliations	15
2.4.1. 3+1-foliation of the whole spacetime	16
2.4.2. 2+1-foliation of the $t = \text{const}$ 3-surfaces	17
2.5. Basic Fields	18
2.5.1. Geometry	18
2.5.2. Matter	19
2.6. Projections	19
2.7. Ancillary fields	21
2.7.1. Geometry	21
2.7.1.1. Logarithm of 2-lapse	21
2.7.1.2. Christoffel symbols	21
2.7.1.3. Exterior curvature	22
2.7.1.4. Projections	22
2.7.1.5. Commutators	23
2.7.2. Matter	23
2.7.2.1. Velocity	23
2.7.2.2. Projections	23
2.8. Geometry equations	24
2.9. Matter equations	24
2.9.1. Energy equation as result of a parallel projection	25
2.9.1.1. Compact form	25
2.9.1.2. Expanded form	25
2.9.1.3. Analytic Solution	26
2.9.2. Relativistic Euler equation as result of an orthogonal projection	27
2.9.2.1. Compact form	27
2.9.2.2. Expanded form of temporal component	28
2.9.2.3. Azimuthal component	28
2.9.2.4. Meridional components	29

2.9.3.	Velocity v^a	34
2.9.4.	Equation of state	37
3.	Numerics	39
3.1.	Basic fields	39
3.2.	Poisson equations	39
3.2.1.	Poisson equation for ν	40
3.2.2.	Poisson equations for N^a	41
3.2.3.	Poisson equation for β	42
3.2.4.	Poisson equations for M^m	44
3.2.4.1.	Identification of potential and source	44
3.2.4.2.	Slicing condition	46
3.2.4.3.	Rotation axis	48
3.2.4.4.	Numerically optimally suited form of source terms	49
3.2.5.	Poisson equation for α	50
3.2.6.	Poisson equation for χ_0	51
3.3.	Numerical grid	52
3.4.	Boundary	53
3.4.1.	Ghost zone	53
3.4.2.	Boundary conditions	54
3.5.	Green functions	55
3.5.1.	2-scalar	55
3.5.1.1.	Analytic solution	55
3.5.1.2.	Numerical solution	55
3.5.1.3.	Von Neumann boundary condition	56
3.5.1.4.	Dirichlet boundary condition	56
3.5.2.	3-scalar	57
3.5.2.1.	Analytic solution	57
3.5.2.2.	Numerical solution	57
3.5.2.3.	Axisymmetry	58
3.5.2.4.	Azimuthal cosine	58
3.5.2.5.	Vanishing surface potential	60
3.5.3.	2-vector	61
3.5.3.1.	Analytic solution	61
3.5.3.2.	Numerical solution	61
3.5.4.	3-vector	62
3.5.4.1.	Analytic solution	62
3.5.4.2.	Numerical solution	62
3.6.	Slicing conditions	66
3.6.1.	Maximal time slicing	66
3.6.2.	Conformally minimal azimuthal slicing	67
3.7.	Final gauge	68
3.7.1.	Origin of the remaining gauge freedom	68
3.7.2.	Final gauge fixing of M^m	69
3.7.3.	Final gauge fixing of α	70
3.8.	Fixed point iteration	70
3.8.1.	Initial configuration	70
3.8.2.	Iteration	70
3.8.3.	Removal of lower modes	71

4. GRNS	73
4.1. Neutron star parameters	73
4.2. Start screen	74
4.3. Overview screen	75
4.4. Field screen	76
4.5. Additional features	76
5. Tests	79
5.1. Resolution	79
5.2. Polynomials	80
5.3. Centimeter	81
5.4. Grid radius	82
6. Results	83
6.1. Assumptions	83
6.2. Case $f(\psi) = \psi$	83
6.2.1. Fundamental mode	83
6.2.2. Higher modes	84
6.3. Case $f(\psi) = 1$	85
7. Conclusions	93
A. Christoffel symbols of the first kind	95
A.1. 2-surfaces $\Sigma_{t\phi}$	95
A.2. 3-surfaces Σ_t	96
B. Derivation of correct 3-lapse equation	99
C. Geometry equations	105
C.1. Equation for ν	105
C.2. Equations for N^a	105
C.3. Equation for β	108
C.4. Equations for M^m	109
C.5. Equation for α	109
D. Determinants	111
E. Polytropic equation of state	113
F. Sources of 3-shift Poisson equation	115
G. Associated Legendre polynomials	119
H. Slicing conditions in flat space	121
H.1. Maximal time slicing	121
H.2. Conformally minimal azimuthal slicing	122
I. Tolman-Oppenheimer-Volkoff solution	125
J. Outlook to electromagnetism	127

Contents

1. Introduction

1.1. The beginning

The goal of physics is to understand nature. This endeavor has developed gradually since man has begun to reason. However, with the discovery of the law of gravitation by Isaac Newton in 1666 a new era has begun in physics. Since then, nature has taught us that eventually all of its phenomena can be described by equations of various complexity. Knowing these equations is, in principle, sufficient to fully understand nature. Every single detail of our world can then be derived, even those aspects whose connection to the equations is rather hidden, like the physical properties of the medium this text is written on. For that purpose, the only requirement is a computer with infinite resources of memory and computing time. Unfortunately, such a machine is not available to us. Therefore, a much more practical approach is used, in which even the derivation of the manifold phenomena from already known equations turns out to be a challenge. This has begun with mere analytic derivations, done by hand and limited to the simplest physical configurations. The advent of the computer age has allowed us to go beyond this scope and to investigate evermore complex scenarios numerically.

In 1915, Albert Einstein generalized Newton's theory of gravitation. The resulting equation is Einstein's field equation. The easiest solution to this equation is an empty universe, a flat spacetime without any matter. Everything beyond this trivial solution requires some additional process of understanding. Black holes are those solutions where gravitation is strongest. This leads to the presence of event horizons and singularities. They are not only of philosophical interest, but also an obstacle for a straightforward numerical implementation. However, it turns out that an extra amount of investigation is required even if only strong gravitation itself is present, without the exotic properties of black holes. This is the realm of neutron stars, the central topic of this work.

1.2. Neutron stars

The gravitational potential of a neutron star is about eight orders of magnitude stronger than the gravitational field of Earth. This tremendous difference is a consequence of the high density of $\approx 10^{15} \text{ g/cm}^3$ inside of a neutron star (see, e.g., [Michel 1991](#)). Such a density usually comes into being when a large fraction of about 1.4 – 3 solar masses of a massive star undergoes a gravitational collapse during a supernova (Fig. 1.1). The collapsing matter is then compressed to a spherical object of only $\approx 10 \text{ km}$ radius, the neutron star. White dwarfs are compact objects whose mass is lighter than the Chandrasekhar limit of ≈ 1.4 solar masses. Their gravitational potential is not as strong as that of neutron stars and therefore not of direct interest in this thesis. On the other hand, if the mass is above the Tolman-Oppenheimer-Volkoff limit of ≈ 3 solar masses, the compact objects are presumed to be exotic objects like quark stars ([Camenzind 2007](#)). For these stellar configurations, the Pauli exclusion principle still produces a pressure

1. Introduction

high enough to compensate gravitation. However, beyond ≈ 5 solar masses, the gravitation pressure becomes so strong that compact objects at the boundary of the validity of general relativity are generated, which are usually believed to be black holes.

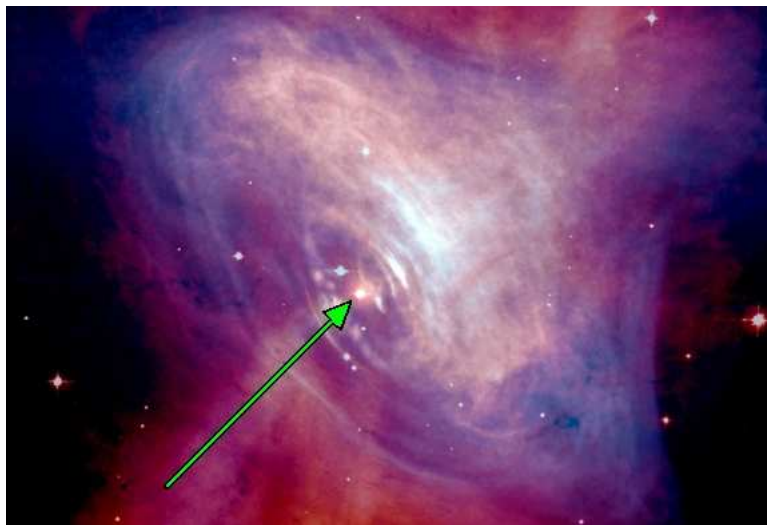


Figure 1.1.: **Crab Nebula with pulsar at its center.** The Crab Nebula in the constellation Taurus is the remnant of the famous supernova observed by Chinese astronomers in 1054. The center of this nebula contains a pulsar (marked by the green arrow), a rotating magnetized neutron star, which periodically emits pulses of radiation. *HubbleSite*.

During the creation of a neutron star, its strong gravitational field compresses protons and electrons of the collapsing stellar matter to neutrons. That way, they become the main constituent and responsible for the naming ‘neutron star’. The compression is strongest in the center, where the gravitational pressure is highest. Realistic neutron star models consist of several concentric layers, the central region being one of them (Shapiro *et al.* 1983). The outermost layers are an atmosphere of a few centimeters thickness and an about one kilometer thick solid crust. The inner layers are not well understood and subdue to speculations about their actual composition. This is a consequence of the lack of direct observations.

The majority of the observed neutron stars are pulsars (Fig. 1.1). Pulsars are rotating neutrons stars, equipped with a strong magnetic field of up to $\approx 10^{14}$ G, whose symmetry axis is inclined towards the rotation axis. The magnetic field accelerates charged particles such that synchrotron radiation is emitted along the symmetry axis of the magnetic field (Kawaler *et al.* 1997). Whenever Earth lies within the conical radiation field, pulses of radiation are observed like from a lighthouse. That way, it is possible to detect neutron stars at galactic distances, which can be pretty old, as long as their magnetic field has not yet decayed too much.

Hot neutron stars in the vicinity of Earth can be observed also directly via their thermal radiation. However, these neutron stars have to be young, because the temperature drops quickly. This is due to the lack of a heat source, like the nuclear burning in the progenitor star. At its creation, the central temperature of a neutron star is $\approx 10^{11}$ K (Becker 2009). It cools down to $\approx 10^9$ K – 10^{10} K during the first day, and after several hundred years the temperature is $\approx 10^6$ K. For the first $\approx 10^5$ years, the energy loss is mostly due to neutrinos, and afterwards photon emission dominates.

The temperature distribution inside the neutron star is not uniform: it drops from the center to the surface. There are also unstable gradients in the temperature and composition distribution, which are strongest for young neutron stars. These gradients lead to convection, i.e. an internal motion of the neutron star fluid. Unstable gradients are only one source for such a fluid motion. The other two possibilities are the influence of the magnetic field via magnetohydrodynamic effects and, most importantly, the conservation of angular momentum during the collapse phase. Like a spinning ice-skater pulling the arms to spin faster, in many cases the collapse leads to a rapid fluid motion around a certain axis. The observed rotation rates of pulsars range from 1.4ms to 8.5s (Becker 2009). In this thesis, we want to get a deeper insight into the fluid motion of neutron stars.

1.3. Modelling

There are three ways to augment the knowledge about the internal motion of neutron stars: the observational, the theoretical and the numerical approach. We do not follow the observational one, because of the already mentioned difficulties in a direct observation of the neutron star interior. From the theoretical viewpoint, we do not expect new knowledge at the current stage, because the required equations of physics are already known to a sufficiently accurate degree, namely Einstein's field equation. Therefore, this work is focused on the **numerical**¹ part by means of a simulation.

A common way to investigate a neutron star numerically is to simulate its evolution in a certain time interval. This is reasonable whenever the neutron star undergoes a significant change of its internal structure. Typically, this occurs after the creation of the neutron star or when it interacts with other stellar objects, like during the merging with a black hole. However, we assume that the neutron star behaves in a quasistationary manner, i.e. we approximately consider the neutron star to be **stationary**. In addition to that, we limit ourselves to **axisymmetric** configurations.

Both kinds of assumptions do not only reduce the required computational resources, they also allow a simplification of Einstein's field equation, used in a **general relativistic** approach. For that purpose, spacetime is split into a set of spacelike hypersurfaces according to the 3+1 decomposition of the ADM formalism, introduced by Arnowitt, Deser and Misner in 1962 (Arnowitt *et al.* 1962 or Misner *et al.* 1973). Every spacelike hypersurface is further split into meridional hypersurfaces, i.e. hypersurfaces containing the symmetry axis. That way, we arrive at a so-called (2+1)+1 decomposition of spacetime, as worked out by Gourgoulhon & Bonazzola 1993. This approach constitutes the theoretical fundamentals describing the curvature of spacetime caused by the neutron star, in our work.

A general relativistic approach always introduces two components: the geometry and the matter part. We make use of a rather simplified matter model. We assume that the neutron star matter is being described by a **perfect fluid**, i.e. there is no viscosity, heat conduction and so on. The equation of state is limited to the **barotropic** case, which means that the total energy density ϵ is a function $\epsilon(p)$ of only the pressure p . The advantage of this restriction is that the equations for the matter part can be solved much easier than without it. A side effect is that temperature is not required to unambiguously specify the state of the neutron star. The total energy density ϵ , the pressure p and the fluid velocity \vec{v} describe the matter part completely. Temperature could then be fixed by

¹In this section, all approximations assumed in this thesis are marked in boldface.

1. Introduction

specifying a thermal equation of state, but this is not done in this work (similarly, for the entropy).

Additional assumptions for the matter part are a **homogeneous chemical composition** and only **one layer**, i.e. there is nothing like a crust. Moreover, there is **no magnetic field** in the considered models.

1.4. Current state

There are many investigations about neutrons stars in literature. However, at our level of approximations they reduce to a manageable amount. They distinguish themselves in the additional simplifications applied on the fluid matter. For that purpose, we have to discern the azimuthal fluid motion around the symmetry axis from the meridional fluid motion inside the meridional planes.

A first simplification is to assume that there exists only an azimuthal fluid motion. This approach is followed by Nick Stergioulas with his RNS code (=‘Rapidly Rotating Neutron Star’, Stergioulas & Friedman 1995 and Nozawa *et al.* 1998). It is based on the general relativistic method of Komatsu *et al.* (1989). They essentially rewrite the geometry equations of the neutron star as Poisson equations in flat space. This means that every such equation consists of a flat-space Laplacian that acts on a potential and gives a source. The advantage of this notation is that the Green functions of the flat-space Laplacians are known. Therefore, these Green functions are used to invert the flat-space Laplacians and to vice versa compute the potentials from the sources. This is performed as a fixed point iteration method. At every iteration step, one computes new sources from old potentials, and afterwards new potentials are determined by inverting the Laplacians. The initial potentials of this procedure describe a non-rotating neutron star, given by the Tolman-Oppenheimer-Volkoff equation (Fließbach 2006). In order to achieve an azimuthal fluid motion, a rotation profile has to be specified. This is part of the matter equations, which have to be solved together with the geometry equations. In Komatsu *et al.* (1989), they are written in a manner suited to the vanishing meridional fluid motion. There are also several other groups, who follow slightly different numerical methods. Here, we refer to the citations in Nozawa *et al.* 1998.

The second type of simplification applied to the fluid motion is to assume that there is both an azimuthal and a meridional flow component, but the meridional one is slow. Then, the meridional fluid motion can be treated in a perturbative manner. This is done by Ioka & Sasaki (2004) in a general relativistic way. They also include a perturbatively treated magnetic field in their approach. There is a much earlier work by Roxburgh (1974), who also uses a perturbation technique, but without any magnetic fields and only in the Newtonian framework.

The third and last way is to have strong meridional currents, but no magnetic fields. As already realized by Randers (1941) and Roxburgh (1974), this leads to the following issue. Let us assume that the neutron star surface rotates. Then, the conservation of angular momentum causes the neutron star fluid to move faster and faster around the rotation axis when dragged by the meridional currents closer to the poles. Eventually, the rotation would become faster than the local speed of light. Therefore, without magnetic fields, the azimuthal component of the fluid motion has to vanish at the neutron star surface. The easiest way to fulfill this requirement is to consider a mere meridional fluid motion, with the azimuthal one vanishing everywhere. This is done by Eriguchi *et al.* (1986) and Eriguchi & Müller (1991). The central constituent of their approach is the usage of a stream function. The stream function is a scalar function, and it completely defines the

two-dimensional meridional fluid motion. Therefore, they rewrite the matter equations in a way somewhat different to that of Komatsu *et al.* (1989). So, it turns out that there are two ways to write the matter equations, the one fitting better a purely azimuthal and the other one a purely meridional fluid motion. Eriguchi *et al.* (1986) solve their equations with a Newton-Raphson iteration to produce a meridional circulation. However, a strong limitation of their approach is the usage of Newtonian physics.

1.5. Investigation goals

The goal of this thesis is to go beyond the limitations described in the last section. Therefore, we investigate the simultaneous presence of both an azimuthal and a meridional fluid motion. None of these components have to be weak. And, the treatment is performed in the framework of general relativity. The curvature of spacetime caused by the neutron star is computed with a generalization of the method of Komatsu *et al.* (1989), and for the matter, the stream function method of Eriguchi *et al.* (1986) is extended to general relativity.

The generalization of Komatsu *et al.* (1989) works in the following manner: We use the same fixed point iteration method idea as in the RNS code, starting from a solution of the Tolman-Oppenheimer-Volkoff equation. However, the presence of a meridional fluid motion requires the usage of more geometry fields. Therefore, there are also additional equations determining these fields, and their shape is more complicated. The exact form of these equations can be found in Gourgoulhon & Bonazzola (1993). However, they are not yet given in a shape applicable to the Green function method. Therefore, they are rewritten as Poisson equations in flat space.

The second part is the extension of the stream function idea of Eriguchi *et al.* (1986). For that purpose, we have to rederive the equations in Eriguchi *et al.* (1986) from scratch, but in the general relativistic framework. Actually, Eriguchi *et al.* (1986) still include an azimuthal fluid motion at the stage where they write down the equations. However, as soon as the solution method is presented they set the azimuthal part equal to zero. We, in contrast, include the azimuthal fluid motion at all steps. That way, one simple additional equation is required, and the remaining equations become somewhat more complicated, due to the more general treatment.

The above generalizations are implemented in a new code, called GRNS (=‘Generally Rotating Neutron Star’). It generalizes the RNS code of N. Stergioulas from the mere azimuthal fluid motion to a general one. The main attention of this thesis lies in the derivation of the theoretical fundamentals of this code and the creation of the GRNS code. However, as it generalizes the Newtonian method of Eriguchi *et al.* (1986), we are also interested in the fluid motion modes described in that paper extended to general relativity.

1.6. Outline

In Chapter 2, we present the basic fields, which unambiguously specify the structure of the neutron star. The rest of this chapter is then devoted to the equations determining the basic fields, including a derivation of the stream function method in general relativity. Chapter 3 deals with the rewriting of the equations into a form applicable for a numerical treatment. Therefore, the geometry equations are converted to flat-space Poisson equations, and the Green functions are computed. The numerical implementation into the GRNS code is briefly explained in Chapter 4. Here, also the graphical user

1. Introduction

interface of the GRNS code is presented, which is based on OpenGL. In Chapter 5, the results of convergence and consistency tests performed with the GRNS code are reported. An analysis of meridional circulation modes is done in Chapter 6. Finally, Chapter 7 summarizes the conclusions of this thesis and discusses possible extensions.

2. Theory

2.1. Notations and conventions

Our investigation is based on the framework of general relativity. Therefore, we keep as close as possible to the notations and conventions of the standard work of [Misner *et al.* \(1973\)](#). In addition to that, we include the definitions of [Gourgoulhon & Bonazzola \(1993\)](#), because this paper contains the fundamentals of how we deal with curved geometry.

We use geometrized units, in which the speed of light c and the gravitational constant G are set equal to unity:

$$c = G = 1 \tag{2.1}$$

That way, all general relativistic expressions become as transparent as possible. An exception to this rule are Chapters 4, 5 and 6. There, the GRNS code is explained and simulation results are presented in more appropriate cgs-units.

The fundamental quantities of general relativity are tensors. We use the component notation for tensors throughout this thesis. In this notation, tensors are written as $T_{\beta\dots}^{\alpha\dots}$. Being a common tool in the context of relativity, we apply Einstein's sum convention: Whenever two tensor indices in a term are denoted with the same letter, one has to sum over all possible values of the indices. We consider three types of indices with different value domains, discerned by the following letters:

$$\begin{aligned} \alpha, \beta, \dots, \omega &\in \{t, r, \theta, \phi\} \\ a, b, \dots, l &\in \{r, \theta, \phi\} \\ m, n, \dots, q &\in \{r, \theta\} \end{aligned} \tag{2.2}$$

This definition differs from the convention chosen in [Gourgoulhon & Bonazzola \(1993\)](#), where $a, b, \dots, k \in \{1, 2\}$ and $i, j, \dots, q \in \{1, 2, 3\}$. The choice (2.2) has two advantages: We perform two successive slicings of spacetime into hypersurfaces in this thesis. The first one removes the time index t and the second one removes the angle index ϕ . Therefore, it is more natural to map the spatial indices $\{r, \theta, \phi\}$ to the first part of the Roman alphabet and the meridional indices $\{r, \theta\}$ to the second one. Moreover, in [Gourgoulhon & Bonazzola \(1993\)](#) there are some scalars and vectors denoted with the same symbol, like the lapse function N and the shift vector N^a . Writing, e.g., the θ -component of the shift vector as N^2 could be misunderstood as the square of the lapse N . This ambiguity is resolved with the convention (2.2), in which the numerical index values of [Gourgoulhon & Bonazzola \(1993\)](#) have been replaced by letters. Note that the usage of the letters for the meridional indices stops at q , because the letters r and t already denote radial and temporal indices.

The 3+1 decomposition of the metric is given in equation (21.42) of [Misner *et al.* \(1973\)](#) and equation (2.9a) of [Gourgoulhon & Bonazzola \(1993\)](#). Unfortunately, there is a sign difference in the definition of the shift vector N^a . It does not arise from a difference in

2. Theory

the signature of the metric, because in both papers the signature is

$$(-, +, +, +)$$

and we follow this convention. We use the shift vector definition of [Gourgoulhon & Bonazzola \(1993\)](#), because then the geometry equations given therein do not have to be modified.

2.2. Fields and equations

We investigate neutron stars in general relativity. The central difference between Newtonian physics and general relativity is the treatment of space and time. In Newtonian physics, spacetime is flat and does not take part in physical phenomena. Gravitation is therefore a force, whose origin remains mysterious in the Newtonian framework. This problem is resolved in general relativity. There, spacetime is a curved manifold, and gravitation is a direct result of its curvature.

The manifold of general relativity is a four-dimensional pseudo-Riemannian manifold \mathcal{M} . Its exact shape is unambiguously specified by the **metric** tensor $g_{\alpha\beta}$. This tensor is symmetric, which means that $g_{\alpha\beta} = g_{\beta\alpha}$. In general relativity, all remaining physical fields are considered as matter fields. We assume that matter is approximately a perfect fluid without electromagnetic forces. Thus, it is completely defined by a **total energy density** ϵ , a **pressure** p and a **4-velocity** u_α .

The metric $g_{\alpha\beta}$ and the matter fields (ϵ, p, u_α) are governed by Einstein's field equation. Let us quickly recapitulate the quantities required to state this equation. The first step is to evaluate the Christoffel symbols of the second kind

$$\Gamma_{\beta\gamma}^\alpha = \frac{1}{2}g^{\alpha\delta}(\partial_\beta g_{\delta\gamma} + \partial_\gamma g_{\beta\delta} - \partial_\delta g_{\beta\gamma}) \quad (2.3)$$

where the tensor $g^{\alpha\beta}$ is the inverse of the tensor $g_{\alpha\beta}$ and $\partial_\alpha = \partial/\partial x^\alpha$ the partial derivative with respect to the coordinates x^α . The Christoffel symbols determine the Ricci tensor

$$R_{\alpha\beta} = \partial_\gamma \Gamma_{\alpha\beta}^\gamma - \partial_\alpha \Gamma_{\gamma\beta}^\gamma + \Gamma_{\gamma\delta}^\gamma \Gamma_{\alpha\beta}^\delta - \Gamma_{\delta\alpha}^\gamma \Gamma_{\gamma\beta}^\delta$$

which can be transformed into the Einstein tensor

$$G_{\alpha\beta} = R_{\alpha\beta} - \frac{1}{2}g_{\alpha\beta}g^{\gamma\delta}R_{\gamma\delta}$$

On the other hand, the matter fields are represented by the stress-energy tensor

$$T_{\alpha\beta} = (\epsilon + p)u_\alpha u_\beta + pg_{\alpha\beta} \quad (2.4)$$

Then, Einstein's field equation takes the form¹

$$\boxed{G_{\alpha\beta} = 8\pi T_{\alpha\beta}} \quad (2.5)$$

In the following sections, we will write the metric $g_{\alpha\beta}$ and the matter fields (ϵ, p, u_α) in terms of new fields, which we call basic fields. These fields still describe the state of the considered neutron star completely, but they are more appropriate for a numerical

¹There are many mathematical formulas in this thesis. In order to guide the reader, the most important ones are highlighted with boxes.

solution of equation (2.5).

2.3. Symmetries

The neutron stars analyzed in this dissertation underlie two symmetry assumptions:

- stationarity
- axisymmetry

Therefore, we consider a time coordinate $t = x^t$ and an angular coordinate $\phi = x^\phi$, limited to the interval $[0, 2\pi)$. These coordinates are chosen in such a manner that the fields depend only on the meridional coordinates x^r and x^θ :

$$g_{\alpha\beta} = g_{\alpha\beta}(x^r, x^\theta)$$

and

$$T_{\alpha\beta} = T_{\alpha\beta}(x^r, x^\theta)$$

In this choice of coordinates, Einstein's field equation (2.5) simplifies, strongly (Gourgoulhon & Bonazzola 1993).

2.4. Foliation

The metric $g_{\alpha\beta}$ consists of ten independent components, due to its symmetry property. Therefore, any invertible set of ten smooth functions $f^1 = f^1(g_{\alpha\beta}), f^2 = f^2(g_{\alpha\beta}), \dots$ can be used to represent the metric. A trivial example is $f^1 = g_{tt}, f^2 = g_{tr}, \dots$, which is a mere renaming of the individual metric components. This does not change the form of Einstein's field equation. However, any non-trivial choice makes it look more complex. We follow a method known as **foliation**, in order to derive a set of non-trivial functions f^1, f^2, \dots . It originates from the intention to write Einstein's field equation as an initial value problem (Arnowitt *et al.* 1962). In our case, the advantage of this approach is that Einstein's field equation can be transformed into a form well suited for numerical work. A foliation works in the following manner:

Starting with an arbitrary manifold, we split it into a continuous sequence of infinitesimally close hypersurfaces, whose dimension is one lower than that of the original manifold (Fig. 2.1). Each of the hypersurfaces is given by its own metric, the **induced metric**. The hypersurfaces alone are not sufficient to fully specify the original manifold. In addition to them, knowledge about the length and the attachment points of the perpendicular connectors between the hypersurfaces is required. The length of the connectors can be encoded in a scalar, called **lapse function**, and the socket positions in a so-called **shift vector**. Hence, the metric of the original manifold is replaced by three quantities: the induced metric, the lapse function and the shift vector.

In the following two sections, we use two successive foliations. The first step (Sect. 2.4.1) is a foliation of the whole four-dimensional spacetime \mathcal{M} into spacelike 3-surfaces Σ_t of constant time t . This way, the ten independent metric components $g_{\alpha\beta}$ are replaced by the induced 3-metric h_{ab} with six independent components, the 3-lapse function N and the shift 3-vector N^a . In the second step (Sect. 2.4.2), each 3-surface Σ_t is foliated into the 2-surfaces $\Sigma_{t\phi}$, which are defined as the intersections between the 3-surfaces Σ_t and the 3-surfaces Σ_ϕ of constant angle ϕ . Consequently, the 3-metric h_{ab} is given by the

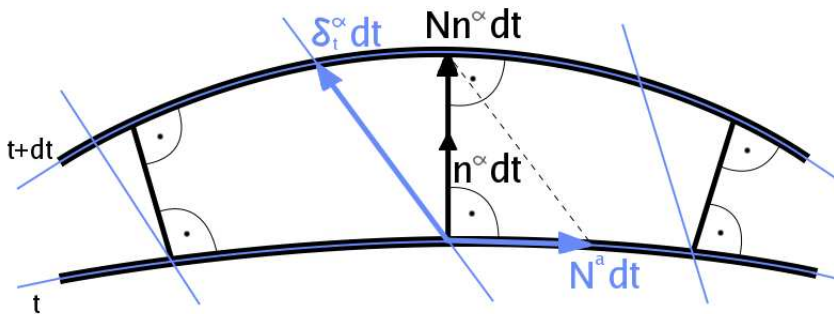


Figure 2.1.: **Foliation into two hypersurfaces with perpendicular connectors.**

For simplicity, we consider only a flat two-dimensional manifold, namely the mere plane upon which the text of this page is written on. This plane is split into infinitesimally close hypersurfaces at times t and $t + dt$, represented by the two horizontal curves. The metric of the original, two-dimensional manifold defines orthogonality. That way, the black, vertical, perpendicular connectors of infinitesimal length are unambiguously given. The direction of these connectors is specified by the unit vector n^α and their $1/dt$ -fold length by the lapse function N . The coordinates on the hypersurfaces may be chosen, arbitrarily. Hence, the timelike coordinate basis vector $\delta_t^\alpha = (1, 0, 0, 0)$ can be inclined with respect to the connectors. The amount of inclination is encoded in the shift vector N^a .

induced 2-metric k_{mn} with three independent components, the 2-lapse function M and the shift 2-vector M^n . The final result of the two foliations are then the fields

$$N, M, N^a, M^n, k_{mn} \quad (2.6)$$

which contain the original ten independent degrees of freedom.

2.4.1. 3+1-foliation of the whole spacetime

We begin by foliating the four-dimensional spacetime \mathcal{M} into spacelike 3-surfaces Σ_t of constant time t . This so-called 3 + 1-foliation is a well known procedure, for example performed in [Misner *et al.* \(1973\)](#) and [Straumann \(2004\)](#). Still, it is reasonable to repeat it here, to better understand the less familiar, but very similar foliation of the 3-surfaces Σ_t , undertaken in Sect. 2.4.2.

The first step of the foliation is to specify the shape of the individual 3-surfaces Σ_t , independent of how they are arranged against each other. This information is located in the induced 3-metric, which is simply given by

$$h_{ab} = g_{ab} \quad (2.7)$$

The second step is to connect the 3-surfaces Σ_t . For that purpose, we specify the perpendicular connectors between them. The $1/dt$ -fold length of the connectors is called 3-lapse N and their direction is denoted by the 4-vector n^α . This timelike vector is normalized to $g_{\alpha\beta}n^\alpha n^\beta = -1$. The orthogonality of the connectors implies $g_{\alpha\beta}n^\alpha X^\beta = 0$ for all spacelike 4-vectors X^α . The condition for being spacelike is $X^t = 0$, i.e. $g_{\alpha b}n^\alpha X^b = 0$. Looking at Fig. 2.1, we realize that the difference $Nn^\alpha - \delta_t^\alpha$ is a 3-vector tangent to the 3-surfaces Σ_t . Therefore, we can write it as $Nn^\alpha - \delta_t^\alpha = (0, N^a)$, with the 3-shift N^a , or

vice versa

$$\delta_t^\alpha = Nn^\alpha - (0, N^a) \quad (2.8)$$

The quantity δ_t^α are four components of the Kronecker symbol δ_β^α , which is equal to unity for $\alpha = \beta$ and zero otherwise. This allows us to compute

$$g_{tt} = g_{\alpha\beta}\delta_t^\alpha\delta_t^\beta = g_{\alpha\beta}N^2n^\alpha n^\beta + 2g_{ab}Nn^\alpha N^b + g_{ab}N^aN^b = -N^2 + N_aN^a \quad (2.9)$$

and

$$g_{ta} = g_{\beta c}\delta_t^\beta\delta_a^c = g_{\beta c}Nn^\beta\delta_a^c - g_{bc}N^b\delta_a^c = -N_a \quad (2.10)$$

with $N_a = h_{ab}N^b$. Introducing the inverse h^{ab} of the 3-metric h_{ab} , we can then summarize the three results (2.7), (2.9) and (2.10) as

$$\boxed{\begin{pmatrix} g_{tt} & g_{tb} \\ g_{at} & g_{ab} \end{pmatrix} = \begin{pmatrix} N_cN^c - N^2 & -N_b \\ -N_a & h_{ab} \end{pmatrix}} \quad (2.11)$$

and

$$\begin{pmatrix} g^{tt} & g^{tb} \\ g^{at} & g^{ab} \end{pmatrix} = \begin{pmatrix} -\frac{1}{N^2} & -\frac{N^b}{N^2} \\ -\frac{N^a}{N^2} & h^{ab} - \frac{N^aN^b}{N^2} \end{pmatrix} \quad (2.12)$$

This is the 3 + 1-decomposition of the spacetime \mathcal{M} , based on the conventions of [Gourgoulhon & Bonazzola \(1993\)](#).

2.4.2. 2+1-foliation of the $t = \text{const}$ 3-surfaces

We proceed by foliating each of the 3-surfaces Σ_t into the meridional 2-surfaces $\Sigma_{t\phi}$ of constant time t and constant angle ϕ . This procedure is very similar to the 3 + 1-decomposition performed in section 2.4.1.

In analogy to equation (2.7), we start with the definition of the induced 2-metric

$$k_{mn} = h_{mn} \quad (2.13)$$

This metric unambiguously specifies the shape of the 2-surfaces $\Sigma_{t\phi}$. The only remaining issue are therefore the perpendicular connectors. The 1/dt-fold length of the connectors is called 2-lapse M and the direction is given by the 4-vector m^α . However, this time the direction vector is spacelike and hence normalized to $g_{\alpha\beta}m^\alpha m^\beta = 1$. Being spacelike means that $m^t = 0$, and in addition to that the orthogonality causes $g_{\alpha\beta}m^\alpha Y^\beta = 0$ for all 4-vectors Y^α tangent to the 2-surfaces $\Sigma_{t\phi}$. This implies $Y^t = Y^\phi = 0$ such that $g_{\alpha m}m^\alpha Y^m = 0$. Similar to the 3 + 1-decomposition, we then use the so-called 2-shift M^m to express $Mm^\alpha - \delta_\phi^\alpha = (0, M^m, 0)$ or

$$\delta_\phi^\alpha = Mm^\alpha - (0, M^m, 0) \quad (2.14)$$

This leads to

$$h_{\phi\phi} = g_{\alpha\beta}\delta_\phi^\alpha\delta_\phi^\beta = g_{\alpha\beta}M^2m^\alpha m^\beta + 2g_{\alpha m}Mm^\alpha M^m + g_{mn}M^m M^n = M^2 + M_m M^m \quad (2.15)$$

and

$$h_{\phi m} = g_{\alpha n}\delta_\phi^\alpha\delta_m^n = g_{\alpha n}Mm^\alpha\delta_m^n - g_{on}M^o\delta_m^n = -M_m \quad (2.16)$$

with $M_m = k_{mn}M^n$. The last step is to define the inverse of the 2-metric k_{mn} as k^{mn} .

2. Theory

Then, we can finally summarize the results (2.13), (2.15) and (2.16) as

$$\boxed{\begin{pmatrix} h_{mn} & h_{m\phi} \\ h_{\phi n} & h_{\phi\phi} \end{pmatrix}} = \begin{pmatrix} k_{mn} & -M_m \\ -M_n & M^2 + M_o M^o \end{pmatrix} \quad (2.17)$$

and

$$\begin{pmatrix} h^{mn} & h^{m\phi} \\ h^{\phi n} & h^{\phi\phi} \end{pmatrix} = \begin{pmatrix} k^{mn} + \frac{M^m M^n}{M^2} & \frac{M^m}{M^2} \\ \frac{M^n}{M^2} & \frac{1}{M^2} \end{pmatrix} \quad (2.18)$$

just as done in [Gourgoulhon & Bonazzola \(1993\)](#).

2.5. Basic Fields

There are twelve basic fields. Every solution of Einstein's field equation (2.5) is uniquely defined by these twelve basic fields. In the following two sections, we will define the **basic geometry** and **basic matter fields**.

2.5.1. Geometry

Let us review the decomposition of a manifold into hypersurfaces from a more general viewpoint. Each such decomposition consists of a lapse function and a shift vector. The purpose of the lapse function is to specify the distance between the hypersurfaces, which are surfaces where one coordinate is constant. Varying this coordinate and fixing all other ones leads to coordinate lines whose direction is set by the shift vector. It is obvious that these coordinate surfaces and coordinate lines can be chosen in an arbitrary manner. Vice versa, this means that there always exists a coordinate transformation which changes the lapse function and the shift vector arbitrarily. Imagining the 2-metric k_{mn} being decomposed in a 1 + 1-manner, it is therefore possible to choose meridional coordinates $(x^r, x^\theta) = (r, \theta)$, limited to $r \in [0, \infty)$ and $\theta \in [0, \pi)$, in such a way that

$$k_{mn} = A^2 \begin{pmatrix} 1 & 0 \\ 0 & r^2 \end{pmatrix} \quad (2.19)$$

with the 2-conformal factor A . This choice of so-called **isotropic polar coordinates** is made in [Gourgoulhon & Bonazzola \(1993\)](#).

Using isotropic polar coordinates, the ten degrees of freedom (2.6) of the metric $g_{\alpha\beta}$ reduce to the eight ones given by

$$N, M, N^a, M^n, A$$

These quantities define the basic geometry fields

$$\boxed{\nu, N^r, N^\theta, N^\phi, \beta, M^r, M^\theta, \alpha} \quad (2.20)$$

with

$$\nu = \ln N \quad (2.21)$$

$$\beta = \ln \frac{M}{r \sin \theta} \quad (2.22)$$

$$\alpha = \ln A \quad (2.23)$$

The basic geometry fields unambiguously specify the curvature of spacetime caused by the neutron star. In flat spacetime, the metric has the form $g_{\alpha\beta} = \text{diag}(-1, 1, r^2, r^2 \sin^2 \theta)$ such that the two shift vectors N^a and M^m are zero. In addition to that, equations (2.11), (2.17) and (2.19) show that $N = 1$, $A=1$ and $M = r \sin \theta$. That way, it is obvious that all basic geometry fields vanish in flat spacetime. This property is of advantage for finding a numerically stable form of the field equations when solved numerically using Green functions.

2.5.2. Matter

In order to deal with the matter the neutron star consists of, our goal is to extend the stream function method of [Eriguchi *et al.* \(1986\)](#) from the Newtonian limit to general relativity. The central idea of this method is express two components of the Newtonian velocity 3-vector in terms of a **stream function** ψ . That way, the continuity equation of the neutron star fluid matter is fulfilled automatically. We proceed in a similar manner. Further below, we will show how two degrees of freedom of the 4-velocity u_α can be expressed in terms of the stream function ψ . There, it will also turn out that it is appropriate to express the third degree of freedom of the 4-velocity as a quantity l_ϕ , the ϕ -component of the so-called **Lagrangian angular momentum**. Note that the 4-velocity u_α has only three degrees of freedom due to the well known velocity constraint ([Misner *et al.* 1973](#))

$$g_{\alpha\beta} u^\alpha u^\beta = -1 \quad (2.24)$$

So, matter is unambiguously described by its total energy density ϵ (=rest energy density+thermal energy density), its pressure p , the stream function ψ and the Lagrangian angular momentum component l_ϕ . In [Eriguchi *et al.* \(1986\)](#), the Poisson equation of the stream function method is written using the modified stream function

$$\chi_0 = \frac{\psi}{r \sin \theta}$$

Therefore, we consider

$$\boxed{\epsilon, p, \chi_0, l_\phi} \quad (2.25)$$

as the basic matter fields.

2.6. Projections

For every basic field, there is one corresponding equation. So, there are eight geometry equations for the eight basic geometry fields (2.20) and four matter equations for the four basic matter fields (2.25). Both sets of equations are treated in a different manner in this thesis. In the following, we will address the basic geometry equations, first.

Einstein's field equation (2.5) contains ten components, because both sides of that equation are symmetric tensors of rank 2 in 4-dimensional spacetime. So, it is actually a set of ten equations. Eight of these ten equations define the eight geometry fields (we do not need all ten equations due to the coordinate choice (2.19)). However, the ten equations are not yet given in such a shape that we can assign one equation to each geometry field. This task is performed in [Gourgoulhon & Bonazzola \(1993\)](#). For that purpose, these authors project Einstein's field equation parallelly and orthogonally to the 4-vectors n^α and m^α . The projections work in the following manner:

We begin with the 4-vector n^α , perpendicular to the hypersurfaces Σ_t of constant time

2. Theory

t. Looking at equation (2.8), we realize that the components of this vector are

$$n^\alpha = \left(\frac{1}{N}, \frac{N^a}{N} \right)$$

Then, the expression

$$n^\alpha n^\beta (G_{\alpha\beta} - 8\pi T_{\alpha\beta}) = 0 \quad (2.26)$$

is what we call a double parallel projection. A second projection consists of a parallel projection combined with an orthogonal one. With this in mind, we need the projector

$$h_\beta^\alpha = \delta_\beta^\alpha + n^\alpha n_\beta$$

along the 4-vector n^α onto the hypersurfaces Σ_t . This quantity is a projector, because using the normalization $g_{\alpha\beta} n^\alpha n^\beta = -1$ we see that

$$h_\beta^\alpha n^\beta = n^\alpha + n^\alpha n_\beta n^\beta = 0$$

and

$$h_\beta^\alpha h_\gamma^\beta = (\delta_\beta^\alpha + n^\alpha n_\beta) (\delta_\gamma^\beta + n^\beta n_\gamma) = \delta_\gamma^\alpha + 2n^\alpha n_\gamma + n^\alpha n_\beta n^\beta n_\gamma = \delta_\gamma^\alpha + n^\alpha n_\gamma = h_\gamma^\alpha$$

Then, we get the projection

$$h_\alpha^\beta n^\gamma (G_{\beta\gamma} - 8\pi T_{\beta\gamma}) = 0 \quad (2.27)$$

The last projection based on the 4-vector n^α is the double orthogonal projection

$$h_\alpha^\gamma h_\beta^\delta (G_{\gamma\delta} - 8\pi T_{\gamma\delta}) = 0 \quad (2.28)$$

So, we have obtained equation (2.26) with only one component, equation (2.27) with three components and finally equation (2.28) with six components.

The next step is to repeat the parallel and orthogonal projections with equations (2.27) and (2.28) but this time with the 4-vector m^α , perpendicular to the hypersurfaces $\Sigma_{t\phi}$ of constant time t and constant angle ϕ . This vector has the components

$$m^\alpha = \left(0, \frac{M^m}{M}, \frac{1}{M} \right)$$

due to equation (2.14). The corresponding projector along the 4-vector m^α onto the hypersurfaces $\Sigma_{t\phi}$ has the form

$$k_\beta^\alpha = \delta_\beta^\alpha - m^\alpha m_\beta$$

In contrast to the projector h_β^α (2.26), there is a minus sign in the definition of the projector k_β^α , because the 4-vector m^α is normalized to $g_{\alpha\beta} m^\alpha m^\beta = 1$.

We do not list the equations resulting from the projections based on the 4-vector m^α here. It is sufficient to understand the basic idea. Moreover, [Gourgoulhon & Bonazzola \(1993\)](#) do not use the resulting projections directly. Instead, some of them are combined and other ones are simply skipped. It is possible to skip equations, because we need only eight equations for the eight basic geometry fields, though Einstein's field equation has ten components.

2.7. Ancillary fields

Based on the projection idea described in the last section, [Gourgoulhon & Bonazzola \(1993\)](#) obtain eight geometry equations from Einstein's field equation (2.5), one for each of the eight basic geometry fields. Afterwards, these equations are reformulated such that their Poisson-like character becomes evident. Note that at this stage the Laplacians therein are still defined in curved spacetime. That is, the Laplacians consist of covariant derivatives and not of partial ones.

In principle, we could now repeat all the steps leading to the final results (B3-B7) in the paper of [Gourgoulhon & Bonazzola \(1993\)](#). Actually, this would be reasonable, because the paper of these authors is written in such a manner that only important steps are given, but many intermediate calculations are omitted. These calculations are definitively not trivial, and they are required for a deeper understanding of this thesis. However, repeating all the tedious computations here would lead us too far off. Therefore, we skip all intermediate steps leading to the final form of the geometry equations, and instead refer only to the results (B3-B7) of [Gourgoulhon & Bonazzola \(1993\)](#).

The equations (B3-B7) of [Gourgoulhon & Bonazzola \(1993\)](#) make use of a large set of ancillary quantities. Every such ancillary field can be computed from the basic fields. It is possible to state the equations (B3-B7) merely in terms of the basic fields. However, then the equations would become unnecessarily long. Therefore, we use the ancillary fields defined by [Gourgoulhon & Bonazzola \(1993\)](#). There are two kinds of such fields, the ancillary geometry fields and the ancillary matter fields. In the following, all these ancillary fields are defined. However, it is beyond the scope of this thesis to give a deeper explanation of their meaning.

2.7.1. Geometry

2.7.1.1. Logarithm of 2-lapse

We start with the ancillary geometry fields (2.20). Similarly to the quantity $\nu = \ln N$ for the 3-lapse N , we define

$$\mu = \ln M \quad (2.29)$$

for the 2-lapse M . Note that we do not use this quantity as one of our basic fields, because it does not vanish in flat spacetime, in contrast to the basic geometry field β .

2.7.1.2. Christoffel symbols

We have already considered the Christoffel symbols of the second kind $\Gamma_{\beta\phi}^{\alpha}$ in equation (2.3). They can be expressed in terms of the Christoffel symbols of the first kind

$$\Gamma_{\alpha\beta\gamma} = \frac{1}{2} (\partial_{\beta} g_{\alpha\gamma} + \partial_{\gamma} g_{\beta\alpha} - \partial_{\alpha} g_{\beta\gamma})$$

as

$$\Gamma_{\beta\gamma}^{\alpha} = g^{\alpha\delta} \Gamma_{\delta\beta\gamma}$$

Both Christoffel symbols are defined in the whole 4-dimensional spacetime \mathcal{M} . However, there are also Christoffel symbols for the 3-surfaces Σ_t and for the 2-surfaces $\Sigma_{t\phi}$. The Christoffel symbols of the first kind on the 3-surfaces Σ_t are

$${}^3\Gamma_{abc} = \Gamma_{abc} \quad (2.30)$$

2. Theory

and on the 2-surfaces $\Sigma_{t\phi}$ they have the form

$${}^2\Gamma_{mno} = \Gamma_{mno} \quad (2.31)$$

The expressions for these Christoffel symbols simplify drastically with our choice of coordinates (see Appendix A). The corresponding Christoffel symbols of the second kind are given by

$${}^3\Gamma_{bc}^a = h^{ad} {}^3\Gamma_{dbc} \quad (2.32)$$

and

$${}^2\Gamma_{no}^m = k^{mp} {}^2\Gamma_{pno} \quad (2.33)$$

They appear in the definition of covariant derivatives on the 3-surfaces Σ_t and on the 2-surfaces $\Sigma_{t\phi}$, respectively. Similarly to [Gourgoulhon & Bonazzola \(1993\)](#), we use a single stroke ‘|’ for the so-called 3-covariant derivative

$$T_{b...|c}^{a...} = \partial_c T_{b...}^{a...} + {}^3\Gamma_{dc}^a T_{b...}^{d...} + \dots - {}^3\Gamma_{bc}^d T_{d...}^{a...} - \dots \quad (2.34)$$

for every tensor field $T_{b...}^{a...}$ on the 3-surfaces Σ_t , and a double one ‘||’ for the 2-covariant derivative

$$T_{n...||o}^{m...} = \partial_o T_{n...}^{m...} + {}^2\Gamma_{po}^n T_{m...}^{p...} + \dots - {}^2\Gamma_{no}^p T_{p...}^{m...} - \dots \quad (2.35)$$

for all tensor fields $T_{n...}^{m...}$ on the 2-surfaces $\Sigma_{t\phi}$. The covariant derivative referring to the whole spacetime \mathcal{M} is written in the usual manner as ‘;’.

2.7.1.3. Exterior curvature

Having introduced the covariant derivatives on the 3-surfaces Σ_t and on the 2-surfaces $\Sigma_{t\phi}$, respectively, we now address the exterior curvature of these hypersurfaces. The exterior curvature is a different way to encode the information given by the lapse function and the shift vector. In this thesis, we have to consider the exterior curvature, because it is part of the equations (B3-B7) in [Gourgoulhon & Bonazzola \(1993\)](#).

Let us start with the exterior curvature on the 3-surfaces Σ_t . It is defined as

$$K_{ab} = -\frac{1}{2N} (N_{a|b} + N_{b|a}) = -\frac{1}{N} \left[\frac{1}{2} (\partial_a N_b + \partial_b N_a) - {}^3\Gamma_{ab}^c N_c \right]$$

and its indices are raised with the 3-metric h_{ab} , as shown in

$$K^{ab} = h^{ac} h^{bd} K_{cd} \quad (2.36)$$

for example. Similarly, we obtain the exterior curvature

$$L_{mn} = -\frac{1}{M} M_{(m|n)} = -\frac{1}{M} (\partial_{(m} M_{n)} - {}^2\Gamma_{mn}^o M_o)$$

on the 2-surfaces $\Sigma_{t\phi}$. Here, we have to use the 2-metric k_{mn} for raising indices, i.e.

$$L^{mn} = k^{mo} k^{np} L_{op}$$

2.7.1.4. Projections

As already mentioned above, the equations (B3-B7) in [Gourgoulhon & Bonazzola \(1993\)](#) are the result of projecting Einstein’s field equation parallelly and orthogonally along the two 4-vectors n^α and m^α , respectively. Therefore, several fields are expressed in terms

of their projections in that paper. Let us begin with the decomposition of the 3-lapse as $N^\alpha = \omega m^\alpha + q^\alpha$, in which we assume $N^0 = 0$. The resulting projections are

$$\begin{aligned}\omega &= m_\alpha N^\alpha \\ q^\alpha &= k_\beta^\alpha N^\beta\end{aligned}\tag{2.37}$$

In a similar manner, we split the exterior 3-curvature K^{ab} , given in equation (2.36). For that purpose, we extend this quantity to $K^{\alpha\beta}$ by demanding $K^{\alpha 0} = K^{0\alpha} = 0$. Then, we perform the split $K^{\alpha\beta} = \kappa m^\alpha m^\beta + m^\alpha \kappa^\beta + \kappa^\alpha m^\beta + \kappa^{\alpha\beta}$, with

$$\begin{aligned}\kappa &= m_\alpha m_\beta K^{\alpha\beta} \\ \kappa^\alpha &= k_\beta^\alpha m_\gamma K^{\beta\gamma} \\ \kappa^{\alpha\beta} &= k_\gamma^\alpha k_\delta^\beta K^{\gamma\delta}\end{aligned}$$

2.7.1.5. Commutators

We conclude the description of the ancillary geometry fields with three commutators, which are defined as

$$\begin{aligned}[M, q]^m &= M^n \partial_n q^m - q^n \partial_n M^m \\ [M, \kappa]^m &= M^n \partial_n \kappa^m - \kappa^n \partial_n M^m \\ [q, \kappa]^m &= q^n \partial_n \kappa^m - \kappa^n \partial_n q^m\end{aligned}$$

2.7.2. Matter

2.7.2.1. Velocity

The second set of ancillary fields are the ancillary matter fields. The three degrees of freedom of the 4-velocity u^α , resulting from the constraint (2.24), can be extracted into the quantity

$$v^a = u^a / u^t\tag{2.38}$$

Vice versa, we obtain

$$\begin{aligned}u^t &= \frac{1}{\sqrt{-(g_{tt} + 2g_{ta}v^a + g_{ab}v^a v^b)}} \\ u^a &= u^t v^a\end{aligned}$$

2.7.2.2. Projections

We will now project the stress-energy tensor in various ways. The first decomposition is $T^{\alpha\beta} = E n^\alpha n^\beta + n^\alpha J^\beta + J^\alpha n^\beta + S^{\alpha\beta}$, with the projections

$$\begin{aligned}E &= n_\alpha n_\beta T^{\alpha\beta} \\ J^\alpha &= -h_\beta^\alpha n_\gamma T^{\beta\gamma} \\ S^{\alpha\beta} &= h_\gamma^\alpha h_\delta^\beta T^{\gamma\delta}\end{aligned}$$

2. Theory

The minus above is used in [Gourgoulhon & Bonazzola \(1993\)](#), too. We proceed with the split $J^\alpha = jm^\alpha + j^\alpha$. This time, the projections are given by

$$\begin{aligned} j &= m_\alpha J^\alpha \\ j^\alpha &= k_\beta^\alpha J^\beta \end{aligned}$$

Finally, we decompose $S^{\alpha\beta} = sm^\alpha m^\beta + m^\alpha s^\beta + s^\alpha m^\beta + s^{\alpha\beta}$, with

$$\begin{aligned} s &= m_\alpha m_\beta S^{\alpha\beta} \\ s^\alpha &= k_\beta^\alpha m_\gamma S^{\beta\gamma} \\ s^{\alpha\beta} &= k_\gamma^\alpha k_\delta^\beta S^{\gamma\delta} \end{aligned}$$

Note that for projections onto the 3-surfaces Σ_t , like S^{ab} , the 3-metric h_{ab} is the tool for raising and lowering indices, whereas for projections onto the 2-surfaces $\Sigma_{t\phi}$, like s^{mn} , this role is taken by the 2-metric k_{mn} .

2.8. Geometry equations

We are now equipped with enough ancillary fields to state the eight geometry equations ([B3](#), [B4a](#), [B4b](#), ..., [B7](#)) of [Gourgoulhon & Bonazzola \(1993\)](#) in this thesis. However, the first three of these equations contain some typos. In [Appendix B](#), we perform a mathematical derivation, which shows how the first equation has to be corrected. For the other two erroneous equations, we have used a computer algebra program. The correct versions of the rather lengthy equations ([B3-B7](#)) of [Gourgoulhon & Bonazzola \(1993\)](#) are listed in [Appendix C](#).

2.9. Matter equations

We proceed with the equations for the four matter fields ([2.25](#)). For that purpose, we recall the contracted Bianchi identity

$$\nabla_\beta G^{\alpha\beta} = 0$$

where ∇_α is the covariant derivative. Applying the contracted Bianchi identity on Einstein's field equation ([2.5](#)) leads to the equation of general relativistic hydrodynamics

$$\boxed{\nabla_\beta T^{\alpha\beta} = 0} \tag{2.39}$$

[Gourgoulhon & Bonazzola \(1993\)](#) rewrite the components of this equation in a manner similar to the geometry equations. The result are equations ([4.3](#)), ([4.5](#)) and ([4.7](#)) of [Gourgoulhon & Bonazzola \(1993\)](#). The first two of these equations are scalar equations, and the third one is a 2-vector equation. However, they are not given in an expanded form like the geometry equations ([B3-B7](#)) of [Gourgoulhon & Bonazzola \(1993\)](#), where in most cases Einstein's sum convention is written out explicitly. Therefore, it turned out to be much easier to extend the Newtonian stream function method of [Eriguchi *et al.* \(1986\)](#) to general relativity. In the following sections, the general relativistic stream function method is derived. For that purpose, we project equation ([2.39](#)) parallelly and orthogonally to the fluid 4-velocity u^α .

2.9.1. Energy equation as result of a parallel projection

2.9.1.1. Compact form

We begin with a projection of equation (2.39) parallel to the 4-velocity u_α . The resulting equation

$$u_\alpha \nabla_\beta T^{\alpha\beta} = 0 \quad (2.40)$$

would lead to the conservation of energy if we neglected p/ϵ terms for a negligibly small pressure, like in the Newtonian limit. In order to show this, we use the velocity constraint (2.24), which gives

$$u_\alpha \nabla_\beta u^\alpha = 0 \quad (2.41)$$

Similar to the projector h_β^α , defined in equation (2.26), we introduce the projector

$$q_\beta^\alpha = \delta_\beta^\alpha + u^\alpha u_\beta \quad (2.42)$$

along the 4-velocity u^α . This quantity obeys

$$q_\beta^\alpha u^\beta = 0 \quad (2.43)$$

Then, equation (2.40) becomes

$$\begin{aligned} 0 &= u_\alpha \nabla_\beta \left(\epsilon u^\alpha u^\beta + p q^{\alpha\beta} \right) \\ &= u_\alpha u^\alpha \nabla_\beta \left(\epsilon u^\beta \right) + u_\alpha p \nabla_\beta \left(g^{\alpha\beta} + u^\alpha u^\beta \right) \\ &= -\nabla_\alpha (\epsilon u^\alpha) - p \nabla_\alpha u^\alpha \end{aligned}$$

That way, we finally arrive at

$$\boxed{\nabla_\alpha [(\epsilon + p) u^\alpha] = u^\alpha \nabla_\alpha p} \quad (2.44)$$

as shown in [Friedman & Stergioulas](#). So, if we neglected p/ϵ terms, this would lead to the conservation $\nabla_\alpha (\epsilon u^\alpha) = 0$ of the total energy density.

2.9.1.2. Expanded form

We expand equation (2.44) as

$$\partial_\alpha [(\epsilon + p) u^\alpha] + (\epsilon + p) \Gamma_{\beta\alpha}^\beta u^\alpha = u^\alpha \partial_\alpha p$$

From [D’Inverno \(1992\)](#), we know

$$\Gamma_{\beta\alpha}^\beta = \partial_\alpha \ln \sqrt{-g}$$

with the determinant $g = \det g_{\alpha\beta}$, such that stationarity and axisymmetry lead to

$$\partial_m [(\epsilon + p) u^m] + (\epsilon + p) u^m \partial_m \ln \sqrt{-g} = u^m \partial_m p \quad (2.45)$$

The results (D.1) and (D.2), proven in Appendix D, have the consequence that

$$\partial_m \ln \sqrt{-g} = \partial_m \left(\nu + \ln \sqrt{h} \right) = \partial_m \left(\nu + \mu + \ln \sqrt{k} \right)$$

2. Theory

We rewrite the ancillary field $\mu = \ln M$ as $\mu = \beta + \ln(r \sin \theta)$ (see equation (2.22)) and compute $\ln \sqrt{k} = 2\alpha + \ln r$ with equation (2.19). Then, we arrive at

$$\partial_m \ln \sqrt{-g} = \partial_m [2\alpha + \gamma + 2 \ln r + \ln(\sin \theta)]$$

with the ancillary field

$$\gamma = \beta + \nu \quad (2.46)$$

We insert this result in equation (2.45):

$$\partial_m [(\epsilon + p) u^m] + (\epsilon + p) \left(\frac{2}{r} u^r + \cot \theta u^\theta \right) = \left[\partial_m p - (\epsilon + p) (2\alpha + \gamma)_{,m} \right] u^m$$

Now, we use the temporal component (2.56) of the relativistic Euler equation, derived further below in Sect. 2.9.2.2. That way,

$$\begin{aligned} \partial_m [(\epsilon + p) u^m] + (\epsilon + p) \left(\frac{2}{r} u^r + \cot \theta u^\theta \right) &= -(\epsilon + p) (2\alpha + \gamma + \ln u_t)_{,m} u^m \\ &= -\ln(e^{2\alpha + \gamma} u_t)_{,m} (\epsilon + p) u^m \end{aligned}$$

and hence

$$\partial_m [e^{2\alpha + \gamma} (\epsilon + p) u_t u^m] + e^{2\alpha + \gamma} u_t (\epsilon + p) \left(\frac{2}{r} u^r + \cot \theta u^\theta \right) = 0 \quad (2.47)$$

The first term is the contraction of a partial derivative and a vector. However, this quantity is not a 3-divergence in flat space, because we do not use Cartesian coordinates, but spherical ones. Still, it is possible to write the above equation in terms of the flat space 3-divergence. For that purpose, we recall from [D'Inverno \(1992\)](#) that for a tensor density of weight +1, like $\sqrt{h} X^a$, with the determinant $h = \det h_{ab}$ and an arbitrary 3-vector X^a , the covariant derivative can be replaced with the partial one:

$$\left(\sqrt{h} X^a \right)_{|a} = \left(\sqrt{h} X^a \right)_{,a}$$

Therefore, we can write the flat space 3-divergence as

$${}^3 \text{div} \vec{X} = X^a_{|a} = \frac{1}{\sqrt{h}} \left(\sqrt{h} X^a \right)_{,a}$$

having taken into account that $h_{|a} = 0$. For flat space, the 3-metric is $h_{ab} = \text{diag}(r^2, r^2 \sin^2 \theta)$ such that $\sqrt{h} = r^2 \sin \theta$ and hence

$${}^3 \text{div} \vec{X} = X^m_{,m} + \frac{2}{r} X^r + \cot \theta X^\theta \quad (2.48)$$

Comparing this result with equation (2.47), we find

$$\boxed{{}^3 \text{div} [e^{2\alpha + \gamma} (\epsilon + p) u_t \vec{u}] = 0} \quad (2.49)$$

2.9.1.3. Analytic Solution

In order to solve equation (2.49), we apply a Helmholtz decomposition. A Helmholtz decomposition is the split of a vector field into the gradient of a scalar field and a solenoidal

field. So, in Cartesian coordinates, denoted with the index c , we decompose

$$e^{2\alpha+\gamma} (\epsilon + p) u_t u_c^m = \partial_m^c \sigma + A_c^m \quad (2.50)$$

with the so called **source function** σ and the solenoidal field A_c^m , i.e. ${}^3\text{div}\vec{A} = 0$. Transforming the decomposition into spherical coordinates, we get

$$e^{2\alpha+\gamma} (\epsilon + p) u_t \begin{pmatrix} u^r \\ u^\theta \end{pmatrix} = \begin{pmatrix} \partial_r \sigma + A^r \\ \frac{1}{r^2} \partial_\theta \sigma + A^\theta \end{pmatrix}$$

with

$${}^3\text{div}\vec{A} = \partial_r A^r + \partial_\theta A^\theta + \frac{2}{r} A^r + \cot \theta A^\theta = 0 \quad (2.51)$$

This condition is automatically satisfied by the **stream function** ψ , defined as

$$\begin{aligned} A^r &= \frac{1}{r^2 \sin \theta} \partial_\theta \psi \\ A^\theta &= -\frac{1}{r^2 \sin \theta} \partial_r \psi \end{aligned}$$

similar to [Eriguchi *et al.* \(1986\)](#). Applying the flat space divergence 3-divergence on both sides of the decomposition (2.50), the equations (2.49) and (2.51) show us that

$${}^3\Delta_c \sigma = 0$$

The only solution to this equation is

$$\sigma = 0$$

Hence, the solution of equation (2.49) is the reduction of the two degrees of freedom of the meridional velocity v^m to the single degree of freedom ψ via

$$\boxed{\begin{pmatrix} v^r \\ v^\theta \end{pmatrix} = \frac{1}{r^2 \sin \theta e^{2\alpha+\gamma} (\epsilon + p) u_t u^t} \begin{pmatrix} \partial_\theta \psi \\ -\partial_r \psi \end{pmatrix}} \quad (2.52)$$

This result generalizes equations (2) and (3) of [Eriguchi *et al.* \(1986\)](#).

2.9.2. Relativistic Euler equation as result of an orthogonal projection

2.9.2.1. Compact form

The relativistic Euler equation is the result of projecting equation (2.39) orthogonally to the 4-velocity u^α , i.e.

$$q_\gamma^\alpha \nabla_\beta T^{\beta\gamma} = 0$$

Using equations (2.41) and (2.43), we find

$$\begin{aligned} 0 &= q_\gamma^\alpha \nabla_\beta (\epsilon u^\beta u^\gamma + p q^{\beta\gamma}) \\ &= q_\gamma^\alpha \epsilon u^\beta \nabla_\beta u^\gamma + q^{\alpha\beta} \nabla_\beta p + q_\gamma^\alpha p \nabla_\beta (u^\beta u^\gamma) \\ &= g_\gamma^\alpha \epsilon u^\beta \nabla_\beta u^\gamma + q^{\alpha\beta} \nabla_\beta p + g_\gamma^\alpha u^\beta p \nabla_\beta u^\gamma \\ &= \epsilon u^\beta \nabla_\beta u^\alpha + q^{\alpha\beta} \nabla_\beta p + p u^\beta \nabla_\beta u^\alpha \end{aligned}$$

2. Theory

This leads to

$$\boxed{(\epsilon + p) u^\beta \nabla_\beta u^\alpha = -q^{\alpha\beta} \nabla_\beta p} \quad (2.53)$$

according to [Friedman & Stergioulas](#).

2.9.2.2. Expanded form of temporal component

Equation (2.53) can be expanded as

$$\begin{aligned} 0 &= (\epsilon + p) u^\beta \nabla_\beta u^\alpha + q_\alpha^\beta \nabla_\beta p \\ &= (\epsilon + p) u^\beta \left(\partial_\beta u^\alpha - \Gamma_{\beta\alpha}^\gamma u^\gamma \right) + \left(\delta_\alpha^\beta + u_\alpha u^\beta \right) \partial_\beta p \\ &= (\epsilon + p) \left(u^\beta \partial_\beta u^\alpha - \Gamma_{\beta\gamma\alpha} u^\beta u^\gamma \right) + \partial_\alpha p + u_\alpha u^\beta \partial_\beta p \\ &= (\epsilon + p) \left[u^m \partial_m u_\alpha - \frac{1}{2} (\partial_\gamma g_{\beta\alpha} + \partial_\alpha g_{\gamma\beta} - \partial_\beta g_{\gamma\alpha}) u^\beta u^\gamma \right] \\ &\quad + \partial_\alpha p + u_\alpha u^m \partial_m p \end{aligned} \quad (2.54)$$

such that

$$\frac{\partial_\alpha p + u_\alpha u^m \partial_m p}{\epsilon + p} = \frac{1}{2} u^\beta u^\gamma \partial_\alpha g_{\beta\gamma} - u^m \partial_m u_\alpha \quad (2.55)$$

The temporal component of this equation is

$$\frac{u_t u^m \partial_m p}{\epsilon + p} = -u^m \partial_m u_t$$

Using equation (2.38), it can be written as

$$\boxed{v^m \partial_m p = -(\epsilon + p) v^m \partial_m \ln u_t} \quad (2.56)$$

2.9.2.3. Azimuthal component

Expanded form

We obtain the spatial components of equation (2.55) by setting $\alpha = a$:

$$\frac{\partial_a p}{\epsilon + p} = \frac{1}{2} \partial_a g_{\beta\gamma} u^\beta u^\gamma - u^m \partial_m u_a - \frac{u_a u^m \partial_m p}{\epsilon + p}$$

Using the temporal component (2.56) of the relativistic Euler equation, we rewrite the spatial components to

$$\begin{aligned} \frac{\partial_a p}{\epsilon + p} &= \frac{1}{2} u^\beta u^\gamma \partial_a g_{\beta\gamma} - u^m \partial_m u_a + \frac{u_a}{u_t} u^m \partial_m u_t \\ &= \frac{1}{2} u^\beta u^\gamma \partial_a g_{\beta\gamma} - u_t u^m \partial_m \frac{u_a}{u_t} \end{aligned}$$

Here, it is reasonable to introduce the Lagrangian angular momentum (see, [Font & Daigne 2002](#))

$$l_\alpha = -\frac{u_\alpha}{u_t} \quad (2.57)$$

such that

$$\frac{\partial_a p}{\epsilon + p} = u_t u^m \partial_m l_a + \frac{1}{2} u^\beta u^\gamma \partial_a g_{\beta\gamma} \quad (2.58)$$

Setting $a = \phi$ and taking axisymmetry into account, we see that the azimuthal component of this equation is

$$\boxed{v^m \partial_m l_\phi = 0} \quad (2.59)$$

This is the general relativistic version of equation (12) of [Eriguchi *et al.* \(1986\)](#). Astonishingly, it has exactly the same form as in the Newtonian case.

Analytic solution

There are three possible solutions of equation (2.59):

- $v^m = 0$ everywhere
- $v^m \neq 0$ somewhere, but not everywhere
- $v^m \neq 0$ everywhere

Note that we perform a slightly different categorization of the solutions of equation (2.59) than [Eriguchi *et al.* \(1986\)](#) and [Eriguchi & Müller \(1991\)](#). In the first case, there is no meridional fluid motion, but merely an azimuthal one. This scenario has already been extensively investigated by N. Stergioulas with the RNS code. Therefore, we are not interested in that possibility. The second case is that there is a meridional fluid motion, but not everywhere in the neutron star. In this thesis, we do not investigate such solutions nor do we analyze whether they exist at all. Instead, we focus on the third possibility where there is a meridional fluid motion everywhere. In that case, we have to choose the ϕ -component l_ϕ of the Lagrangian angular momentum in such a manner that equation (2.59) is obeyed. For that purpose, we rewrite the meridional fluid velocity v^m in terms of the stream function ψ using the result (2.52):

$$\partial_\theta \psi \partial_r l_\phi - \partial_r \psi \partial_\theta l_\phi = 0$$

This equation is solved by

$$\boxed{l_\phi = L(\psi)} \quad (2.60)$$

in which $L(\psi)$ is an arbitrary function of the stream function ψ .

2.9.2.4. Meridional components

Expanded form

We obtain the meridional components of equation (2.58) by setting $a = m$:

$$\frac{\partial_m p}{\epsilon + p} = u_t u^n \partial_n l_m + \frac{1}{2} u^\alpha u^\beta \partial_m g_{\alpha\beta} \quad (2.61)$$

In the following, we will write these components in a manner similar to equations (7) and (8) of [Eriguchi *et al.* \(1986\)](#). For that purpose, we expand

$$\begin{aligned} u^n \partial_n l_m &= \begin{pmatrix} (u^r \partial_r + u^\theta \partial_\theta) l_r \\ (u^r \partial_r + u^\theta \partial_\theta) l_\theta \end{pmatrix} \\ &= \begin{pmatrix} u^\theta (\partial_\theta l_r - \partial_r l_\theta) + u^r \partial_r l_r + u^\theta \partial_r l_\theta \\ -u^r (\partial_\theta l_r - \partial_r l_\theta) + u^r \partial_\theta l_r + u^\theta \partial_\theta l_\theta \end{pmatrix} \\ &= r \begin{pmatrix} u^\theta \\ -u^r \end{pmatrix} w - u^n \partial_m \begin{pmatrix} u_n \\ u_t \end{pmatrix} \end{aligned} \quad (2.62)$$

2. Theory

with

$$w = \frac{1}{r} (\partial_\theta l_r - \partial_r l_\theta) \quad (2.63)$$

The ancillary field w is defined in such a way that its Newtonian limit is equal to the quantity ‘ ω ’ defined in [Eriguchi *et al.* \(1986\)](#). Unfortunately, we cannot use the same symbol here, because in equation (2.37) we have introduced $\omega = m_\alpha N^\alpha$, following the conventions of [Gourgoulhon & Bonazzola \(1993\)](#).

Next, we rewrite

$$u_t u^n \partial_m \left(\frac{u_n}{u_t} \right) = u^n \partial_m u_n + u_t u^n u_n \partial_m \frac{1}{u_t}$$

Using the 4-velocity constraint $u_t u^t + u_m u^m + u_\phi u^\phi = -1$, the second term on the right hand side of this equation becomes

$$u_t u^n u_n \partial_m \frac{1}{u_t} = -u_t \left(1 + u_t u^t + u_\phi u^\phi \right) \partial_m \frac{1}{u_t} = \left(\frac{1}{u_t} + u^t \right) \partial_m u_t - u_t u_\phi u^\phi \partial_m \frac{1}{u_t}$$

That way, we get

$$\begin{aligned} u_t u^n \partial_m \left(\frac{u_n}{u_t} \right) &= \partial_m \ln u_t + u^\alpha \partial_m u_\alpha - u^\phi \partial_m u_\phi - u_t u_\phi u^\phi \partial_m \frac{1}{u_t} \\ &= \partial_m \ln u_t + u^\alpha \partial_m \left(g_{\alpha\beta} u^\beta \right) - u_t u^\phi \partial_m \frac{u_\phi}{u_t} \end{aligned}$$

Here, the 4-velocity constraint, written as $g_{\alpha\beta} u^\alpha u^\beta = -1$, allows us to transform the second term to

$$u^\alpha \partial_m \left(g_{\alpha\beta} u^\beta \right) = u^\alpha u^\beta \partial_m g_{\alpha\beta} + \frac{1}{2} g_{\alpha\beta} \partial_m \left(u^\alpha u^\beta \right) = \frac{1}{2} u^\alpha u^\beta \partial_m g_{\alpha\beta}$$

Therefore, we arrive at

$$-u_t u^n \partial_m \left(\frac{u_n}{u_t} \right) + \frac{1}{2} u^\alpha u^\beta \partial_m g_{\alpha\beta} = -\partial_m \ln u_t + u_t u^\phi \partial_m \frac{u_\phi}{u_t} \quad (2.64)$$

Eventually, we use the two results (2.62) and (2.64) in equation (2.61). This leads to

$$\boxed{\frac{1}{2} \partial_m \ln (u_t)^2 + \frac{\partial_m p}{\epsilon + p} = r u_t \begin{pmatrix} u^\theta \\ -u^r \end{pmatrix} w - u_t u^\phi \partial_m l_\phi} \quad (2.65)$$

which is the general relativistic version of the two equations (7) and (8) of [Eriguchi *et al.* \(1986\)](#).

Solenoidal part

In order to solve equation (2.65), we proceed similar to [Eriguchi *et al.* \(1986\)](#) in the Newtonian limit. For that purpose, we extend equation (15) of [Eriguchi *et al.* \(1986\)](#) to general relativity with the help of equation (2.52). We recall $v^a = u^a / u^t$ and begin with

$$\begin{aligned} &\partial_r^2 \psi + \frac{\sin \theta}{r^2} \partial_\theta \left(\frac{1}{\sin \theta} \partial_\theta \psi \right) \\ &= \sin \theta \left\{ -\partial_r \left[r^2 e^{2\alpha+\gamma} (\epsilon + p) u_t u^\theta \right] + \partial_\theta \left[e^{2\alpha+\gamma} (\epsilon + p) u_t u^r \right] \right\} \end{aligned} \quad (2.66)$$

On the right hand side of this relation, we use the decompositions (2.12) and (2.18) to rewrite

$$u^m = g^{m\alpha} u_\alpha = \left(k^{mn} + \frac{M^m M^n}{M^2} - \frac{N^m N^n}{N^2} \right) u_n - \frac{N^m}{N^2} u_t + \left(\frac{M^m}{M^2} - \frac{N^m N^\phi}{N^2} \right) u_\phi$$

In order to make the resulting equation more compact, we introduce the 2-vector (note that below $o \in \{r, \theta\}$ is an index and not a zero)

$$c_m = u_t e^\gamma (\epsilon + p) k_{mn} \left[(m^n m^o - n^n n^o) u_o - n^t n^n u_t + (m^n m^\phi - n^n n^\phi) u_\phi \right]$$

such that

$$u^m = k^{mn} \left[-u_t l_n + \frac{e^{-\gamma}}{u_t (\epsilon + p)} c_n \right] \quad (2.67)$$

Then, equation (2.19) allows us to compute

$$\begin{aligned} \partial_r \left[r^2 e^{2\alpha+\gamma} (\epsilon + p) u_t u^\theta \right] &= \partial_r \left\{ e^\gamma (\epsilon + p) u_t \left[-u_t l_\theta + \frac{e^{-\gamma}}{u_t (\epsilon + p)} c_\theta \right] \right\} \\ &= -\partial_r \left[e^\gamma (\epsilon + p) (u_t)^2 l_\theta \right] + \partial_r c_\theta \end{aligned}$$

and in a similar manner

$$\begin{aligned} \partial_\theta \left[e^{2\alpha+\gamma} (\epsilon + p) u_t u^r \right] &= \partial_\theta \left\{ e^\gamma (\epsilon + p) u_t \left[-u_t l_r + \frac{e^{-\gamma}}{u_t (\epsilon + p)} c_r \right] \right\} \\ &= -\partial_\theta \left[e^\gamma (\epsilon + p) (u_t)^2 l_r \right] + \partial_\theta c_r \end{aligned}$$

Inserting these two results into equation (2.66), one finds

$$\begin{aligned} &\partial_r^2 \psi + \frac{\sin \theta}{r^2} \partial_\theta \left(\frac{1}{\sin \theta} \partial_\theta \psi \right) \\ &= \sin \theta \left\{ -e^\gamma (\epsilon + p) (u_t)^2 \partial_r (-l_\theta) - (-l_\theta) \partial_r \left[e^\gamma (\epsilon + p) (u_t)^2 \right] \right. \\ &\quad \left. + e^\gamma (\epsilon + p) (u_t)^2 \partial_\theta (-l_r) + (-l_r) \partial_\theta \left[e^\gamma (\epsilon + p) (u_t)^2 \right] + \partial_\theta c_r - \partial_r c_\theta \right\} \end{aligned}$$

The Lagrangian angular momentum l_m appears four times on the right hand side. For the two occurrences without derivatives in front, we revert equation (2.67) to

$$l_m = -\frac{1}{u_t} \left[k_{mn} u^n - \frac{e^{-\gamma}}{u_t (\epsilon + p)} c_m \right]$$

That way, using the abbreviation (2.63), we obtain

$$\begin{aligned} &\partial_r^2 \psi + \frac{\sin \theta}{r^2} \partial_\theta \left(\frac{1}{\sin \theta} \partial_\theta \psi \right) \\ &= -r \sin \theta e^\gamma (\epsilon + p) (u_t)^2 w + \sin \theta (\partial_\theta c_r - \partial_r c_\theta) \\ &\quad \frac{\sin \theta}{u_t} \left\{ - \left[k_{\theta n} u^n - \frac{e^{-\gamma}}{u_t (\epsilon + p)} c_\theta \right] \partial_r + \left[k_{r n} u^n - \frac{e^{-\gamma}}{u_t (\epsilon + p)} c_r \right] \partial_\theta \right\} \left[e^\gamma (\epsilon + p) (u_t)^2 \right] \end{aligned}$$

2. Theory

Here, we focus on the last line. We use equations (2.19) and (2.52) to rewrite

$$k_{\theta n} u^n - \frac{e^{-\gamma}}{u_t (\epsilon + p)} c_\theta = u^t r^2 e^{2\alpha} v^\theta - \frac{e^{-\gamma}}{u_t (\epsilon + p)} c_\theta = -\frac{e^{-\gamma}}{u_t (\epsilon + p)} \left(\frac{\partial_r \psi}{\sin \theta} + c_\theta \right)$$

and

$$k_{rn} u^n - \frac{e^{-\gamma}}{u_t (\epsilon + p)} c_r = u^t e^{2\alpha} v^r - \frac{e^{-\gamma}}{u_t (\epsilon + p)} c_r = \frac{e^{-\gamma}}{u_t (\epsilon + p)} \left(\frac{\partial_\theta \psi}{r^2 \sin \theta} - c_r \right)$$

Hence, we arrive at the general relativistic extension

$$\begin{aligned} & \partial_r^2 \psi + \frac{\sin \theta}{r^2} \partial_\theta \left(\frac{1}{\sin \theta} \partial_\theta \psi \right) \\ &= -e^\gamma (\epsilon + p) (u_t)^2 r \sin \theta w + \sin \theta (\partial_\theta c_r - \partial_r c_\theta) \\ &+ \left[(\partial_r \psi + c_\theta \sin \theta) \partial_r + \left(\frac{\partial_\theta \psi}{r^2} - c_r \sin \theta \right) \partial_\theta \right] \ln \left[e^\gamma (\epsilon + p) (u_t)^2 \right] \quad (2.68) \end{aligned}$$

of equation (15) of [Eriguchi *et al.* \(1986\)](#).

The next step is to use the function

$$\chi = \chi(r, \theta, \phi) = \frac{\psi \cos \phi}{r \sin \theta}$$

of equation (16) of [Eriguchi *et al.* \(1986\)](#). Note that the field χ is correlated to the basic matter field χ_0 by

$$\chi_0(r, \theta) = \chi(r, \theta, 0)$$

Then, we find that the first squared bracket in the last line of equation (2.68) takes the form

$$\begin{aligned} & (\partial_r \psi + c_\theta \sin \theta) \partial_r + \left(\frac{\partial_\theta \psi}{r^2} - c_r \sin \theta \right) \partial_\theta \\ &= \frac{r \sin \theta}{\cos \phi} \left\{ \left[\frac{\partial_r (r\chi)}{r} + \frac{c_\theta}{r} \cos \phi \right] \partial_r + \frac{1}{r^2} \left[\frac{\partial_\theta (\sin \theta \chi)}{\sin \theta} - r c_r \cos \phi \right] \partial_\theta \right\} \end{aligned}$$

such that

$$\begin{aligned} & \partial_r^2 \psi + \frac{\sin \theta}{r^2} \partial_\theta \left(\frac{1}{\sin \theta} \partial_\theta \psi \right) \\ &= \frac{r \sin \theta}{\cos \phi} \left\{ -e^\gamma (\epsilon + p) (u_t)^2 w \cos \phi + \frac{\cos \phi}{r} (\partial_\theta c_r - \partial_r c_\theta) \right. \\ &\quad + \left[\left(\partial_r \chi + \frac{\chi}{r} + \frac{c_\theta}{r} \cos \phi \right) \partial_r \right. \\ &\quad \left. \left. + \frac{1}{r^2} (\partial_\theta \chi + \cot \theta \chi - r c_r \cos \phi) \partial_\theta \right] \ln \left[e^\gamma (\epsilon + p) (u_t)^2 \right] \right\} \end{aligned}$$

We compare this result with equations (17) and (18) of [Eriguchi *et al.* \(1986\)](#). That way, it is obvious that these two equations have to be generalized to

$$\begin{aligned}
\Delta (\chi_0 \cos \phi) &= S_{\chi_0} \cos \phi & (2.69) \\
S_{\chi_0} &= -e^\gamma (\epsilon + p) (u_t)^2 w + \frac{1}{r} (\partial_\theta c_r - \partial_r c_\theta) \\
&\quad + \left[\left(\partial_r \chi_0 + \frac{\chi_0}{r} + \frac{c_\theta}{r} \right) \partial_r \right. \\
&\quad \left. + \frac{1}{r^2} (\partial_\theta \chi_0 + \cot \theta \chi_0 - r c_r) \right] \partial_\theta \ln \left[e^\gamma (\epsilon + p) (u_t)^2 \right]
\end{aligned}$$

Note that the expression $S_{\chi_0} \cos \phi$ introduced above corresponds to the quantity ‘ $T(r, \theta, \phi)$ ’ defined in [Eriguchi *et al.* \(1986\)](#).

Finally, we have to constrain the quantity w similarly to equation (13) of [Eriguchi *et al.* \(1986\)](#) in such a manner that the solenoidal part of equation (2.65) vanishes. For that purpose, we restrict ourselves to a **barotropic equation of state**, from now on. This means that the total energy density ϵ is a function $\epsilon(p)$ of the pressure p only. The advantage of this limitation is that then the left hand side of equation (2.65) is a mere gradient field and therefore its solenoidal part is zero. As a result, the solenoidal part on the right hand side has to vanish, too. We achieve this by choosing the quantity w appropriately. With this in mind, we use equations (2.52) and (2.60) to rewrite the right hand side of equation (2.65) to

$$\begin{aligned}
r u_t \begin{pmatrix} u^\theta \\ -u^r \end{pmatrix} w - u_t u^\phi \partial_m l_\phi &= -\frac{w}{r \sin \theta e^{2\alpha+\gamma} (\epsilon + p)} \partial_m \psi - u_t u^\phi \partial_m L(\psi) \\
&= -\left[\frac{w}{r \sin \theta e^{2\alpha+\gamma} (\epsilon + p)} + u_t u^\phi L'(\psi) \right] \partial_m \psi & (2.70)
\end{aligned}$$

The solenoidal part vanishes if the expression in the squared bracket is a mere function of the stream function ψ . We call this function $f(\psi)$ such that

$$\boxed{w = e^{2\alpha+\gamma} (\epsilon + p) r \sin \theta (f(\psi) - u_t u^\phi L'(\psi))} \quad (2.71)$$

This is the generalization of equation (13) of [Eriguchi *et al.* \(1986\)](#).

Gradient part

Inserting (2.71) into equation (2.70) gives

$$r u_t \begin{pmatrix} u^\theta \\ -u^r \end{pmatrix} w - u_t u^\phi \partial_m l_\phi = -f(\psi) \partial_m \psi$$

Thus, equation (2.65) becomes

$$\frac{1}{2} \partial_m \ln (u_t)^2 + \frac{\partial_m p}{\epsilon + p} + f(\psi) \partial_m \psi = 0$$

Due to the limitation to the barotropic case, i.e. $\epsilon = \epsilon(p)$, we can integrate this equation to

$$\boxed{\frac{1}{2} \ln (u_t)^2 + \int_0^p \frac{dp'}{\epsilon(p') + p'} + \int_0^\psi d\psi' f(\psi') = C} \quad (2.72)$$

with an arbitrary integration constant C . This the generalization of equation (14) of [Eriguchi *et al.* \(1986\)](#).

2. Theory

Analytic solution of gradient part

In order to solve equation (2.72), we introduce the heat function (see, e.g., [Friedman & Stergioulas](#))

$$H(p) = \int_0^p \frac{dp'}{\epsilon(p') + p'}$$

and the ancillary function

$$I(\psi) = \int_0^\psi d\psi' f(\psi')$$

Then, we can simplify equation (2.72) to

$$\frac{1}{2} \ln(u_t)^2 + H(p) + I(\psi) = C$$

The constant C is fixed by the requirement

$$\frac{1}{2} \ln(u_t^c)^2 + H(p_c) + I(\psi_c) = C$$

with the central pressure p_c , the central stream function ψ_c and the central covariant temporal component u_t^c of the 4-velocity. Due to $\epsilon \geq 0$, the heat function $H(p)$ is invertible such that we then get the solution

$$\boxed{p = H^{-1} \left(H(p_c) + \frac{1}{2} \ln(u_t^c)^2 - \frac{1}{2} \ln(u_t)^2 + I(\psi_c) - I(\psi) \right)} \quad (2.73)$$

2.9.3. Velocity v^a

In section 2.7.2.1, we have expressed the three degrees of freedom of the 4-velocity u^α in terms of the 3-velocity $v^a = u^a/u^t$. We will now explain how the velocity v^a can be computed from the basic fields. For that purpose, we have a closer look at equation (2.52). The fields α , ϵ , p and ψ appearing on the right hand side of this equation are basic fields. The ancillary field γ is the sum of the basic geometry fields β and ν . Thus, only the 4-velocity components u_t and u^t are an obstacle for a straightforward computation of the meridional velocity v^m from the basic fields. In contrast to the Newtonian limit, where the components u_t and u^t are equal to unity, general relativity leads to contributions of the meridional velocity v^m , hidden in the components u_t and u^t . In the following, we will therefore rewrite equation (2.52) in such a manner that the meridional velocity v^m appears only on the left hand side.

In order to rewrite equation (2.52), we have to address the azimuthal velocity v^ϕ first. This velocity component can be expressed in terms of the meridional velocity v^m . For that purpose, we expand the ϕ -component of definition (2.57) to

$$l_\phi = -\frac{u_\phi}{u_t} = -\frac{g_{\phi\alpha}v^\alpha}{g_{t\beta}v^\beta} = -\frac{g_{\phi t} + g_{\phi m}v^m + g_{\phi\phi}v^\phi}{g_{tt} + g_{tn}v^n + g_{t\phi}v^\phi}$$

such that

$$v^\phi = -\frac{g_{t\phi} + g_{m\phi}v^m + (g_{tt} + g_{tm}v^m)l_\phi}{g_{\phi\phi} + g_{t\phi}l_\phi}$$

or

$$\boxed{v^\phi = A_1 + A_{2r}v^r + A_{2\theta}v^\theta} \quad (2.74)$$

with the abbreviations

$$A_1 = -\frac{g_{t\phi} + g_{tt}l_\phi}{g_{\phi\phi} + g_{t\phi}l_\phi} \stackrel{\text{SR}}{=} 0$$

and

$$A_{2m} = -\frac{g_{m\phi} + g_{tm}l_\phi}{g_{\phi\phi} + g_{t\phi}l_\phi} \stackrel{\text{SR}}{=} 0$$

Further below, we will have to investigate the values of several quantities, like A_1 and A_{2m} , in the special relativistic case under the assumptions $l_\phi = 0$ and $\partial_r\psi = 0$. Therefore, we will always compute the values of such quantities in the special relativistic case, and we denote this by $\stackrel{\text{SR}}{=}$, as done in the above two definitions.

Next, we consider the component v^θ . With this in mind, we introduce the quantity

$$A_3^m = \frac{1}{r^2 \sin\theta e^{2\alpha+\gamma} (\epsilon + p)} \begin{pmatrix} \partial_\theta\psi \\ -\partial_r\psi \end{pmatrix} \stackrel{\text{SR}}{=} \delta_r^m A_3^r \quad (2.75)$$

Then, equation (2.52) allows us to express the component v^θ as

$$\boxed{v^\theta = \frac{A_3^\theta}{A_3^r} v^r} \quad (2.76)$$

Eventually, we address the radial velocity component v^r . In order to simplify the following computations, we introduce the quantity

$$A_4 = \frac{A_3^\theta}{A_3^r} \stackrel{\text{SR}}{=} 0$$

Then, we can write

$$v^\theta = A_4 v^r \quad (2.77)$$

Using this result, we express equation (2.74) as

$$v^\phi = A_1 + A_5 v^r \quad (2.78)$$

with

$$A_5 = A_{2r} + A_{2\theta} A_4 \stackrel{\text{SR}}{=} 0$$

Next, we use (2.75) to write equation (2.52) as

$$A_3^m = u_t u^t v^m = g_{t\alpha} (u^t)^2 v^\alpha v^m$$

On the very right hand side of the above line, the 4-velocity constraint tells us

$$(u^t)^2 = -\frac{1}{g_{\alpha\beta} v^\alpha v^\beta}$$

such that we can write

$$g_{t\alpha} v^\alpha v^r + A_3^r g_{\alpha\beta} v^\alpha v^\beta = 0$$

Using equation (2.77), the first term in this relation becomes

$$g_{t\alpha} v^\alpha v^r = g_{tt} v^r + (g_{tr} + A_4 g_{t\theta}) (v^r)^2 + g_{t\phi} v^r v^\phi \quad (2.79)$$

2. Theory

and for the second one we use the expansion

$$g_{\alpha\beta}v^\alpha v^\beta = g_{tt} + 2g_{tr}v^r + 2g_{t\theta}v^\theta + 2g_{t\phi}v^\phi + g_{rr}(v^r)^2 + 2g_{r\theta}v^r v^\theta + 2g_{r\phi}v^r v^\phi + g_{\theta\theta}(v^\theta)^2 + 2g_{\theta\phi}v^\theta v^\phi + g_{\phi\phi}(v^\phi)^2$$

such that

$$g_{\alpha\beta}v^\alpha v^\beta = g_{tt} + 2(g_{tr} + A_4 g_{t\theta})v^r + 2g_{t\phi}v^\phi + \left[g_{rr} + 2A_4 g_{r\theta} + (A_4)^2 g_{\theta\theta} \right] (v^r)^2 + 2(g_{r\phi} + 2A_4 g_{\theta\phi})v^r v^\phi + g_{\phi\phi}(v^\phi)^2 \quad (2.80)$$

Then, we combine the results (2.79) and (2.80) to

$$A_3^r g_{tt} + A_6 v^r + A_7 v^\phi + A_8 (v^r)^2 + A_9 v^r v^\phi + A_{10} (v^\phi)^2 = 0 \quad (2.81)$$

with

$$\begin{aligned} A_6 &= g_{tt} + 2A_3^r (g_{tr} + A_4 g_{t\theta}) \stackrel{\text{SR}}{=} -1 \\ A_7 &= 2A_3^r g_{t\phi} \stackrel{\text{SR}}{=} 0 \\ A_8 &= g_{tr} + A_4 g_{t\theta} + A_3^r \left[g_{rr} + 2A_4 g_{r\theta} + (A_4)^2 g_{\theta\theta} \right] \stackrel{\text{SR}}{=} A_3^r \\ A_9 &= g_{t\phi} + 2A_3^r (g_{r\phi} + A_4 g_{\theta\phi}) \stackrel{\text{SR}}{=} 0 \\ A_{10} &= A_3^r g_{\phi\phi} \stackrel{\text{SR}}{=} r^2 \sin^2 \theta A_3^r \end{aligned}$$

We will now replace the v^ϕ -component with the help of equation (2.78). That way, equation (2.81) becomes

$$B_1 + B_2 v^r + B_3 (v^r)^2 = 0 \quad (2.82)$$

with

$$\begin{aligned} B_1 &= A_3^r g_{tt} + A_1 A_7 + (A_1)^2 A_{10} \stackrel{\text{SR}}{=} -A_3^r \\ B_2 &= A_6 + A_5 A_7 + A_1 A_9 + 2A_1 A_5 A_{10} \stackrel{\text{SR}}{=} -1 \\ B_3 &= A_8 + A_5 A_9 + (A_5)^2 A_{10} \stackrel{\text{SR}}{=} A_3^r \end{aligned}$$

For equation (2.82), we get

$$v^r = \frac{1}{2B_3} \left(-B_2 \pm \sqrt{(B_2)^2 - 4B_1 B_3} \right) \quad (2.83)$$

that is two solutions corresponding to the two signs \pm . In order to find the physically relevant solution, we investigate the special relativistic limit with the assumptions $l_\phi = 0$ and $\partial_r \psi = 0$. Then, we find

$$v^r \stackrel{\text{SR}}{=} \frac{1}{2A_3^r} \left(1 \pm \sqrt{1 - 4(A_3^r)^2} \right) \quad (2.84)$$

Now, we analyze what happens in the limit $\partial_\theta \psi \rightarrow 0$. Due to equation (2.75), this means

that $A_3^r \rightarrow 0$. In this limit, we find

$$\lim_{A_3^r \rightarrow 0} \frac{1}{2A_3^r} \left(1 + \sqrt{1 - 4(A_3^r)^2} \right) = \lim_{A_3^r \rightarrow 0} \frac{1}{A_3^r} = \infty$$

Therefore, the physically relevant solution of equation (2.83) is

$$v^r = -\frac{1}{2B_3} \left(B_2 + \sqrt{(B_2)^2 - 4B_1B_3} \right)$$

This result together with equation (2.76) defines the velocity component v^θ . Then, it is possible to evaluate the component v^ϕ by using equation (2.74).

2.9.4. Equation of state

We conclude the theoretical part by having a closer look at the equation of state. In Sect. 2.9.2.4, we have limited ourselves to a barotropic equation of state, where the total energy density ϵ is an arbitrary function $\epsilon(p)$ of the pressure p only. We recall that the reason for this limitation was a simplification of the solution method of the equation of general relativistic hydrodynamics. In this investigation, we perform another such simplification. We restrict ourselves to a special barotropic equation of state (it is easy to extend the GRNS code to the general barotropic case), namely a polytropic one, i.e.

$$p = K\rho^\Gamma \tag{2.85}$$

with the polytropic constant K , the rest mass density ρ and the polytropic exponent Γ . In Appendix E, we rewrite this equation to the less familiar form (E.2):

$$\epsilon = \frac{p}{\Gamma - 1} + \left(\frac{p}{K} \right)^{\frac{1}{\Gamma}} \tag{2.86}$$

This equation allows us to compute the total energy density ϵ , one of our basic matter fields.

2. *Theory*

3. Numerics

3.1. Basic fields

In Chapter 2, we have introduced the twelve basic fields

$$\nu, N^r, N^\theta, N^\phi, \beta, M^r, M^\theta, \alpha, \epsilon, p, \chi_0, l_\phi \quad (3.1)$$

These fields are governed by Einstein's field equation (2.5). For three of them, we have even found an analytic solution. Each such analytic solution allows us to explicitly compute one of the twelve basic fields under the assumption that the other eleven fields are known. The three analytic solutions are equations (2.60), (2.73) and (2.86), which solve for the Lagrangian angular momentum component l_ϕ , the pressure p and the total energy density ϵ . For the remaining nine fields

$$\nu, N^r, N^\theta, N^\phi, \beta, M^r, M^\theta, \alpha, \chi_0 \quad (3.2)$$

no analytic solution is available. However, for each of these fields there is a partial differential equation, which can be rewritten as a Poisson equation in flat space. Such equations can be solved via Green functions. That way, we will be able to compute each of the basic fields (3.2) if all other eleven basic fields are known. Eventually, all twelve basic fields together will be computed via a fixed point iteration method.

3.2. Poisson equations

In the following sections, we will state the Poisson equations. Each such equation has the structure

$$\hat{O}\Phi = S$$

in which \hat{O} , Φ and S are a Laplacian, a potential and a source, respectively. The form of these Poisson equations is not unambiguous. Instead of the potential Φ , we can choose a slightly different potential, like $r\Phi$. In that case, we get

$$\hat{O}(r\Phi) = S'$$

with some modified source S' . Unfortunately, the numerical stability of the fixed point iteration method is highly sensitive to such changes of the potential. Therefore, it is mandatory to find the appropriate way to write the Poisson equations. However, a deeper analysis of this issue would have gone beyond the scope of this investigation. Therefore, we simply experimented around, until we found the form of the equations presented below, which turns out to be numerically stable.

3. Numerics

3.2.1. Poisson equation for ν

We start with the Poisson equation for the basic field ν . This field is governed by equation (C.1). Actually, equation (C.1) originates from equation (3.11) of Gourgoulhon & Bonazzola (1993), which is of the form

$$N^{|a}{}_{|a} = \dots \quad (3.3)$$

Here, the index a runs from 1 to 3 and the vertical stroke denotes a 3-covariant derivative. Therefore, we realize that a covariant 3-scalar Laplacian is applied on the 3-lapce N . This Laplacian consists of two parts. The first one is the **axisymmetric, flat space 3-scalar Laplacian**

$$\boxed{{}^3\Delta = \partial_r^2 + \frac{1}{r^2}\partial_\theta^2 + \frac{2}{r}\partial_r + \frac{\cot\theta}{r^2}\partial_\theta} \quad (3.4)$$

This is the commonly known Laplacian $\Delta = \partial_x^2 + \partial_y^2 + \partial_z^2$ rewritten in spherical coordinates (without ϕ -derivatives). The second part are additional terms which account for the curvature of the 3-surfaces Σ_t . Moving these terms to the right hand side in equation (C.1), we find

$$\begin{aligned} & \nu_{,rr} + \frac{1}{r^2}\nu_{,\theta\theta} + \frac{2}{r}\nu_{,r} + \frac{\cot\theta}{r^2}\nu_{,\theta} \\ = & A^2 \left\{ 4\pi(E + S_a^a) + K_{ab}K^{ab} + \frac{L^2}{2} - \left[\frac{1}{A^2} + (m^r)^2 \right] (\nu_{,r})^2 - \left[\frac{1}{(rA)^2} + (m^\theta)^2 \right] (\nu_{,\theta})^2 \right. \\ & - (m^r)^2 \nu_{,rr} - 2m^r m^\theta \nu_{,r\theta} - (m^\theta)^2 \nu_{,\theta\theta} \\ & \left. - (m^r m^r{}_{,r} + m^\theta m^r{}_{,\theta}) \nu_{,r} - (m^r m^\theta{}_{,r} + m^\theta m^\theta{}_{,\theta}) \nu_{,\theta} - 2m^r m^\theta \nu_{,r}\nu_{,\theta} \right\} \\ & + \left(\frac{1}{r} - \mu_{,r} \right) \nu_{,r} + \frac{1}{r^2} (\cot\theta - \mu_{,\theta}) \nu_{,\theta} \end{aligned}$$

Then,

$$\mu = \ln(r \sin\theta) + \beta \quad (3.5)$$

which is a result of equations (2.22) and (2.29), produces

$$\boxed{\begin{aligned} {}^3\Delta\nu &= S_\nu & (3.6) \\ S_\nu &= A^2 \left\{ 4\pi(E + S_a^a) + K_{ab}K^{ab} + \frac{L^2}{2} - \left[\frac{1}{A^2} + (m^r)^2 \right] (\nu_{,r})^2 \right. \\ & - \left[\frac{1}{(rA)^2} + (m^\theta)^2 \right] (\nu_{,\theta})^2 - (m^r)^2 \nu_{,rr} - 2m^r m^\theta \nu_{,r\theta} - (m^\theta)^2 \nu_{,\theta\theta} \\ & \left. - (m^r m^r{}_{,r} + m^\theta m^r{}_{,\theta}) \nu_{,r} - (m^r m^\theta{}_{,r} + m^\theta m^\theta{}_{,\theta}) \nu_{,\theta} - 2m^r m^\theta \nu_{,r}\nu_{,\theta} \right\} \\ & - \beta_{,r}\nu_{,r} - \frac{\beta_{,\theta}\nu_{,\theta}}{r^2} \end{aligned}}$$

This is a Poisson equation consisting of the Laplacian ${}^3\Delta$, the potential ν and the source S_ν .

3.2.2. Poisson equations for N^a

The 3-shift N^a is determined by equations (C.2), (C.3) and (C.4). These three equations arise from equation (3.12) of Gourgoulhon & Bonazzola (1993), which starts with

$$N^{a|b}{}_b = \dots$$

So, in contrast to the covariant 3-scalar Laplacian of equation (3.3), we now encounter a covariant 3-vector Laplacian. The analog in flat space, the flat space 3-vector Laplacian, has the usual form ${}^c\Delta^a{}_b = (\partial_x^2 + \partial_y^2 + \partial_z^2) \text{diag}(1, 1, 1)$ in Cartesian coordinates (denoted by the index c), in which Cartesian coordinates are correlated to spherical ones via $x = r \sin \theta \cos \phi$, $y = r \sin \theta \sin \phi$ and $z = r \cos \theta$. However, in spherical coordinates, its form is not very widely known. Therefore, we briefly repeat the computation of the Laplacian in these coordinates. For that purpose, we consider an arbitrary 3-vector potential Φ^a , and then we find

$$\begin{aligned} & h^{bc} \Phi^a{}_{|bc} \\ = & h^{bc} \left[\partial_b \left(\partial_c \Phi^a + {}^3\Gamma_{cd}^a \Phi^d \right) - {}^3\Gamma_{bc}^e \left(\partial_e \Phi^a + {}^3\Gamma_{ed}^a \Phi^d \right) + {}^3\Gamma_{be}^a \left(\partial_e \Phi^e + {}^3\Gamma_{cd}^e \Phi^d \right) \right] \\ = & {}^3\Delta_b^a \Phi^b \end{aligned} \quad (3.7)$$

Choosing the flat space 3-metric

$$h_{ab} = \begin{pmatrix} 1 & 0 & 0 \\ 0 & r^2 & 0 \\ 0 & 0 & r^2 \sin^2 \theta \end{pmatrix}$$

and additionally assuming axisymmetry, the quantity ${}^3\Delta_b^a$ becomes what we call **axisymmetric, flat space 3-vector Laplacian**. A somewhat lengthy but still straightforward computation leads to the result

$${}^3\Delta^a{}_b = \begin{pmatrix} {}^3\Delta - \frac{2}{r^2} & -\frac{2}{r} \partial_\theta - 2 \frac{\cot \theta}{r} & 0 \\ \frac{2}{r^3} \partial_\theta & {}^3\Delta + \frac{2}{r} \partial_r + \frac{1 - \cot^2 \theta}{r^2} & 0 \\ 0 & 0 & {}^3\Delta + \frac{2}{r} \partial_r + 2 \frac{\cot \theta}{r^2} \partial_\theta \end{pmatrix} \quad (3.8)$$

Therefore, we have to extract this Laplacian from equations (C.2), (C.3) and (C.4). In order to do this, we rewrite equation (2.22) to $M = r \sin \theta e^\beta$. Then, we compute

$$M_{,\theta} = r e^\beta (\cos \theta + \sin \theta \beta_{,\theta})$$

such that

$$\frac{M_{,\theta r}}{M} = \frac{\cot \theta}{r} + \frac{1}{r} \beta_{,\theta} + \cot \theta \beta_{,r} + \beta_{,r\theta} + \beta_{,r} \beta_{,\theta}$$

and

$$\frac{M_{,\theta\theta}}{M} = -1 + 2 \cot \theta \beta_{,\theta} + \beta_{,\theta\theta} + (\beta_{,\theta})^2$$

3. Numerics

Using these two results together with $\mu = \ln(r \sin \theta) + \beta$ and the commutativity of partial derivatives, we rewrite

$$\begin{aligned}
& \left[\frac{1}{A^2} - (m^r)^2 \right] \frac{M_{,r\theta}}{M} + \left[\frac{1}{A^2} + (m^r)^2 \right] \mu_{,r}\mu_{,\theta} \\
&= \left[\frac{1}{A^2} - (m^r)^2 \right] \left(\frac{\cot \theta}{r} + \frac{1}{r} \beta_{,\theta} + \cot \theta \beta_{,r} + \beta_{,r\theta} + \beta_{,r}\beta_{,\theta} \right) \\
&\quad + \left[\frac{1}{A^2} + (m^r)^2 \right] \left(\frac{1}{r} + \beta_{,r} \right) (\cot \theta + \beta_{,\theta}) \\
&= \frac{1}{A^2} \left(2 \frac{\cot \theta}{r} + \frac{2}{r} \beta_{,\theta} + 2 \cot \theta \beta_{,r} + \beta_{,r\theta} + 2 \beta_{,r}\beta_{,\theta} \right) - (m^r)^2 \beta_{,r\theta}
\end{aligned}$$

in equation (C.2) and

$$\begin{aligned}
& \left[\frac{1}{(rA)^2} + (m^\theta)^2 \right] (\mu_{,\theta})^2 + \left[\frac{1}{(rA)^2} - (m^\theta)^2 \right] \frac{M_{,\theta\theta}}{M} \\
&= \left[\frac{1}{(rA)^2} + (m^\theta)^2 \right] (\cot \theta + \beta_{,\theta})^2 \\
&\quad + \left[\frac{1}{(rA)^2} - (m^\theta)^2 \right] \left[-1 + 2 \cot \theta \beta_{,\theta} + \beta_{,\theta\theta} + (\beta_{,\theta})^2 \right] \\
&= \frac{1}{(rA)^2} \left[\cot^2 \theta + 4 \cot \theta \beta_{,\theta} + 2 (\beta_{,\theta})^2 - 1 + \beta_{,\theta\theta} \right] + (m^\theta)^2 (\cot^2 \theta + 1 - \beta_{,\theta\theta})
\end{aligned}$$

in (C.3). In the latter equation, we also reformulate

$$\begin{aligned}
& \left(\frac{2}{r^3 A^2} - \frac{1}{(rA)^2} \mu_{,r} \right) \mu_{,\theta} - \frac{1}{(rA)^2} \frac{M_{,r\theta}}{M} \\
&= \frac{1}{(rA)^2} \left\{ \left[\frac{2}{r} - \left(\frac{1}{r} + \beta_{,r} \right) \right] (\cot \theta + \beta_{,\theta}) - \left(\frac{\cot \theta}{r} + \frac{1}{r} \beta_{,\theta} + \cot \theta \beta_{,r} + \beta_{,r\theta} + \beta_{,r}\beta_{,\theta} \right) \right\} \\
&= -\frac{1}{(rA)^2} (2 \cot \theta \beta_{,r} + \beta_{,r\theta} + 2 \beta_{,r}\beta_{,\theta})
\end{aligned}$$

in order to avoid a numerical instability, which otherwise turned out to appear in our simulation. That way, we eventually arrive at the 3-vector Poisson equation

$$\boxed{{}^3\Delta^a{}_b N^b = S_N^a} \tag{3.9}$$

where the rather lengthy expressions for the sources S_N^a are given in Appendix F.

3.2.3. Poisson equation for β

In order to compute the basic field β , we have to solve equation (C.5). This equation originates from equation (3.13) of [Gourgoulhon & Bonazzola \(1993\)](#), which has the form

$$(MN) \parallel_m^m = \dots$$

Here, we have the covariant 2-scalar Laplacian. Hence, we have to identify the **flat space 2-scalar Laplacian**

$$\boxed{{}^2\Delta = \partial_r^2 + \frac{\partial_\theta^2}{r^2} + \frac{1}{r}\partial_r} \quad (3.10)$$

in equation (C.5). This is an easy task, because the Laplacian ${}^2\Delta$ is directly applied to the product MN in that equation, which gives the terms

$$(MN)_{,rr} + \frac{1}{r}(MN)_{,r} + \frac{1}{r^2}(MN)_{,\theta\theta}$$

However, a problem occurs in the context of the Green function iteration process. Even though we set the product MN to a positive value at the initial step of the iteration, the Green function iteration method does not guarantee that positivity is conserved. Therefore, at later iteration steps, the product MN might become negative. We have to avoid such outcomes, because physically reasonable lapse functions are always positive. Therefore, we cannot use MN as the potential of the sought Poisson equation, instead we have to use a modified potential. For that purpose, we use equations (2.21), (2.22) and (2.46) to rewrite

$$MN = r \sin \theta e^{\beta+\nu} = r \sin \theta e^\gamma$$

Then, we get the first derivatives

$$(MN)_{,r} = \left[(r \sin \theta \gamma)_{,r} + \sin \theta (1 - \gamma) \right] e^\gamma$$

and

$$(MN)_{,\theta} = \left[(r \sin \theta \gamma)_{,\theta} + r \cos \theta (1 - \gamma) \right] e^\gamma$$

such that the second derivatives are

$$(MN)_{,rr} = \left[(r \sin \theta \gamma)_{,rr} + (r \sin \theta \gamma)_{,r} \gamma_{,r} - \sin \theta \gamma_{,r} + \sin \theta (1 - \gamma) \gamma_{,r} \right] e^\gamma$$

and

$$\begin{aligned} & (MN)_{,\theta\theta} \\ = & \left[(r \sin \theta \gamma)_{,\theta\theta} + (r \sin \theta \gamma)_{,\theta} \gamma_{,\theta} - r \sin \theta (1 - \gamma) - r \cos \theta \gamma_{,\theta} + r \cos \theta (1 - \gamma) \gamma_{,\theta} \right] e^\gamma \end{aligned}$$

As a result of all these derivatives, we find

$$\begin{aligned} & (MN)_{,rr} + \frac{1}{r}(MN)_{,r} + \frac{1}{r^2}(MN)_{,\theta\theta} \\ = & e^\gamma \left\{ (r \sin \theta \gamma)_{,rr} + \frac{1}{r^2} (r \sin \theta \gamma)_{,\theta\theta} + \frac{1}{r} (r \sin \theta \gamma)_{,r} \right. \\ & \quad \left. + (r \sin \theta \gamma)_{,r} \gamma_{,r} - \sin \theta \gamma_{,r} + \frac{1}{r} \sin \theta (1 - \gamma) \right. \\ & \quad \left. + \frac{1}{r^2} \left[(r \sin \theta \gamma)_{,\theta} \gamma_{,\theta} - r \sin \theta (1 - \gamma) - r \cos \theta \gamma_{,\theta} \right] \right\} \end{aligned}$$

With the help of equation (3.10), we can then write

$$(MN)_{,rr} + \frac{1}{r}(MN)_{,r} + \frac{1}{r^2}(MN)_{,\theta\theta} = e^\gamma \left\{ {}^2\Delta (r \sin \theta \gamma) + r \sin \theta \left[(\gamma_r)^2 + \frac{1}{r^2} (\gamma_\theta)^2 \right] \right\}$$

3. Numerics

On the right hand side of this relation, the Laplacian ${}^2\Delta$ is applied on the expression $r \sin \theta \gamma$. This quantity leads to physically reasonable configurations even if it is negative. Therefore, we use $r \sin \theta \gamma$ (this quantity also appears on the left hand side of equation (24) of Komatsu *et al.* (1989)) as the sought modified potential. That way, equation (C.5) becomes

$$\begin{aligned}
 {}^2\Delta [r \sin \theta (\beta + \nu)] &= S_\beta \\
 S_\beta &= \frac{A^2}{e^\gamma} \left\{ 8\pi MN s_m^m - 2\kappa_r [M, q]^r - 2\kappa_\theta [M, q]^\theta \right. \\
 &\quad - M (q^r + \omega m^r) \kappa_{,r} - M (q^\theta + \omega m^\theta) \kappa_{,\theta} \\
 &\quad \left. + MN (\kappa_{mn} \kappa^{mn} + \kappa^2 - L_{mn} L^{mn}) \right\} \\
 &\quad - r \sin \theta \left[(\gamma_r)^2 + \frac{1}{r^2} (\gamma_\theta)^2 \right]
 \end{aligned} \tag{3.11}$$

3.2.4. Poisson equations for M^m

3.2.4.1. Identification of potential and source

Equations (C.6) and (C.7) originate from equation (3.14) of Gourgoulhon & Bonazzola (1993). This equation has the form

$$M^{m||n}{}_n = \dots$$

which uses the covariant 2-vector Laplacian. So, this time our task is to extract the **flat space 2-vector Laplacian** from equations (C.6) and (C.7). In Cartesian coordinates, this Laplacian is equal to the flat space 2-scalar Laplacian and has the form $\partial_x^2 + \partial_z^2$. However, in spherical coordinates we have to proceed similarly to equation (3.7). That way, we find

$$\begin{aligned}
 &k^{no} {}^2\nabla_n {}^2\nabla_o \Phi^m \\
 &= k^{no} [\partial_n (\partial_o \Phi^m + {}^2\Gamma_{op}^m \Phi^p) - {}^2\Gamma_{no}^q (\partial_q \Phi^m + {}^2\Gamma_{qp}^m \Phi^p) + {}^2\Gamma_{nq}^m (\partial_o \Phi^q + {}^2\Gamma_{op}^q \Phi^p)] \\
 &= {}^2\Delta_n^m \Phi^n
 \end{aligned}$$

Then, we choose the flat space 2-metric

$$k_{mn} = \begin{pmatrix} 1 & 0 \\ 0 & r^2 \end{pmatrix}$$

such that we obtain

$${}^2\Delta_n^m = \begin{pmatrix} {}^2\Delta - \frac{1}{r^2} & -\frac{2}{r} \partial_\theta \\ \frac{2}{r^3} \partial_\theta & \partial_r^2 + \frac{1}{r^2} \partial_\theta^2 + \frac{3}{r} \partial_r \end{pmatrix} \tag{3.12}$$

In addition to that, we use equations (2.21) and (2.29) to compute

$$N \left(\frac{M}{N} \right)_{,m} = \frac{M_{,m} N - M N_{,m}}{N} = M (\mu_{,m} - \nu_{,m})$$

and

$$\frac{1}{N} (MN)_{,m} = M_{,m} + M \frac{N_{,m}}{N} = M (\mu_{,m} + \nu_{,m})$$

With the help of equation (3.5), these two results lead to the components

$$\begin{aligned} N \left(\frac{M}{N} \right)_{,r} &= M \left(\frac{1}{r} + \beta_{,m} - \nu_{,r} \right) \\ N \left(\frac{M}{N} \right)_{,\theta} &= M (\cot \theta + \beta_{,\theta} - \nu_{,\theta}) \\ \frac{1}{N} (MN)_{,r} &= M \left(\frac{1}{r} + \beta_{,r} + \nu_{,r} \right) \\ \frac{1}{N} (MN)_{,\theta} &= M (\cot \theta + \beta_{,\theta} + \nu_{,\theta}) \end{aligned}$$

Together with

$$\frac{M^2}{N} \left(\frac{\omega}{M} \right)_{,m} = \frac{M^2}{N} \frac{\omega_{,m} M - \omega M_{,m}}{M^2} = \frac{M}{N} (\omega_{,m} - \omega \mu_{,m})$$

we eventually find

$${}^2 \Delta_n^m M^n = S_M^m \quad (3.13)$$

where

$$\begin{aligned} S_M^r &= A^2 \left[16\pi M s^r - 2L^{rr} M \left(\frac{1}{r} + \beta_{,r} - \nu_{,r} \right) - 2L^{r\theta} M (\cot \theta + \beta_{,\theta} - \nu_{,\theta}) \right. \\ &\quad + \frac{L}{A^2} M \left(\frac{1}{r} + \beta_{,r} + \nu_{,r} \right) + 2 \frac{M}{N} [q, \kappa]^r + 2 \frac{\omega}{N} [M, \kappa]^r \\ &\quad + 2 \left(\frac{\kappa}{A^2} - \kappa^{rr} \right) \frac{M}{N} (\omega_{,r} - \omega \mu_{,r}) - 2\kappa^{r\theta} \frac{M}{N} (\omega_{,\theta} - \omega \mu_{,\theta}) \\ &\quad \left. - 2M \left(2\kappa^r_{,r} \kappa^r + 2\kappa^r_{,\theta} \kappa^\theta - \kappa \kappa^r \right) \right] \\ &\quad - 2 \left[\alpha_{,r} \left(M^r_{,r} - M^\theta_{,\theta} - \frac{1}{r} M^r \right) + \alpha_{,\theta} \left(M^\theta_{,r} + \frac{1}{r^2} M^r_{,\theta} \right) \right] \end{aligned} \quad (3.14)$$

and

$$\begin{aligned} S_M^\theta &= A^2 \left[16\pi M s^\theta - 2L^{\theta r} M \left(\frac{1}{r} + \beta_{,r} - \nu_{,r} \right) - 2L^{\theta\theta} M (\cot \theta + \beta_{,\theta} - \nu_{,\theta}) \right. \\ &\quad + \frac{L}{r^2 A^2} M (\cot \theta + \beta_{,\theta} + \nu_{,\theta}) + 2 \frac{M}{N} [q, \kappa]^\theta + 2 \frac{\omega}{N} [M, \kappa]^\theta \\ &\quad + \left[\frac{\kappa}{(rA)^2} - \kappa^{\theta\theta} \right] \frac{M}{N} (\omega_{,\theta} - \omega \mu_{,\theta}) - 2\kappa^{\theta r} \frac{M}{N} (\omega_{,r} - \omega \mu_{,r}) \\ &\quad \left. - 2M \left(2\kappa^\theta_{,r} \kappa^r + 2\kappa^\theta_{,\theta} \kappa^\theta - \kappa \kappa^\theta \right) \right] \\ &\quad - 2 \left[\frac{1}{r^2} \alpha_{,\theta} \left(M^\theta_{,\theta} - M^r_{,r} + \frac{1}{r} M^r \right) + \alpha_{,r} \left(M^\theta_{,r} + \frac{1}{r^2} M^r_{,\theta} \right) \right] \end{aligned} \quad (3.15)$$

Unfortunately, these Poisson equations suffer from two severe problems. The first one is that they do not take into account that the geometry fields obey so-called slicing conditions. We will have a closer look at this issue in the next section. The subsequent section deals with another obstacle. A straightforward numerical implementation of the

3. Numerics

above two Poisson equations turns out to be numerically unstable. In order to solve this problem, we will set the sources to zero in the vicinity of the rotation axis.

3.2.4.2. Slicing condition

The 2-shift M^m has to obey the slicing condition (3.4) of Gourgoulhon & Bonazzola (1993). According to equation (H.8), this condition can be rewritten as

$${}^2\text{div} \left(e^{2(\alpha+\nu)} \vec{M} \right) = 0 \quad (3.16)$$

where the operator ${}^2\text{div}$ is the flat space 2-divergence. This operator is the analog of the flat space 3-divergence ${}^3\text{div}$ already encountered in Sect. 2.9.1.2. Similarly to the calculations performed in that section, we can compute the flat space 2-divergence ${}^2\text{div}$ in spherical coordinates. The only differences are that we have to replace the 3-vector X^a , the 3-metric h_{ab} , the determinant h and the 3-covariant derivative $|$ with the 2-vector Y^m , the 2-metric k_{mn} , the determinant $k = \det k_{mn}$ and the 2-covariant derivative $\|$, respectively. Then, setting $k_{mn} = \text{diag}(r^2, r^2 \sin^2 \theta)$ for flat space such that $\sqrt{k} = r^2 \sin \theta$, we obtain the result

$${}^2\text{div} \vec{Y} = Y^m{}_{,m} + \frac{1}{r} Y^r \quad (3.17)$$

The slicing condition (3.16) causes a problem in combination with the Poisson equation (3.13). In order to see this, we consider the Poisson equation (3.13) in Cartesian coordinates, i.e.

$$\begin{aligned} (\partial_x^2 + \partial_z^2) M^x &= \dots \\ (\partial_x^2 + \partial_z^2) M^z &= \dots \end{aligned}$$

with the Cartesian components M^x and M^z of the 2-shift vector. Having a solution (M^x, M^z) of this equation, also $(M^x, M^z + \text{const})$ is a solution, in which const is an arbitrary constant. There is no such constant for the M^x -component, because this would violate axisymmetry. On the other hand, the slicing condition (3.16) has the form

$$\partial_x \left(e^{2(\alpha+\nu)} M^x \right) + \partial_z \left(e^{2(\alpha+\nu)} M^z \right) = 0$$

in Cartesian coordinates. This equation is not invariant under the transformation $M^z \rightarrow M^z + \text{const}$, except when $(\alpha + \nu)_{,z} = 0$. In total, this means that the Poisson equation (3.13) forces us to somehow fix the constant in $M^z \rightarrow M^z + \text{const}$, whereas the slicing condition tells us that the choice is not arbitrary. Unfortunately, there does not seem to be a way to directly compute the constant with the help of the slicing condition. Therefore, we choose a different way and rewrite the Poisson equation (3.13) as

$$\boxed{{}^2\Delta^m_n \left[e^{2(\alpha+\nu)} M^n \right] = S_M^m} \quad (3.18)$$

with the new potential $e^{2(\alpha+\nu)} M^m$ and the new source S_M^m . This Poisson equation is invariant under the transformation $e^{2(\alpha+\nu)} M^z \rightarrow e^{2(\alpha+\nu)} M^z + \text{const}$. As the slicing condition (3.16) is invariant under that transformation, too, we can then fix the constant arbitrarily.

In order to determine the new source S_M^m , we compute

$$\partial_m \left(e^{2(\alpha+\nu)} M^o \right) = M^o \partial_m e^{2(\alpha+\nu)} + e^{2(\alpha+\nu)} \partial_m M^o = e^{2(\alpha+\nu)} [2M^o \partial_m (\alpha + \nu) + \partial_m M^o]$$

and for $m = n$

$$\begin{aligned} \partial_{mn} \left(e^{2(\alpha+\nu)} M^o \right) &= M^o \partial_{mn} e^{2(\alpha+\nu)} + 2\partial_m e^{2(\alpha+\nu)} \partial_n M^o + e^{2(\alpha+\nu)} \partial_{mn} M^o \\ &= e^{2(\alpha+\nu)} \{ 2M^o [\partial_{mn} (\alpha + \nu) + 2\partial_m (\alpha + \nu) \partial_n (\alpha + \nu)] \\ &\quad + 4\partial_m (\alpha + \nu) \partial_n M^o + \partial_{mn} M^o \} \end{aligned}$$

Then, equation (3.12) tells us that

$$\begin{aligned} &S_M^r \\ &= \left(\partial_r^2 + \frac{1}{r^2} \partial_\theta^2 + \frac{1}{r} \partial_r - \frac{1}{r^2} \right) \left(e^{2(\alpha+\nu)} M^r \right) - \frac{2}{r} \partial_\theta \left(e^{2(\alpha+\nu)} M^\theta \right) \\ &= e^{2(\alpha+\nu)} \left\{ 2M^r \left[\partial_r^2 (\alpha + \nu) + 2(\partial_r (\alpha + \nu))^2 \right] + 4\partial_r (\alpha + \nu) \partial_r M^r + \partial_r^2 M^r \right. \\ &\quad \left. + \frac{2}{r^2} M^r \left[\partial_\theta^2 (\alpha + \nu) + 2(\partial_\theta (\alpha + \nu))^2 \right] + \frac{4}{r^2} \partial_\theta (\alpha + \nu) \partial_\theta M^r + \frac{1}{r^2} \partial_\theta^2 M^r \right. \\ &\quad \left. + \frac{2}{r} M^r \partial_r (\alpha + \nu) + \frac{1}{r} \partial_r M^r - \frac{1}{r^2} M^r - \frac{4}{r} M^\theta \partial_\theta (\alpha + \nu) - \frac{2}{r} \partial_\theta M^\theta \right\} \end{aligned}$$

and

$$\begin{aligned} &S_M^\theta \\ &= \left(\partial_r^2 + \frac{1}{r^2} \partial_\theta^2 + \frac{3}{r} \partial_r \right) \left(e^{2(\alpha+\nu)} M^\theta \right) + \frac{2}{r^3} \partial_\theta \left(e^{2(\alpha+\nu)} M^r \right) \\ &= e^{2(\alpha+\nu)} \left\{ 2M^\theta \left[\partial_r^2 (\alpha + \nu) + 2(\partial_r (\alpha + \nu))^2 \right] + 4\partial_r (\alpha + \nu) \partial_r M^\theta + \partial_r^2 M^\theta \right. \\ &\quad \left. + \frac{2}{r^2} M^\theta \left[\partial_\theta^2 (\alpha + \nu) + 2(\partial_\theta (\alpha + \nu))^2 \right] + \frac{4}{r^2} \partial_\theta (\alpha + \nu) \partial_\theta M^\theta + \frac{1}{r^2} \partial_\theta^2 M^\theta \right. \\ &\quad \left. + \frac{6}{r} M^\theta \partial_r (\alpha + \nu) + \frac{3}{r} \partial_r M^\theta + \frac{4}{r^3} M^r \partial_\theta (\alpha + \nu) + \frac{2}{r^3} \partial_\theta M^r \right\} \end{aligned}$$

Due to equations (2.21) and (2.23), we can replace $e^{2(\alpha+\nu)} = A^2 N^2$. And, equations (3.10) and (3.12) allow us to write

$$\begin{aligned} S_M^r &= A^2 N^2 \left\{ 4M^r [\partial_r (\alpha + \nu)]^2 + 4\partial_r (\alpha + \nu) \partial_r M^r + \frac{4}{r^2} M^r [\partial_\theta (\alpha + \nu)]^2 \right. \\ &\quad \left. + \frac{4}{r^2} \partial_\theta (\alpha + \nu) \partial_\theta M^r - \frac{4}{r} M^\theta \partial_\theta (\alpha + \nu) + {}^2\Delta M^r + 2M^r {}^2\Delta (\alpha + \nu) \right\} \end{aligned}$$

and

$$\begin{aligned} S_M^\theta &= A^2 N^2 \left\{ 4M^\theta [\partial_r (\alpha + \nu)]^2 + 4\partial_r (\alpha + \nu) \partial_r M^\theta + \frac{4}{r^2} M^\theta [\partial_\theta (\alpha + \nu)]^2 \right. \\ &\quad \left. + \frac{4}{r^2} \partial_\theta (\alpha + \nu) \partial_\theta M^\theta + \frac{4}{r} M^\theta \partial_r (\alpha + \nu) + \frac{4}{r^3} M^r \partial_\theta (\alpha + \nu) \right. \\ &\quad \left. + {}^2\Delta M^\theta + 2M^\theta {}^2\Delta (\alpha + \nu) \right\} \end{aligned}$$

3. Numerics

Then, equations (3.13) and (3.23), the latter one being derived further below, eventually give

$$\begin{aligned}
 S_M^r &= A^2 N^2 \left\{ 4\partial_r(\alpha + \nu) [M^r \partial_r(\alpha + \nu) + \partial_r M^r] \right. \\
 &\quad \left. + \frac{4}{r^2} \partial_\theta(\alpha + \nu) [M^r \partial_\theta(\alpha + \nu) + \partial_\theta M^r] - \frac{4}{r} M^\theta \partial_\theta(\alpha + \nu) \right. \\
 &\quad \left. + S_M^{rr} + 2M^r S_\alpha \right\} \\
 S_M^\theta &= A^2 N^2 \left\{ 4\partial_r(\alpha + \nu) [M^\theta \partial_r(\alpha + \nu) + \partial_r M^\theta] \right. \\
 &\quad \left. + \frac{4}{r^2} \partial_\theta(\alpha + \nu) [M^\theta \partial_\theta(\alpha + \nu) + \partial_\theta M^\theta] \right. \\
 &\quad \left. + \frac{4}{r} M^\theta \partial_r(\alpha + \nu) + \frac{4}{r^3} M^r \partial_\theta(\alpha + \nu) + S_M^{\theta\theta} + 2M^\theta S_\alpha \right\}
 \end{aligned}$$

3.2.4.3. Rotation axis

Let us have a closer look at the expressions

$$E_1 = A^2 \left(-2L^{rr} M \frac{1}{r} - 2L^{r\theta} M \cot \theta + \frac{L}{A^2} M \frac{1}{r} \right) \quad (3.19)$$

and

$$E_2 = A^2 \left(-2L^{\theta r} M \frac{1}{r} - 2L^{\theta\theta} M \cot \theta + \frac{L}{r^2 A^2} M \cot \theta \right) \quad (3.20)$$

in equations (3.14) and (3.15). It can be shown (with the computer algebra program Mathematica) that these two expressions can be written as

$$E_1 = -\frac{1}{r^2} M^r + \frac{\cot \theta}{r^2} \partial_\theta M^r - \frac{1}{r} \partial_\theta M^\theta + \frac{1}{r} \partial_r M^r + \cot \theta \partial_r M^\theta$$

and

$$E_2 = \frac{\cot \theta}{r^3} M^r + \frac{1}{r^3} \partial_\theta M^r + \frac{\cot \theta}{r^2} \partial_\theta M^\theta - \frac{\cot \theta}{r^2} \partial_r M^r + \frac{1}{r} \partial_r M^\theta$$

In Cartesian coordinates, they take the form

$$E_1 = \frac{1}{x} (\partial_x M^x - \partial_z M^z)$$

and

$$E_2 = \frac{1}{x} (\partial_z M^x + \partial_x M^z)$$

That way, it is obvious that the rotation axis $x = 0$ is somehow problematic, as there a division by zero occurs. However, in our numerical approach, we place the cells of the numerical grid in such a manner that they end on the rotation axis. With the grid points lying in the center of the cells, the rotation axis does therefore not contain any grid points. Instead, the innermost radial grid line (grid lines connect grid points) is given at the radius $r = r_{\min} > 0$, and the minimal and maximal angular grid lines are set at $\theta = \theta_{\min} > 0$ and $\theta = \theta_{\max} < \pi$, respectively. Then, the Cartesian coordinate x is never zero at anyone of our grid points and no division by zero occurs. Unfortunately, merely having no grid points on the rotation axis has turned out to still cause the fixed point iteration method to be divergent. Numerically experimenting with the iteration,

we found out that this problem can be solved by setting $S_M^m = 0$ on the three grid lines $r = r_{\min}$, $\theta = \theta_{\min}$ and $\theta = \theta_{\max}$.

3.2.4.4. Numerically optimally suited form of source terms

The final problem is that for very high numerical resolutions the source terms (3.19) and (3.20) have turned out to cause the fixed point iteration method to become divergent. Therefore, we had to rewrite them. For the two terms containing the trace L of the exterior 2-curvature, we do not compute the trace L via $L = k^{mn} L_{mn}$ but instead use equation (3.10)

$$L = \frac{2M^m}{MN} N_{||m} = 2m^m \nu_{,m} \quad (3.21)$$

of Gourgoulhon & Bonazzola (1993), which results from the slicing condition (3.16). From a perturbative viewpoint, where all basic fields are small and of the order of Δ , it is now obvious that L is of the order Δ^2 , because it contains the two basic fields M^m and ν . Therefore, L does no longer affect stability.

The only remaining problematic expressions are therefore

$$E'_1 = A^2 \left(-2L^{rr} M \frac{1}{r} - 2L^{r\theta} M \cot \theta \right)$$

and

$$E'_2 = A^2 \left(-2L^{\theta r} M \frac{1}{r} - 2L^{\theta\theta} M \cot \theta \right)$$

They can be rewritten as (again with Mathematica)

$$E'_1 = \cot \theta \left(\frac{1}{r^2} M^r_{,\theta} + M^\theta_{,r} \right) + \frac{2}{r} M^r_{,r} + \frac{2}{r} \left(M^r \alpha_{,r} + M^\theta \alpha_{,\theta} \right)$$

and

$$E'_2 = \frac{1}{r} \left(\frac{1}{r^2} M^r_{,\theta} + M^\theta_{,r} \right) + 2 \frac{\cot \theta}{r^2} \left(\frac{1}{r} M^r + M^\theta_{,\theta} + M^r \alpha_{,r} + M^\theta \alpha_{,\theta} \right) \quad (3.22)$$

On the other hand, it is also possible to show (with Mathematica by explicitly evaluating the trace L) that equation (3.21) can be put in the form

$$M^\theta_{,\theta} + M^r_{,r} + \frac{1}{r} M^r + 2M^r (\alpha_{,r} + \nu_{,r}) + 2M^\theta (\alpha_{,\theta} + \nu_{,\theta}) = 0$$

Then, we can reduce the number of stability relevant terms in expression (3.22) by writing it as

$$E'_2 = \frac{1}{r} \left(\frac{1}{r^2} M^r_{,\theta} + M^\theta_{,r} \right) - 2 \frac{\cot \theta}{r^2} M^r_{,r} - 2 \frac{\cot \theta}{r^2} \left[M^r (\alpha_{,r} + 2\nu_{,r}) + M^\theta (\alpha_{,\theta} + 2\nu_{,\theta}) \right]$$

such that we finally obtain

$$\begin{aligned}
S_M^r &= \cot \theta \left(\frac{1}{r^2} M^r_{,\theta} + M^\theta_{,r} \right) + \frac{2}{r} M^r_{,r} \\
&+ A^2 \left[16\pi M s^r - 2L^{rr} M(\beta_{,r} - \nu_{,r}) - 2L^{r\theta} M(\beta_{,\theta} - \nu_{,\theta}) \right. \\
&\quad + \frac{2M^m \nu_{,m}}{A^2} (\mu_{,r} + \nu_{,r}) + 2\frac{M}{N} [q, \kappa]^r + 2\frac{\omega}{N} [M, \kappa]^r \\
&\quad + 2 \left(\frac{\kappa}{A^2} - \kappa^{rr} \right) \frac{M}{N} (\omega_{,r} - \omega \mu_{,r}) - 2\kappa^{r\theta} \frac{M}{N} (\omega_{,\theta} - \omega \mu_{,\theta}) \\
&\quad \left. - 2M \left(2\kappa^r_{,r} \kappa^r + 2\kappa^r_{,\theta} \kappa^\theta - \kappa \kappa^r \right) \right] \\
&- 2 \left[\alpha_{,r} \left(M^r_{,r} - M^\theta_{,\theta} - \frac{2}{r} M^r \right) + \alpha_{,\theta} \left(M^\theta_{,r} + \frac{1}{r^2} M^r_{,\theta} - \frac{1}{r} M^\theta \right) \right] \\
S_M^\theta &= \frac{1}{r} \left(\frac{1}{r^2} M^r_{,\theta} + M^\theta_{,r} \right) - 2\frac{\cot \theta}{r^2} M^r_{,r} \\
&+ A^2 \left[+16\pi M s^\theta - 2L^{\theta r} M(\beta_{,r} - \nu_{,r}) - 2L^{\theta\theta} M(\beta_{,\theta} - \nu_{,\theta}) \right. \\
&\quad + \frac{2M^m \nu_{,m}}{r^2 A^2} (\mu_{,\theta} + \nu_{,\theta}) + 2\frac{M}{N} [q, \kappa]^\theta + 2\frac{\omega}{N} [M, \kappa]^\theta \\
&\quad + \left[\frac{\kappa}{(rA)^2} - \kappa^{\theta\theta} \right] \frac{M}{N} (\omega_{,\theta} - \omega \mu_{,\theta}) - 2\kappa^{\theta r} \frac{M}{N} (\omega_{,r} - \omega \mu_{,r}) \\
&\quad \left. - 2M \left(2\kappa^\theta_{,r} \kappa^r + 2\kappa^\theta_{,\theta} \kappa^\theta - \kappa \kappa^\theta \right) \right] \\
&- 2 \left[\frac{1}{r^2} \alpha_{,\theta} \left(M^\theta_{,\theta} - M^r_{,r} + \frac{1}{r} M^r \right) + \alpha_{,r} \left(M^\theta_{,r} + \frac{1}{r^2} M^r_{,\theta} \right) \right] \\
&- 2\frac{\cot \theta}{r^2} \left[M^r (\alpha_{,r} + 2\nu_{,r}) + M^\theta (\alpha_{,\theta} + 2\nu_{,\theta}) \right]
\end{aligned}$$

3.2.5. Poisson equation for α

Equation (C.8) follows from equation (3.25) of Gourgoulhon & Bonazzola (1993), having the form

$$N^{|m}_m = \dots$$

This equation uses the covariant 2-scalar Laplacian, and so we look for the flat space 2-scalar Laplacian ${}^2\Delta$ in equation (2.9), which is directly applied to the sum $\alpha + \nu$ there. Hence, we immediately obtain

$$\begin{aligned}
{}^2\Delta(\alpha + \nu) &= S_\alpha \tag{3.23} \\
S_\alpha &= A^2 \left\{ 8\pi s + \frac{1}{N} \left[(q^r + \omega m^r) \kappa_{,r} + (q^\theta + \omega m^\theta) \kappa_{,\theta} \right] \right. \\
&\quad + \frac{2}{MN} \left[\kappa_r [M, q]^r + \kappa_\theta [M, q]^\theta \right] + 3\kappa_m \kappa^m \\
&\quad \left. + \frac{1}{2} (\kappa_{mn} \kappa^{mn} + \kappa^2 + L_{mn} L^{mn}) \right\} \\
&\quad - (\nu_{,r})^2 - \left(\frac{\nu_{,\theta}}{r} \right)^2
\end{aligned}$$

3.2.6. Poisson equation for χ_0

For the basic matter field χ_0 , we have already found a Poisson equation (2.69). In order to invert the Laplacian in that equation, we have to specify boundary conditions. For that purpose, it is best to rewrite equation (2.69) in **coordinates adapted to the surface of the neutron star**. Denoting the radial coordinate of the surface in the old coordinates (r, θ, ϕ) as $R(\theta)$, the new coordinates are defined by

$$\begin{aligned} r'(r, \theta, \phi) &= \frac{r}{R(\theta)} \\ \theta'(r, \theta, \phi) &= \theta \\ \phi'(r, \theta, \phi) &= \phi \end{aligned}$$

So, we have scaled the coordinates radially, such that in the new coordinates (r', θ', ϕ') the radial coordinate of the surface is equal to unity everywhere, i.e. $r'(R(\theta'), \theta', \phi') = 1$. Then, the chain rule produces the first derivatives

$$\partial_r = \frac{1}{R(\theta')} \partial_{r'}$$

and

$$\partial_\theta = -\frac{r \partial_\theta R(\theta)}{R(\theta)^2} \partial_{r'} + \partial_{\theta'} = \partial_{\theta'} - \frac{r' \partial_{\theta'} R(\theta')}{R(\theta')} \partial_{r'}$$

whereas $\partial_\phi = \partial_{\phi'}$. That way, we find the two second derivatives

$$\partial_r^2 = \frac{1}{R(\theta')^2} \partial_{r'}^2$$

and

$$\begin{aligned} \partial_\theta^2 &= \partial_{\theta'}^2 - \partial_{\theta'} \left(\frac{r' \partial_{\theta'} R(\theta')}{R(\theta')} \partial_{r'} \right) - \frac{r' \partial_{\theta'} R(\theta')}{R(\theta')} \partial_{r' \theta'} + \frac{r' \partial_{\theta'} R(\theta')}{R(\theta')} \partial_{r'} \left(\frac{r' \partial_{\theta'} R(\theta')}{R(\theta')} \partial_{r'} \right) \\ &= \partial_{\theta'}^2 + \left(\frac{r' \partial_{\theta'} R(\theta')}{R(\theta')} \right)^2 \partial_{r'}^2 - 2 \frac{r' \partial_{\theta'} R(\theta')}{R(\theta')} \partial_{r' \theta'} \\ &\quad + \frac{r'}{R(\theta')} \left[2 \frac{(\partial_{\theta'} R(\theta'))^2}{R(\theta')} - \partial_{\theta'}^2 R(\theta') \right] \partial_{r'} \end{aligned}$$

Using all the above derivatives, we get

$$\begin{aligned} \Delta &= \partial_r^2 + \frac{1}{r^2} \partial_\theta^2 + \frac{1}{r^2 \sin^2 \theta} \partial_\phi^2 + \frac{2}{r} \partial_r + \frac{\cot \theta}{r^2} \partial_\theta \\ &= \frac{1}{R(\theta')^2} \left\{ \Delta' + \left(\frac{\partial_{\theta'} R(\theta')}{R(\theta')} \right)^2 \partial_{r'}^2 - 2 \frac{\partial_{\theta'} R(\theta')}{r' R(\theta')} \partial_{r' \theta'} \right. \\ &\quad \left. + \frac{1}{r' R(\theta')} \left[2 \frac{(\partial_{\theta'} R(\theta'))^2}{R(\theta')} - \partial_{\theta'}^2 R(\theta') - \cot \theta' \partial_{\theta'} R(\theta') \right] \partial_{r'} \right\} \end{aligned} \quad (3.24)$$

in which Δ' is equal to Δ , except for the replacement $(r, \theta, \phi) \rightarrow (r', \theta', \phi')$. Hence, we finally arrive at

3. Numerics

$$\begin{aligned} \Delta'(\chi_0 \cos \phi') &= S'_{\chi_0} \cos \phi' & (3.25) \\ S'_{\chi_0} &= R(\theta')^2 S_{\chi_0} - \left(\frac{\partial_{\theta'} R(\theta')}{R(\theta')} \right)^2 \partial_{r'}^2 \chi_0 + 2 \frac{\partial_{\theta'} R(\theta')}{r' R(\theta')} \partial_{r' \theta'} \chi_0 \\ &\quad - \frac{1}{r' R(\theta')} \left[2 \frac{(\partial_{\theta'} R(\theta'))^2}{R(\theta')} - \partial_{\theta'}^2 R(\theta') + \cot \theta' \partial_{\theta'} R(\theta') \right] \partial_{r'} \chi_0 \end{aligned}$$

So, we have found Poisson equations for all nine basic fields given in the list (3.2). Therefore, we will focus on how these Poisson equations are solved numerically, in the following.

3.3. Numerical grid

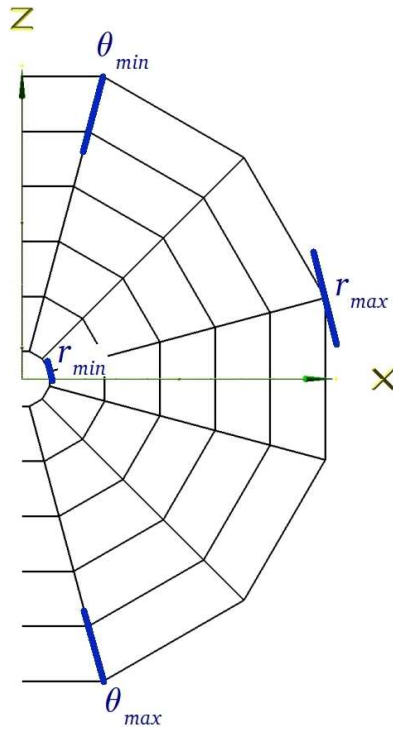


Figure 3.1.: **Numerical grid.** Due to axisymmetry, it is sufficient to store the values of the fields in a single meridional plane. For that purpose, we choose the (x, z) -plane and a two-dimensional polar grid with the coordinates r and θ . The figure shows the radial and angular grid lines, given in black color. In addition to that, the minimal and maximal radial and angular grid lines are highlighted, denoted with r_{\min} , r_{\max} , θ_{\min} and θ_{\max} , respectively.

In order to solve the Poisson equations for the basic fields in the series (3.2), we have to specify a numerical grid. The numerical grid consists of the two coordinates r and θ shown in Fig. 3.1. The minimal and maximal radial grid lines are denoted with r_{\min} and r_{\max} , respectively, in which r_{\max} is chosen sufficiently larger than the radius of the physically interesting region around the neutron star. The minimal and maximal angular grid lines are θ_{\min} and θ_{\max} , connected by the relation $\theta_{\max} = \pi - \theta_{\min}$. The angular grid lines are equidistant, with the angle between two neighboring grid lines being $2\theta_{\min}$, whereas

the radial ones can be placed arbitrarily. In many cases, including those studied in this investigation, the best choice are equidistant radial grid lines. Therefore, the radial grid lines in Fig. 3.1 are distributed equidistantly, though in our numerical implementation, the GRNS code, arbitrarily placed radial grid lines are supported in principle.

3.4. Boundary

3.4.1. Ghost zone

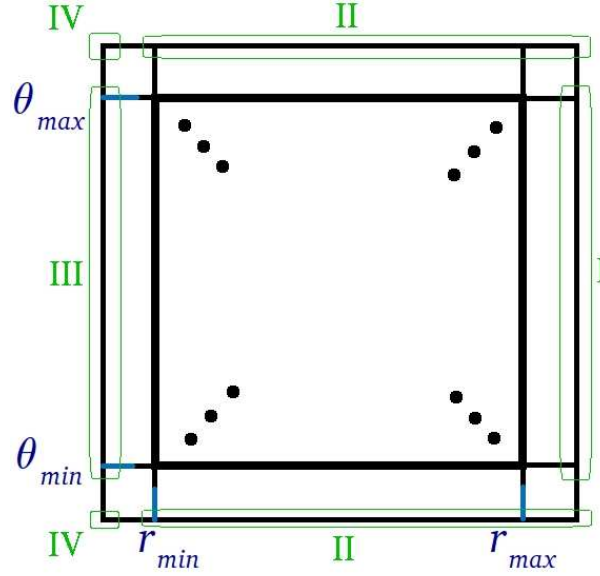


Figure 3.2.: **Ghost zone.** In order to compute derivatives on the boundary of the numerical grid of Fig. 3.1, we use a ghost zone. The ghost zone extends the numerical grid by one zone in both directions of the radial and angular dimensions. It consists of four regions, denoted by *I*, *II*, *III* and *IV*. The values of the fields in the ghost zone are specified by the chosen boundary conditions.

We do not only have to specify the values of the fields on the numerical grid, but we also have to compute first and second derivatives. For that purpose, we call the radial and angular grid lines of the numerical grid r_i and θ_j , where $i \in \{i_{\min}, \dots, i_{\max}\}$ and $j \in \{j_{\min}, \dots, j_{\max}\}$, respectively. Then, the value of an arbitrary field $F(r, \theta)$ at the grid point (r_i, θ_j) can be written as $F_{i,j}$ (the comma is no partial derivative here). Similarly to equation (5.69) of [Dimmelmeier \(2001\)](#), we evaluate the derivatives of the field $F(r, \theta)$ via

$$\begin{aligned}
 \left. \frac{\partial F}{\partial r} \right|_{i,j} &= \frac{\Delta r_{i-1}^2 (F_{i+1,j} - F_{i,j}) + \Delta r_i^2 (F_{i,j} - F_{i-1,j})}{\Delta r_{i-1} \Delta r_i (\Delta r_{i-1} + \Delta r_i)} \\
 \left. \frac{\partial F}{\partial \theta} \right|_{i,j} &= \frac{F_{i,j+1} - F_{i,j-1}}{2\Delta \theta} \\
 \left. \frac{\partial^2 F}{\partial r^2} \right|_{i,j} &= 2 \frac{\Delta r_{i-1} (F_{i+1,j} - F_{i,j}) + \Delta r_i (F_{i-1,j} - F_{i,j})}{\Delta r_{i-1} \Delta r_i (\Delta r_{i-1} + \Delta r_i)} \quad (3.26)
 \end{aligned}$$

3. Numerics

$$\begin{aligned}\frac{\partial^2 F}{\partial \theta^2} \Big|_{i,j} &= \frac{F_{i,j+1} - 2F_{i,j} + F_{i,j-1}}{\Delta \theta^2} \\ \frac{\partial^2 F}{\partial r \partial \theta} \Big|_{i,j} &= \frac{F_{i-1,j-1} - F_{i-1,j+1} - F_{i+1,j-1} + F_{i+1,j+1}}{2(\Delta r_{i-1} + \Delta r_i) \Delta \theta}\end{aligned}$$

with

$$\begin{aligned}\Delta r_i &= r_{i+1} - r_i \\ \Delta \theta &= \theta_{i+1} - \theta_i = \text{const}\end{aligned}$$

These formulas show that we have to go beyond the computational domain, i.e. $i \in \{i_{\min}, \dots, i_{\max}\}$ and $j \in \{j_{\min}, \dots, j_{\max}\}$, in order to compute derivatives on its boundary. This problem is solved with the help of a ghost zone, as shown in Fig. 3.2. The values of the ghost zone are specified by the boundary conditions.

3.4.2. Boundary conditions

Boundary conditions are necessary for the four regions of Fig. 3.2. Let us consider region *I* first. Similarly to the five equations (3.26), the radial, left, third derivative is

$$\begin{aligned}\frac{\partial^3 F}{\partial r^3} \Big|_{i,j}^{\text{left}} &= -\frac{6F_{i-2,j}}{\Delta r_{i-2}(\Delta r_{i-2} + \Delta r_{i-1})(\Delta r_{i-2} + \Delta r_{i-1} + \Delta r_i)} \\ &+ \frac{6F_{i-1,j}}{\Delta r_{i-2}\Delta r_{i-1}(\Delta r_{i-1} + \Delta r_i)} - \frac{6F_{i,j}}{\Delta r_{i-1}(\Delta r_{i-2} + \Delta r_{i-1})\Delta r_i} \\ &+ \frac{6F_{i+1,j}}{\Delta r_i(\Delta r_{i-1} + \Delta r_i)(\Delta r_{i-2} + \Delta r_{i-1} + \Delta r_i)}\end{aligned}$$

We set this quantity equal to zero at the outermost radial grid line i_{\max} , i.e.

$$\frac{\partial^3 F}{\partial r^3} \Big|_{i_{\max},j}^{\text{left}} = 0$$

That way, we can evaluate $F_{i_{\max}+1,j}$ for $j \in \{j_{\min}, \dots, j_{\max}\}$, i.e. in the ghost zone region *I*.

The boundary of region *II* is reflective. This means that

$$F_{i,j_{\min}-1} = F_{i,j_{\min}}$$

and

$$F_{i,j_{\max}+1} = F_{i,j_{\max}}$$

for $i \in \{i_{\min}, \dots, i_{\max} + 1\}$. For region *III*, the boundary is reflective, too, i.e.

$$F_{i_{\min}-1,j} = F_{i_{\min},j}$$

where $j \in \{j_{\min}, \dots, j_{\max}\}$. In region *IV*, the boundary condition has the form

$$F_{i_{\min}-1,j_{\min}-1} = F_{i_{\min},j_{\max}}$$

and

$$F_{i_{\min}-1,j_{\max}+1} = F_{i_{\min},j_{\min}}$$

We do not only have to specify the field values $F_{i,j}$ in the ghost zones to compute the derivatives in the five equations (3.26), but also the radial grid line distances Δr_i . Here, we use

$$\Delta r_{\min-1} = \Delta r_{\min}$$

consistent with the reflective nature of the radial boundary.

3.5. Green functions

3.5.1. 2-scalar

3.5.1.1. Analytic solution

The flat space 2-scalar Poisson equation is

$${}^2\Delta\Phi = S \quad (3.27)$$

with the flat space 2-scalar Laplacian ${}^2\Delta$, defined in equation (3.10), a potential Φ and a source S . Due to equation (24) of Komatsu *et al.* (1989), the Green function of the Laplacian ${}^2\Delta$ is

$$G(\vec{x}, \vec{x}') = \frac{1}{2\pi} \ln |\vec{x} - \vec{x}'|$$

where $\vec{x} = (r \sin \theta, r \cos \theta)$ and $\vec{x}' = (r' \sin \theta', r' \cos \theta')$ are 2-dimensional vectors. This Green function allows us to write the analytic solution of equation (3.27) as

$$\boxed{\Phi(\vec{x}) = \frac{1}{2\pi} \int d^2x' S(\vec{x}') \ln |\vec{x} - \vec{x}'|} \quad (3.28)$$

3.5.1.2. Numerical solution

In order to write equation (3.28) in a form applicable for a numerical evaluation, the easiest way would be to replace the 2-dimensional integral in that equation with two Riemann sums. However, this approach is computationally very expensive. Therefore, we use equation (28) of Komatsu *et al.* (1989):

$$\ln |\vec{x} - \vec{x}'| = \ln \max(r, r') - \sum_{l=1}^{\infty} \frac{1}{l} \frac{\min^l(r, r')}{\max^l(r, r')} (\cos(l\theta) \cos(l\theta') + \sin(l\theta) \sin(l\theta')) \quad (3.29)$$

Then, equation (3.28) becomes

$$\begin{aligned} & \Phi(r, \theta) \\ &= \frac{1}{2\pi} \int_0^{\infty} dr' \int_0^{2\pi} d\theta' r' S(r', \theta') \\ & \cdot \left[\ln \max(r, r') - \sum_{l=1}^{\infty} \frac{1}{l} \frac{\min^l(r, r')}{\max^l(r, r')} (\cos(l\theta) \cos(l\theta') + \sin(l\theta) \sin(l\theta')) \right] \quad (3.30) \end{aligned}$$

Having a closer look at the angular integral, we realize that the angle θ is not restricted to the usual interval $\theta \in [0, \pi]$, but instead the upper integration boundary is equal to 2π (see equation (24) of Komatsu *et al.* 1989). Therefore, we have to specify the value of the integrand and thus the source $S(r, \theta)$ in the interval $\theta \in [\pi, 2\pi]$. For that purpose, we impose boundary conditions.

3. Numerics

3.5.1.3. Von Neumann boundary condition

The von Neumann boundary condition is a result of the requirement

$$S(r, \pi + \theta) = S(r, \pi - \theta)$$

such that

$$\int_0^{2\pi} d\theta' S(r', \theta') = 2 \int_0^\pi d\theta' S(r', \theta')$$

Taking into account

$$\begin{aligned} \begin{pmatrix} \cos(l(\pi + \theta)) \\ \sin(l(\pi + \theta)) \end{pmatrix} S(r, \pi + \theta) &= \begin{pmatrix} \cos(-l(\pi + \theta)) \\ -\sin(-l(\pi + \theta)) \end{pmatrix} S(r, \pi - \theta) \\ &= \begin{pmatrix} \cos(l(\pi - \theta) - 2\pi l) \\ -\sin(l(\pi - \theta) - 2\pi l) \end{pmatrix} S(r, \pi - \theta) \\ &= \begin{pmatrix} \cos(l(\pi - \theta)) \\ -\sin(l(\pi - \theta)) \end{pmatrix} S(r, \pi - \theta) \end{aligned} \quad (3.31)$$

we additionally find

$$\int_0^{2\pi} d\theta' \begin{pmatrix} \cos(l\theta') \\ \sin(l\theta') \end{pmatrix} S(r', \theta') = 2 \int_0^\pi d\theta' \begin{pmatrix} \cos(l\theta') \\ 0 \end{pmatrix} S(r', \theta')$$

Hence, we obtain

$$\begin{aligned} \Phi(r, \theta) &= -\frac{1}{\pi} \sum_{l=1}^{\infty} \frac{1}{l} \cos(l\theta) \int_0^\infty dr' r' \frac{\min^l(r, r')}{\max^l(r, r')} \int_0^\pi d\theta' \cos(l\theta') S(r', \theta') \\ &\quad + \frac{1}{\pi} \int_0^\infty dr' r' \ln \max(r, r') \int_0^\pi d\theta' S(r', \theta') \end{aligned} \quad (3.32)$$

We use this equation to solve the Poisson equation (3.23) of the basic field α . In that case, the potential is $\Phi = \alpha + \nu$ and the source $S = S_\alpha$. We are not allowed to use equation (3.32) for the Poisson equation (3.11) of the basic field β , because there the potential is $\Phi = r \sin \theta (\beta + \nu)$, which has to vanish on the rotation axis due to the presence of the factor $r \sin \theta$. Therefore, we have to apply the Dirichlet boundary condition for the basic field β .

3.5.1.4. Dirichlet boundary condition

For the von Dirichlet boundary condition we assume

$$S(r, \pi + \theta) = -S(r, \pi - \theta)$$

which results in

$$\int_0^{2\pi} d\theta' S(r', \theta') = 0$$

Moreover, in analogy to equation (3.31), we get

$$\begin{pmatrix} \cos(l(\pi + \theta)) \\ \sin(l(\pi + \theta)) \end{pmatrix} S(r, \pi + \theta) = \begin{pmatrix} -\cos(l(\pi - \theta)) \\ \sin(l(\pi - \theta)) \end{pmatrix} S(r, \pi - \theta)$$

and therefore

$$\int_0^{2\pi} d\theta' \sin \theta' \begin{pmatrix} \cos(l\theta') \\ \sin(l\theta') \end{pmatrix} S(r', \theta') = 2 \int_0^\pi d\theta' \sin \theta' \begin{pmatrix} 0 \\ \sin(l\theta') \end{pmatrix} S(r', \theta')$$

Then, we finally arrive at

$$\boxed{\Phi(r, \theta) = -\frac{1}{\pi} \sum_{l=1}^{\infty} \frac{1}{l} \sin(l\theta) \int_0^\infty dr' r' \frac{\min^l(r, r')}{\max^l(r, r')} \int_0^\pi d\theta' \sin(l\theta') S(r', \theta')} \quad (3.33)$$

As mentioned above, we use this equation for the Poisson equation (3.11) of the basic field β . The potential is $\Phi = r \sin \theta (\beta + \nu)$ in that case, and the source is $S = S_\beta$.

3.5.2. 3-scalar

3.5.2.1. Analytic solution

The flat space 3-scalar Poisson equation is

$$\Delta \Phi = S$$

where the flat space 3-scalar Laplacian Δ is given in equation (3.24). For this case, the Green function is commonly known (see, e.g., [Fließbach 1996](#)) to be

$$G(\vec{x}, \vec{x}') = -\frac{1}{4\pi |\vec{x} - \vec{x}'|} \quad (3.34)$$

in which \vec{x} and \vec{x}' are 3-dimensional vectors. They are defined as $\vec{x} = (r \sin \theta \cos \phi, r \sin \theta \sin \phi, r \cos \theta)$, and analogously for \vec{x}' . Then, the analytic solution is

$$\boxed{\Phi(\vec{x}) = -\frac{1}{4\pi} \int d^3 x' \frac{S(\vec{x}')}{|\vec{x} - \vec{x}'|}} \quad (3.35)$$

3.5.2.2. Numerical solution

Equation (11.38) of [Fließbach \(1996\)](#) tells us that the analog of equation (3.29) for the Green function (3.34) is

$$\frac{1}{|\vec{x} - \vec{x}'|} = 4\pi \sum_{l=0}^{\infty} \sum_{m=-l}^l \frac{1}{2l+1} \frac{\min^l(r, r')}{\max^{l+1}(r, r')} Y_{lm}^*(\theta', \phi') Y_{lm}(\theta, \phi)$$

with the spherical harmonics

$$Y_{lm}(\theta, \phi) = \sqrt{\frac{(2l+1)(l-m)!}{4\pi(l+m)!}} P_l^m(\cos \theta) e^{im\phi} \quad (3.36)$$

and the associated Legendre polynomials

$$P_l^m(x) = \frac{(-)^m}{2^l l!} (1-x^2)^{\frac{m}{2}} \frac{d^{l+m}}{dx^{l+m}} (x^2-1)^l$$

3. Numerics

That way, equation (3.35) becomes

$$\begin{aligned} \Phi(\vec{x}) &= -\sum_{l=0}^{\infty} \sum_{m=-l}^l \frac{1}{2l+1} Y_{lm}(\theta, \phi) \int_0^{\infty} dr' r'^2 \frac{\min^l(r, r')}{\max^{l+1}(r, r')} \\ &\quad \cdot \int_0^{\pi} d\theta' \sin \theta' \int_0^{2\pi} d\phi' Y_{lm}^*(\theta', \phi') S(\vec{x}') \end{aligned}$$

which can be rewritten as

$$\begin{aligned} \Phi(\vec{x}) &= -\frac{1}{4\pi} \sum_{l=0}^{\infty} \sum_{m=-l}^l \frac{(l-m)!}{(l+m)!} P_l^m(\cos \theta) e^{im\phi} \int_0^{\infty} dr' r'^2 \frac{\min^l(r, r')}{\max^{l+1}(r, r')} \\ &\quad \cdot \int_0^{\pi} d\theta' P_l^m(\cos \theta') \sin \theta' \int_0^{2\pi} d\phi' S(\vec{x}') e^{-im\phi'} \end{aligned} \quad (3.37)$$

3.5.2.3. Axisymmetry

Now, we assume axisymmetry, i.e.

$$S(\vec{x}) = S(r, \theta)$$

such that

$$\begin{aligned} \Phi(r, \theta) &= -\frac{1}{4\pi} \sum_{l=0}^{\infty} \sum_{m=-l}^l \frac{(l-m)!}{(l+m)!} P_l^m(\cos \theta) e^{im\phi} \int_0^{\infty} dr' r'^2 \frac{\min^l(r, r')}{\max^{l+1}(r, r')} \\ &\quad \cdot \int_0^{\pi} d\theta' P_l^m(\cos \theta') \sin \theta' S(r', \theta') \int_0^{2\pi} d\phi' e^{-im\phi'} \end{aligned}$$

Obviously,

$$\int_0^{2\pi} d\phi' e^{-im\phi'} = \int_0^{2\pi} d\phi' (\cos(m\phi') - i \sin(m\phi')) = 2\pi \delta_0^m$$

Therefore, using the Legendre polynomials

$$P_l(x) = \frac{1}{2^l l!} \frac{d^l}{dx^l} (x^2 - 1)^l$$

we finally obtain

$$\boxed{\Phi(r, \theta) = -\frac{1}{2} \sum_{l=0}^{\infty} P_l(\cos \theta) \int_0^{\infty} dr' r'^2 \frac{\min^l(r, r')}{\max^{l+1}(r, r')} \int_0^{\pi} d\theta' P_l(\cos \theta') \sin \theta' S(r', \theta')} \quad (3.38)$$

We use this equation for the Poisson equation (3.6) of the basic field ν . For that field, the potential is $\Phi = \nu$ and the source $S = S_\nu$.

3.5.2.4. Azimuthal cosine

Next, we assume that

$$S(\vec{x}) = S(r, \theta) \cos \phi \quad (3.39)$$

of which we will make use further below. Then, we acquire

$$\begin{aligned} \Phi(r, \theta, \phi) &= -\frac{1}{4\pi} \sum_{l=0}^{\infty} \sum_{m=-l}^l \frac{(l-m)!}{(l+m)!} P_l^m(\cos \theta) e^{im\phi} \int_0^{\infty} dr' r'^2 \frac{\min^l(r, r')}{\max^{l+1}(r, r')} \\ &\quad \cdot \int_0^{\pi} d\theta' P_l^m(\cos \theta') \sin \theta' S(r', \theta') \int_0^{2\pi} d\phi' e^{-im\phi'} \cos \phi' \end{aligned}$$

Due to the equations (3.45) and (3.46) further below, we see that

$$\int_0^{2\pi} d\phi' e^{-im\phi'} \cos \phi' = \pi \delta_1^{|m|}$$

such that we get

$$\begin{aligned} \Phi(r, \theta, \phi) &= -\frac{1}{4} \sum_{l=1}^{\infty} \sum_{m=-1,1} \frac{(l-m)!}{(l+m)!} P_l^m(\cos \theta) e^{im\phi} \\ &\quad \cdot \int_0^{\infty} dr' r'^2 \frac{\min^l(r, r')}{\max^{l+1}(r, r')} \int_0^{\pi} d\theta' P_l^m(\cos \theta') \sin \theta' S(r', \theta') \end{aligned}$$

We proceed with the relation (equation (3.51) of Jackson 2006)

$$P_l^{-m} = (-)^m \frac{(l-m)!}{(l+m)!} P_l^m \quad (3.40)$$

and find

$$\begin{aligned} \Phi(r, \theta, \phi) &= -\frac{1}{4} \sum_{l=1}^{\infty} \sum_{m=1} \frac{(l-m)!}{(l+m)!} P_l^m(\cos \theta) \left(e^{-im\phi} + e^{im\phi} \right) \\ &\quad \cdot \int_0^{\infty} dr' r'^2 \frac{\min^l(r, r')}{\max^{l+1}(r, r')} \int_0^{\pi} d\theta' P_l^m(\cos \theta') \sin \theta' S(r', \theta') \end{aligned}$$

such that

$$\begin{aligned} \Phi(r, \theta, \phi) &= -\frac{1}{2} \cos \phi \sum_{l=1}^{\infty} \frac{(l-1)!}{(l+1)!} P_l^1(\cos \theta) \\ &\quad \cdot \int_0^{\infty} dr' r'^2 \frac{\min^l(r, r')}{\max^{l+1}(r, r')} \int_0^{\pi} d\theta' P_l^1(\cos \theta') \sin \theta' S(r', \theta') \end{aligned}$$

Then, we eventually arrive at

$$\begin{aligned} \Phi(r, \theta, \phi) &= \Phi(r, \theta) \cos \phi \\ \Phi(r, \theta) &= -\frac{1}{2} \sum_{l=1}^{\infty} \frac{1}{l(l+1)} P_l^1(\cos \theta) \\ &\quad \cdot \int_0^{\infty} dr' r'^2 \frac{\min^l(r, r')}{\max^{l+1}(r, r')} \int_0^{\pi} d\theta' P_l^1(\cos \theta') \sin \theta' S(r', \theta') \quad (3.41) \end{aligned}$$

3. Numerics

3.5.2.5. Vanishing surface potential

Equation (19) of [Eriguchi *et al.* \(1986\)](#) tells us that for the boundary condition (3.39) equation (3.35) can be generalized to

$$\Phi(r, \theta) = \Phi_0(r, \theta) + \sum_{l=1}^{\infty} a_l r^l P_l^1(\cos \theta)$$

Here, $\phi_0(r, \theta)$ is given by equation (3.41) and the a_l are arbitrary coefficients, to allow for a much larger set of boundary conditions. Let us now assume the boundary condition

$$\begin{aligned} S(\vec{x}) &= S(r, \theta) \cos \phi \\ \Phi(R, \theta) &= 0 \end{aligned}$$

with the surface radius R (in surface adapted coordinates, see Sect. 3.2.6). Then, we get

$$\Phi_0(R, \theta) + \sum_{l=1}^{\infty} a_l R^l P_l^1(\cos \theta) = 0$$

We define $\Phi_l = -a_l R^l$ such that

$$\Phi_0(R, \theta) = \sum_{l=1}^{\infty} \Phi_l P_l^1(\cos \theta)$$

Comparing this with equation (G.1), equation (G.2) gives

$$\Phi_l = \frac{(2l+1)}{2l(l+1)} \int_0^\pi d\theta \Phi_0(R, \theta) P_l^1(\cos \theta) \sin \theta$$

such that

$$a_l = -\frac{(2l+1)}{2l(l+1)R^l} \int_0^\pi d\theta \Phi_0(R, \theta) P_l^1(\cos \theta) \sin \theta$$

Hence, we finally arrive at the solution

$$\begin{aligned} \Phi_0(r, \theta) &= -\frac{1}{2} \sum_{l=1}^{\infty} \frac{1}{l(l+1)} P_l^1(\cos \theta) \\ &\quad \cdot \int_0^\infty dr' r'^2 \frac{\min^l(r, r')}{\max^{l+1}(r, r')} \int_0^\pi d\theta' P_l^1(\cos \theta') \sin \theta' S(r', \theta') \\ \Phi(r, \theta) &= \Phi_0(r, \theta) - \frac{1}{2} \sum_{l=1}^{\infty} \frac{2l+1}{l(l+1)} P_l^1(\cos \theta) \frac{r^l}{R^l} \int_0^\pi d\theta' P_l^1(\cos \theta') \sin \theta' \phi_0(R, \theta') \end{aligned}$$

which is used for the basic matter field χ_0 . For that purpose, we rename the coordinates (r, θ) appearing in the above box to (r', θ') (and those in the integrands to (r'', θ'')). Then, we set $\Phi(r', \theta') = \chi_0(r', \theta')$ and $S(r', \theta') = S'_{\chi_0}(r', \theta')$, in which the fields $\chi_0(r', \theta')$ and $S'_{\chi_0}(r', \theta')$ are the two quantities appearing in equation (3.25).

3.5.3. 2-vector

3.5.3.1. Analytic solution

We proceed with the flat space 2-vector Poisson equation

$${}^2\Delta_n^m \Phi^n = S^n$$

where the flat space 2-vector Laplacian ${}^2\Delta_n^m$ is encountered already in equation (3.12), and Φ^n and S^n are a 2-vector potential and a 2-vector source, respectively. Due to equation (3.28), it is obvious that in Cartesian coordinates (denoted with the index c)

$$\Phi_c^m(x, z) = \frac{1}{2\pi} \int d^2x' S_c^m(x', z') \ln |\vec{x} - \vec{x}'|$$

The spherical components $\Phi^m(r, \theta)$ can be computed from the Cartesian ones via

$$\Phi^m(r, \theta) = \frac{\partial(r, \theta)^m}{\partial(x, z)^n} \Phi_c^n(x, z)$$

where $\partial(r, \theta)^m / \partial(x, z)^n$ is a Jacobian. Using the inverse Jacobian $\partial(x, z)^m / \partial(r, \theta)^n$, we find

$$\Phi^m(r, \theta) = \frac{1}{2\pi} \frac{\partial(r, \theta)^m}{\partial(x, z)^n} \int d^2x' \frac{\partial(x', z')^n}{\partial(r', \theta')^o} S^o(r', \theta') \ln |\vec{x} - \vec{x}'|$$

3.5.3.2. Numerical solution

We assume **axisymmetry** such that we have to specify a boundary condition for $\theta = 0$ and $\theta = \pi$, similar to the flat space 2-scalar Poisson equation (see Sect. 3.5.1.2). Obviously, $\Phi_c^x(x, z)$ has to obey a Dirichlet and $\Phi_c^z(x, z)$ a von Neumann boundary condition. In the following, we use the Jacobians

$$\frac{\partial(r, \theta)^m}{\partial(x, z)^n} = \begin{pmatrix} \sin \theta & \cos \theta \\ \frac{\cos \theta}{r} & -\frac{\sin \theta}{r} \end{pmatrix}$$

and

$$\frac{\partial(x, z)^m}{\partial(r, \theta)^n} = \begin{pmatrix} \sin \theta & r \cos \theta \\ \cos \theta & -r \sin \theta \end{pmatrix}$$

In addition to that, we recall equations (3.32) and (3.33). Eventually, we apply

$$\tilde{T}^m(r, \theta) = T_c^m(x(r, \theta), z(r, \theta))$$

where either $T = S$ or $T = \phi$. Then, we find

3. Numerics

$$\begin{aligned}
\Phi^r(r, \theta) &= \sin \theta \tilde{\Phi}^x(r, \theta) + \cos \theta \tilde{\Phi}^z(r, \theta) \\
\Phi^\theta(r, \theta) &= \frac{\cos \theta}{r} \tilde{\Phi}^x(r, \theta) - \frac{\sin \theta}{r} \tilde{\Phi}^z(r, \theta) \\
\tilde{\Phi}^x(r, \theta) &= -\frac{1}{\pi} \sum_{l=1}^{\infty} \frac{1}{l} \sin(l\theta) \int_0^\infty dr' r' \frac{\min^l(r, r')}{\max^l(r, r')} \int_0^\pi d\theta' \sin(l\theta') \tilde{S}^x(r', \theta') \\
\tilde{\Phi}^z(r, \theta) &= -\frac{1}{\pi} \sum_{l=1}^{\infty} \frac{1}{l} \cos(l\theta) \int_0^\infty dr' r' \frac{\min^l(r, r')}{\max^l(r, r')} \int_0^\pi d\theta' \cos(l\theta') \tilde{S}^z(r', \theta') \\
&\quad + \frac{1}{\pi} \int_0^\infty dr' r' \ln \max(r, r') \int_0^\pi d\theta' \tilde{S}^z(r', \theta') \\
\tilde{S}^x(r, \theta) &= \sin \theta S^r(r, \theta) + r \cos \theta S^\theta(r, \theta) \\
\tilde{S}^z(r, \theta) &= \cos \theta S^r(r, \theta) - r \sin \theta S^\theta(r, \theta)
\end{aligned} \tag{3.42}$$

We use this result for the Poisson equation (3.18) of the 2-shift M^m , i.e. for $\Phi^m = e^{2(\alpha+\nu)} M^m$ and $S^m = S_M^m$.

3.5.4. 3-vector

3.5.4.1. Analytic solution

The last Poisson equation to be addressed in this investigation is the axisymmetric, flat space 3-vector one

$${}^3\Delta^a{}_b \Phi^b = S^a$$

with the Laplacian ${}^3\Delta^a{}_b$ from equation (3.8), the 3-vector potential Φ^a and the 3-vector source S^a . Looking at equation (3.35), it is evident that

$$\Phi_c^a(x, y, z) = -\frac{1}{4\pi} \int d^3x' \frac{S_c^a(x', y', z')}{|\vec{x} - \vec{x}'|}$$

Hence, using the two 3-dimensional Jacobians $\partial(r, \theta, \phi)^a / \partial(x, y, z)^b$ and $\partial(x, y, z)^a / \partial(r, \theta, \phi)^b$, we find

$$\Phi^a(r, \theta) = -\frac{1}{4\pi} \frac{\partial(r, \theta, \phi)^a}{\partial(x, y, z)^b} \int d^3x' \frac{\partial(x', y', z')^b}{\partial(r', \theta', \phi')^c} \frac{S^c(r', \theta')}{|\vec{x} - \vec{x}'|} \tag{3.43}$$

3.5.4.2. Numerical solution

The Jacobian inside of the integral of equation (3.43) is

$$\frac{\partial(x, y, z)^a}{\partial(r, \theta, \phi)^b} = \begin{pmatrix} \sin \theta \cos \phi & r \cos \theta \cos \phi & -r \sin \theta \sin \phi \\ \sin \theta \sin \phi & r \cos \theta \sin \phi & r \sin \theta \cos \phi \\ \cos \theta & -r \sin \theta & 0 \end{pmatrix} \tag{3.44}$$

Hence, depending on the choice of the indices b and c , the integrand of equation (3.43) (not considering the denominator $|\vec{x} - \vec{x}'|$) depends either on $\cos \phi$, $\sin \phi$ or not at all on the angle ϕ . The latter case has already been treated in equation (3.38). However, the two possible trigonometric dependencies have to be addressed now. Therefore, we return

to equation (3.35) and modify it to

$$\Psi^n(r, \theta, \phi) = -\frac{1}{4\pi} \int d^3x' \begin{pmatrix} \cos \phi' \\ \sin \phi' \end{pmatrix} \frac{S(\vec{x}')}{|\vec{x} - \vec{x}'|}$$

We have introduced the new 2-vector Ψ^n here to avoid any confusion with the 3-vector Φ^a used in this section. It is then obvious from equation (3.37) that

$$\begin{aligned} \Psi^n(r, \theta, \phi) &= -\frac{1}{4\pi} \sum_{l=0}^{\infty} \sum_{m=-l}^l \frac{(l-m)!}{(l+m)!} P_l^m(\cos \theta) e^{im\phi} \int_0^{\infty} dr' r'^2 \frac{\min^l(r, r')}{\max^{l+1}(r, r')} \\ &\cdot \int_0^{\pi} d\theta' \sin \theta' P_l^m(\cos \theta') S(r', \theta') \int_0^{2\pi} d\phi' \begin{pmatrix} \cos \phi' \\ \sin \phi' \end{pmatrix} e^{-im\phi'} \end{aligned}$$

For $m^2 \neq 1$, we obtain

$$\int_0^{2\pi} d\phi' \begin{pmatrix} \cos \phi' \\ \sin \phi' \end{pmatrix} e^{-im\phi'} = \frac{1}{m^2 - 1} \begin{pmatrix} im \cos \phi' - \sin \phi' \\ im \sin \phi' + \cos \phi' \end{pmatrix} e^{-im\phi'} \Big|_0^{2\pi} = \begin{pmatrix} 0 \\ 0 \end{pmatrix} \quad (3.45)$$

and for $m = \pm 1$

$$\int_0^{2\pi} d\phi' \begin{pmatrix} \cos \phi' \\ \sin \phi' \end{pmatrix} e^{\mp i\phi'} = \frac{1}{2} \begin{pmatrix} \phi' \pm \frac{i}{2} e^{\mp 2i\phi'} \\ \mp i\phi' - \frac{1}{2} e^{\mp 2i\phi'} \end{pmatrix} \Big|_0^{2\pi} = \begin{pmatrix} \pi \\ \mp i\pi \end{pmatrix} \quad (3.46)$$

Thus,

$$\begin{aligned} \Psi^n(r, \theta, \phi) &= -\frac{1}{4\pi} \sum_{l=1}^{\infty} \int_0^{\infty} dr' r'^2 \frac{\min^l(r, r')}{\max^{l+1}(r, r')} \int_0^{\pi} d\theta' \sin \theta' \\ &\cdot \left[\frac{(l+1)!}{(l-1)!} P_l^{-1}(\cos \theta) e^{-i\phi} P_l^{-1}(\cos \theta') \begin{pmatrix} \pi \\ i\pi \end{pmatrix} \right. \\ &\quad \left. + \frac{(l-1)!}{(l+1)!} P_l^1(\cos \theta) e^{i\phi} P_l^1(\cos \theta') \begin{pmatrix} \pi \\ -i\pi \end{pmatrix} \right] S(r', \theta') \end{aligned}$$

Due to relation (3.40), we see

$$\frac{(l+1)!}{(l-1)!} P_l^{-1}(\cos \theta) P_l^{-1}(\cos \theta') = \frac{(l-1)!}{(l+1)!} P_l^1(\cos \theta) P_l^1(\cos \theta')$$

Hence, using

$$e^{-i\phi} \begin{pmatrix} \pi \\ i\pi \end{pmatrix} + e^{i\phi} \begin{pmatrix} \pi \\ -i\pi \end{pmatrix} = 2\pi \begin{pmatrix} \cos \phi \\ \sin \phi \end{pmatrix}$$

allows us to continue with

$$\begin{aligned} \Psi^n(r, \theta, \phi) &= -\frac{1}{2} \begin{pmatrix} \cos \phi \\ \sin \phi \end{pmatrix} \sum_{l=1}^{\infty} \frac{1}{l(l+1)} P_l^1(\cos \theta) \\ &\cdot \int_0^{\infty} dr' r'^2 \frac{\min^l(r, r')}{\max^{l+1}(r, r')} \int_0^{\pi} d\theta' \sin \theta' P_l^1(\cos \theta') S(r', \theta') \end{aligned}$$

3. Numerics

So, using equation (3.38) and the abbreviations

$$\begin{aligned}\hat{O}_0 &= -\frac{1}{2} \sum_{l=0}^{\infty} P_l(\cos \theta) \int_0^{\infty} dr' r'^2 \frac{\min^l(r, r')}{\max^{l+1}(r, r')} \int_0^{\pi} d\theta' P_l(\cos \theta') \sin \theta' \\ \hat{O}_1 &= -\frac{1}{2} \sum_{l=1}^{\infty} \frac{1}{l(l+1)} P_l^1(\cos \theta) \int_0^{\infty} dr' r'^2 \frac{\min^l(r, r')}{\max^{l+1}(r, r')} \int_0^{\pi} d\theta' P_l^1(\cos \theta') \sin \theta'\end{aligned}$$

we obtain

$$-\frac{1}{4\pi} \int d^3x' \begin{pmatrix} \cos \phi' \\ \sin \phi' \\ 1 \end{pmatrix} \frac{S(\vec{x}')}{|\vec{x} - \vec{x}'|} = \begin{pmatrix} \begin{pmatrix} \cos \phi \\ \sin \phi \end{pmatrix} \hat{O}_1 \\ \hat{O}_0 \end{pmatrix} S(r', \theta')$$

Note that the quantities \hat{O}_0 and \hat{O}_1 are no operators in the strict mathematical sense, but a mere tool to keep the expressions below short. To understand this issue more thoroughly, we consider a much easier example, like the integral $I = \int dx f(x) g(x)$, where $f(x)$ and $g(x)$ are arbitrary functions. Then, it is possible to abbreviate $\hat{O} = \int dx f(x)$ such that $I = \hat{O}g(x)$. In this example, it is also clear that the integral appearing in the quantity \hat{O} cannot be evaluated unless the function $g(x)$ is included, a fact also valid for the operators \hat{O}_0 and \hat{O}_1 .

Next, we use the Jacobian (3.44) such that

$$\begin{aligned}& \frac{\partial (x', y', z')^a}{\partial (r', \theta', \phi')^b} S^b(r', \theta') \\ &= \begin{pmatrix} \sin \theta' \cos \phi' & r' \cos \theta' \cos \phi' & -r' \sin \theta' \sin \phi' \\ \sin \theta' \sin \phi' & r' \cos \theta' \sin \phi' & r' \sin \theta' \cos \phi' \\ \cos \theta' & -r \sin \theta' & 0 \end{pmatrix} \begin{pmatrix} S^r(r', \theta') \\ S^\theta(r', \theta') \\ S^\phi(r', \theta') \end{pmatrix} \\ &= \begin{pmatrix} \sin \theta' \cos \phi' S^r(r', \theta') + r' \cos \theta' \cos \phi' S^\theta(r', \theta') - r' \sin \theta' \sin \phi' S^\phi(r', \theta') \\ \sin \theta' \sin \phi' S^r(r', \theta') + r' \cos \theta' \sin \phi' S^\theta(r', \theta') + r' \sin \theta' \cos \phi' S^\phi(r', \theta') \\ \cos \theta' S^r(r', \theta') - r \sin \theta' S^\theta(r', \theta') \end{pmatrix}\end{aligned}$$

Hence, we find

$$\begin{aligned}& -\frac{1}{4\pi} \int d^3x' \frac{\partial (x', y', z')^a}{\partial (r', \theta', \phi')^b} \frac{S^b(r', \theta')}{|\vec{x} - \vec{x}'|} \\ &= \begin{pmatrix} \hat{O}_1 \cdot \begin{pmatrix} \cos \phi \tilde{S}^X(r', \theta') - \sin \phi r' \sin \theta' S^\phi(r', \theta') \\ \sin \phi \tilde{S}^X(r', \theta') + \cos \phi r' \sin \theta' S^\phi(r', \theta') \end{pmatrix} \\ \hat{O}_0 \tilde{S}^z(r', \theta') \end{pmatrix}\end{aligned}$$

with

$$\begin{aligned}\tilde{S}^X(r, \theta) &= \sin \theta S^r(r, \theta) + r \cos \theta S^\theta(r, \theta) \\ \tilde{S}^z(r, \theta) &= \cos \theta S^r(r, \theta) - r \sin \theta S^\theta(r, \theta)\end{aligned}$$

Here, the quantity $\tilde{S}^X(r, \theta)$ is the x -component of the source vector at the angle $\phi = 0$, i.e. $\tilde{S}^X(r, \theta) = \tilde{S}^x(r, \theta, \phi = 0)$, whereas the z -component $\tilde{S}^z(r, \theta)$ is ϕ -independent due

to the assumed axisymmetry. The last step is to use the second Jacobian

$$\frac{\partial (r, \theta, \phi)^a}{\partial (x, y, z)^b} = \begin{pmatrix} \frac{\sin \theta \cos \phi}{\cos \theta \cos \phi} & \frac{\sin \theta \sin \phi}{\cos \theta \sin \phi} & \frac{\cos \theta}{-\frac{\sin \theta}{r}} \\ -\frac{r}{r \sin \theta} & \frac{r}{r \sin \theta} & 0 \end{pmatrix}$$

Then,

$$\begin{aligned} & \begin{pmatrix} \frac{\sin \theta \cos \phi}{\cos \theta \cos \phi} & \frac{\sin \theta \sin \phi}{\cos \theta \sin \phi} & \frac{\cos \theta}{-\frac{\sin \theta}{r}} \\ -\frac{r}{r \sin \theta} & \frac{r}{r \sin \theta} & 0 \end{pmatrix} \\ & \cdot \begin{pmatrix} \hat{O}_1 \begin{pmatrix} \cos \phi \tilde{S}^X(r', \theta') - \sin \phi r' \sin \theta' S^\phi(r', \theta') \\ \sin \phi \tilde{S}^X(r', \theta') + \cos \phi r' \sin \theta' S^\phi(r', \theta') \end{pmatrix} \\ \hat{O}_0 \tilde{S}^z(r', \theta') \end{pmatrix} \\ = & \hat{O}_1 \begin{pmatrix} \sin \theta \cos \phi \left(\cos \phi \tilde{S}^X(r', \theta') - \sin \phi r' \sin \theta' S^\phi(r', \theta') \right) \\ \frac{\cos \theta}{r} \cos \phi \left(\cos \phi \tilde{S}^X(r', \theta') - \sin \phi r' \sin \theta' S^\phi(r', \theta') \right) \\ -\frac{1}{r \sin \theta} \sin \phi \left(\cos \phi \tilde{S}^X(r', \theta') - \sin \phi r' \sin \theta' S^\phi(r', \theta') \right) \end{pmatrix} \\ & + \hat{O}_1 \begin{pmatrix} \sin \theta \sin \phi \left(\sin \phi \tilde{S}^X(r', \theta') + \cos \phi r' \sin \theta' S^\phi(r', \theta') \right) \\ \frac{\cos \theta}{r} \sin \phi \left(\sin \phi \tilde{S}^X(r', \theta') + \cos \phi r' \sin \theta' S^\phi(r', \theta') \right) \\ \frac{1}{r \sin \theta} \cos \phi \left(\sin \phi \tilde{S}^X(r', \theta') + \cos \phi r' \sin \theta' S^\phi(r', \theta') \right) \end{pmatrix} \\ & + \hat{O}_0 \begin{pmatrix} \cos \theta \\ -\frac{\sin \theta}{r} \\ 0 \end{pmatrix} \tilde{S}^z(r', \theta') \end{aligned}$$

such that

$$\begin{aligned} & -\frac{1}{4\pi} \frac{\partial (r, \theta, \phi)^a}{\partial (x, y, z)^b} \int d^3x' \frac{\partial (x', y', z')^b}{\partial (r', \theta', \phi')^c} \frac{S^c(r', \theta')}{|\vec{x} - \vec{x}'|} \\ = & \hat{O}_1 \begin{pmatrix} \sin \theta \tilde{S}^X(r', \theta') \\ \frac{\cos \theta}{r} \tilde{S}^X(r', \theta') \\ \frac{r' \sin \theta'}{r \sin \theta} S^\phi(r', \theta') \end{pmatrix} + \hat{O}_0 \begin{pmatrix} \cos \theta \\ -\frac{\sin \theta}{r} \\ 0 \end{pmatrix} \tilde{S}^z(r', \theta') \end{aligned}$$

Hence, using equation (3.43), we arrive at

$$\begin{aligned} & \Phi^a(r, \theta) \\ = & -\frac{1}{2} \begin{pmatrix} \sin \theta & 0 \\ \frac{\cos \theta}{r} & 0 \\ 0 & \frac{1}{r \sin \theta} \end{pmatrix} \sum_{l=1}^{\infty} \frac{1}{l(l+1)} P_l^1(\cos \theta) \int_0^{\infty} dr' r'^2 \frac{\min^l(r, r')}{\max^{l+1}(r, r')} \\ & \cdot \int_0^{\pi} d\theta' P_l^1(\cos \theta') \sin \theta' \begin{pmatrix} \sin \theta' S^r(r', \theta') + r' \cos \theta' S^\theta(r', \theta') \\ r' \sin \theta' S^\phi(r', \theta') \end{pmatrix}^T \\ & -\frac{1}{2} \begin{pmatrix} \cos \theta \\ -\frac{\sin \theta}{r} \\ 0 \end{pmatrix} \sum_{l=0}^{\infty} P_l(\cos \theta) \int_0^{\infty} dr' r'^2 \frac{\min^l(r, r')}{\max^{l+1}(r, r')} \\ & \cdot \int_0^{\pi} d\theta' P_l(\cos \theta') \sin \theta' \left(\cos \theta' S^r(r', \theta') - r' \sin \theta' S^\theta(r', \theta') \right) \quad (3.47) \end{aligned}$$

3. Numerics

This result is used for the Poisson equation (3.9) of the 3-shift N^a , i.e. $\Phi^a = N^a$ and $S^a = S_N^a$.

3.6. Slicing conditions

In Sect. 3.2.4.2, we mentioned that the 2-shift M^m has to obey a slicing condition. There is another such slicing condition for the 3-shift N^a . Both of these slicing conditions are specified in Gourgoulhon & Bonazzola (1993). In the following, we will rewrite the two slicing conditions in terms of our basic fields in flat space. Afterwards, we will explain how the boxes (3.42) and (3.47) have to be modified to take the slicing conditions into account.

3.6.1. Maximal time slicing

We begin with the slicing condition for the 3-shift N^a , called maximal time slicing and given in equation (3.8) of Gourgoulhon & Bonazzola (1993):

$$N^a|_a = 0$$

Appendix H.1 shows that this slicing condition can be rewritten to (see equation (H.5))

$${}^3\text{div} \left(e^{2\alpha+\beta} \vec{N} \right) = 0 \quad (3.48)$$

In general, the inversion of the Laplacian ${}^3\Delta^a_b$ in equation (3.9) with the help of the result (3.47) does not produce a 3-shift N^a which obeys the slicing condition (3.48). The reason is that the boundary conditions for the Green function were chosen too weak. However, it is possible to tighten them. For that purpose, we consider the quantity

$$\vec{N}_e = e^{2\alpha+\beta} \vec{N} \quad (3.49)$$

and apply a Helmholtz decomposition:

$$\vec{N}_e(\vec{x}) = -\frac{1}{4\pi} {}^3\text{grad} \int d^3x' \frac{{}^3\text{div} \vec{N}_e(\vec{x}')}{|\vec{x} - \vec{x}'|} + \frac{1}{4\pi} {}^3\text{rot} \int d^3x' \frac{{}^3\text{rot} \vec{N}_e(\vec{x}')}{|\vec{x} - \vec{x}'|}$$

This result is valid in general, even if the slicing condition (3.48) is not obeyed. Replacing

$$\vec{N}_e(\vec{x}) \rightarrow \vec{N}'_e(\vec{x}) = \frac{1}{4\pi} {}^3\text{rot} \int d^3x' \frac{{}^3\text{rot} \vec{N}_e(\vec{x}')}{|\vec{x} - \vec{x}'|} \quad (3.50)$$

leads to a new field $\vec{N}'_e(\vec{x})$ which obeys the slicing condition (3.48), because the divergence of a curl vanishes. Therefore, the replacement (3.50) is an appropriate tool to enforce the slicing condition. Actually, we do not use the replacement (3.50) but the analytically equal one

$$\vec{N}_e(\vec{x}) \rightarrow \vec{N}_e(\vec{x}) + \frac{1}{4\pi} {}^3\text{grad} \int d^3x' \frac{{}^3\text{div} \vec{N}_e(\vec{x}')}{|\vec{x} - \vec{x}'|} \quad (3.51)$$

because that way we obtain smoother numerical results in the vicinity of $r = 0$. In the following we will bring this result in a different form by performing several steps. For that purpose, we use definitions (2.48) and (3.49). In addition to that, we apply spherical coordinates and reword the integral by looking at equations (3.35) and (3.38). Then, it

is obvious that we eventually arrive at

$$\begin{aligned}
 \begin{pmatrix} N^r \\ N^\theta \\ N^\phi \end{pmatrix} (r, \theta) &\rightarrow \begin{pmatrix} N^r \\ N^\theta \\ N^\phi \end{pmatrix} (r, \theta) + e^{-2\alpha(r, \theta) - \beta(r, \theta)} \begin{pmatrix} \partial_r \\ \frac{1}{r^2} \partial_\theta \\ 0 \end{pmatrix} \frac{1}{2} \sum_{l=0}^{\infty} P_l(\cos \theta) \\
 &\cdot \int_0^\infty dr' r'^2 \frac{\min^l(r, r')}{\max^{l+1}(r, r')} \int_0^\pi d\theta' P_l(\cos \theta') \sin \theta' \\
 &\cdot \left(N_{e, m}^m(r', \theta') + \frac{2}{r'} N_e^{r'}(r', \theta') + \cot \theta' N_e^{\theta'}(r', \theta') \right) \quad (3.52)
 \end{aligned}$$

3.6.2. Conformally minimal azimuthal slicing

We proceed with the conformally minimal azimuthal slicing, the slicing condition for the 2-shift M^m . This condition is given in equation (3.4) of Gourgoulhon & Bonazzola (1993) and has the form

$$(N^2 M^m)_{||m} = 0$$

In equation (H.8), we show that this slicing condition can be reworded to

$${}^2 \operatorname{div} \left(e^{2(\alpha+\nu)} \vec{M} \right) = 0 \quad (3.53)$$

The next steps are similar to those of Sect. 3.6.1. We define the quantity

$$\vec{M}_e = e^{2(\alpha+\nu)} \vec{M} \quad (3.54)$$

and apply a Helmholtz decomposition

$$\vec{M}_e = {}^2 \operatorname{grad} \phi + \vec{A} \quad (3.55)$$

where ϕ is a scalar and \vec{A} a 2-dimensional solenoidal vector, i.e. ${}^2 \operatorname{div} \vec{A} = 0$. Applying a 2-divergence on equation (3.55), we find

$${}^2 \operatorname{div} \vec{M}_e = {}^2 \Delta \phi$$

On the other hand, equations (3.27) and (3.28) tell us that

$$\phi(\vec{x}) = \frac{1}{2\pi} \int d^2 x' \ln |\vec{x} - \vec{x}'| {}^2 \Delta \phi(\vec{x}')$$

That way, we see

$${}^2 \operatorname{grad} \phi(\vec{x}) = \frac{1}{2\pi} {}^2 \operatorname{grad} \int d^2 x' \ln |\vec{x} - \vec{x}'| {}^2 \operatorname{div} \vec{M}_e(\vec{x}')$$

Hence, equation (3.55) leads to

$$\vec{A} = \vec{M}_e - \frac{1}{2\pi} {}^2 \operatorname{grad} \int d^2 x' \ln |\vec{x} - \vec{x}'| {}^2 \operatorname{div} \vec{M}_e(\vec{x}')$$

Similarly to the replacement (3.51), we apply

$$\vec{M}_e(\vec{x}) \rightarrow \vec{M}_e(\vec{x}) - \frac{1}{2\pi} {}^2 \operatorname{grad} \int d^2 x' \ln |\vec{x} - \vec{x}'| {}^2 \operatorname{div} \vec{M}_e(\vec{x}')$$

3. Numerics

Eventually, we bring this result in a form like equation (3.52). For that purpose, we use definitions (3.54) and spherical coordinates. Moreover, equations (3.28) and (3.32) allow us to reformulate the integral. Hence, we arrive at

$$\begin{aligned} \begin{pmatrix} M^r \\ M^\theta \end{pmatrix} (r, \theta) &\rightarrow \begin{pmatrix} M^r \\ M^\theta \end{pmatrix} (r, \theta) + e^{-2(\alpha(r,\theta)+\nu(r,\theta))} \begin{pmatrix} \partial_r \\ \frac{1}{r^2} \partial_\theta \end{pmatrix} \\ &\cdot \left(\frac{1}{\pi} \sum_{l=1}^{\infty} \frac{1}{l} \cos(l\theta) \int_0^\infty dr' r' \frac{\min^l(r, r')}{\max^l(r, r')} \int_0^\pi d\theta' \cos(l\theta') \right) \\ &- \frac{1}{\pi} \int_0^\infty dr' r' \ln \max(r, r') \int_0^\pi d\theta' \end{aligned} \quad {}^2 \text{div} \vec{M}_e(r', \theta')$$

We do not write the expression ${}^2 \text{div} \vec{M}_e(r', \theta')$ in spherical coordinates by using relation (3.17), because numerical tests have shown that this leads to a weak convergence in the iteration process. Instead, we express the divergence in terms of Cartesian coordinates:

$$\begin{aligned} M_e^x &= \sin \theta M_e^r + r \cos \theta M_e^\theta \\ M_e^z &= \cos \theta M_e^r - r \sin \theta M_e^\theta \\ \begin{pmatrix} M^r \\ M^\theta \end{pmatrix} (r, \theta) &\rightarrow \begin{pmatrix} M^r \\ M^\theta \end{pmatrix} (r, \theta) + e^{-2(\alpha(r,\theta)+\nu(r,\theta))} \begin{pmatrix} \partial_r \\ \frac{1}{r^2} \partial_\theta \end{pmatrix} \\ &\cdot \left(\frac{1}{\pi} \sum_{l=1}^{\infty} \frac{1}{l} \cos(l\theta) \int_0^\infty dr' r' \frac{\min^l(r, r')}{\max^l(r, r')} \int_0^\pi d\theta' \cos(l\theta') \right) \\ &- \frac{1}{\pi} \int_0^\infty dr' r' \ln \max(r, r') \int_0^\pi d\theta' \\ &\cdot \left(\sin \theta' M_{e, r'}^{x'}(r', \theta') + \cos \theta' M_{e, r'}^{z'}(r', \theta') \right) \\ &+ \frac{\cos \theta'}{r'} M_{e, \theta'}^{x'}(r', \theta') - \frac{\sin \theta'}{r'} M_{e, \theta'}^{z'}(r', \theta') \end{aligned}$$

3.7. Final gauge

3.7.1. Origin of the remaining gauge freedom

Let us consider Cartesian coordinates. Then, the d -dimensional ($d \in \{2, 3\}$) scalar and vector Poisson equations have the simple form

$$\begin{aligned} \sum_{i=1}^d \partial_i^2 \phi &= S \\ \sum_{i=1}^d \partial_i^2 \phi^A &= S^A \end{aligned}$$

with $A = 1, \dots, d$. Having solutions ϕ and ϕ^A , it is obvious that also $\phi + \text{const}$ and $\phi^A + \text{const}^A$ are solutions, respectively. This gauge freedom is fixed in the 3-dimensional

case by the requirement

$$\begin{aligned}\lim_{r \rightarrow \infty} \phi(\vec{x}) &= 0 \\ \lim_{r \rightarrow \infty} \phi^A(\vec{x}) &= 0\end{aligned}$$

which is provided by the 3-dimensional Green's function

$$G(\vec{x}, \vec{x}') = -\frac{1}{4\pi |\vec{x} - \vec{x}'|}$$

However, in the 2-dimensional case the Green's function is

$$G(\vec{x}, \vec{x}') = \frac{1}{2\pi} \ln |\vec{x} - \vec{x}'|$$

which is not bounded for $|\vec{x} - \vec{x}'| \rightarrow \infty$. Therefore, in the 2-dimensional case, we always have the gauge freedom to add an arbitrary constant to a solution of the scalar Poisson equation which obeys a von Neumann boundary condition. For the vector Poisson equation, we have to care for the axisymmetry, which demands

$$\lim_{x \rightarrow 0} \phi^x(\vec{x}) = 0$$

Thus, we are allowed to add an arbitrary constant only to the ϕ^z -component, where z is the direction along the symmetry axis.

3.7.2. Final gauge fixing of M^m

From equation (3.18), we know that the field M_e^m obeys a 2-dimensional vector Poisson equation. Therefore, if M_e^m is a solution of equation (3.18), then also

$$M_e'^z = M_e^z + \text{const}_M$$

solves this equation, with an arbitrary constant const_M . Due to equation (3.54), this result can be rewritten as

$$\begin{aligned}M'^r &= M^r + \text{const}_M \cos \theta e^{-2(\alpha+\nu)} \\ M'^\theta &= M^\theta - \text{const}_M \frac{\sin \theta}{r} e^{-2(\alpha+\nu)}\end{aligned}$$

in spherical coordinates. Such a gauge transformation is allowed, because it does not violate the slicing conditions (3.48) and (3.53). We choose the constant in such a manner that

$$M_e'^z(r = r_{\min}) = 0$$

with the minimal radius r_{\min} of the computational domain. This leads to

$$\text{const}_M = -M_e^z(r = r_{\min})$$

such that

$$\boxed{\text{const}_M = -\cos \theta M_e^r(r = r_{\min}) + r_{\min} \sin \theta M_e^\theta(r = r_{\min})}$$

3.7.3. Final gauge fixing of α

Due to equation (3.23), the quantity $\alpha + \nu$ obeys a 2-dimensional scalar Poisson equation. Moreover, at the end of Sect. 3.5.1.3, we have mentioned that the quantity $\alpha + \nu$ is governed by a von Neumann boundary condition. Therefore, we have the gauge freedom to add an arbitrary constant const_α to every solution α , i.e.

$$\alpha' = \alpha + \text{const}_\alpha$$

As this gauge transformation does not violate the slicing conditions (3.48) and (3.53), we can choose the constant in such a manner that

$$\alpha'(r = r_{\min}) = \beta(r = r_{\min})$$

(we have made this choice, because the TOV solutions considered further below meets this condition). Then, we find

$$\boxed{\text{const}_\alpha = \beta(r = r_{\min}) - \alpha(r = r_{\min})}$$

3.8. Fixed point iteration

In the preceding sections, we have shown how the Laplacian of each Poisson equation of the nine fields (3.2) can be inverted with Green functions. Together with the three analytic solutions mentioned in Sect. 3.1, we are thus equipped with the knowledge to evaluate a new value for every single one of the twelve basic fields (3.1) if we have old values for all twelve basic fields that do not necessarily represent a valid physical solution. The remaining sections of the numerical part show how neutron star models are computed with the already mentioned fixed point iteration method.

3.8.1. Initial configuration

The initial configuration of the fixed point iteration is constructed in the following manner. We take a solution of the Tolman-Oppenheimer-Volkoff (TOV) equation. Such solutions are spherically symmetric and do not contain any meridional fluid motion. Appendix I explains how they can be computed for our choice of basic fields. There, we also see that the solutions of the TOV-equation are uniquely specified by the polytropic constant K , the polytropic exponent Γ and the central pressure p_c .

In order to get solutions with a meridional fluid motion from the fixed point iteration, we do not use the chosen TOV-solution as the initial configuration but a modified variant. For that purpose, we set the basic field χ_0 (which vanishes for the TOV solution) to

$$\chi_0(r', \theta') = \chi_0^{\max} \sin[(1 + M_r)r'\pi] \sin[(1 + M_\theta)\theta'] \quad (3.56)$$

in surface-adapted coordinates ($r' = 1$ at the surface of the neutron star, see Sect. 3.2.6), with an arbitrary constant χ_0^{\max} and parameters $M_r, M_\theta \in \{0, 1, \dots\}$ (Fig. 3.3).

3.8.2. Iteration

Let us consider the twelve basic fields (3.1) (geometry fields $\nu, N^r, N^\theta, N^\phi, \beta, M^r, M^\theta$ and matter fields $\alpha, \epsilon, p, \chi_0, l_\phi$). We denote their initial values by $\nu_0, \dots, l_{\phi,0}$, while $\nu_s, \dots, l_{\phi,s}$

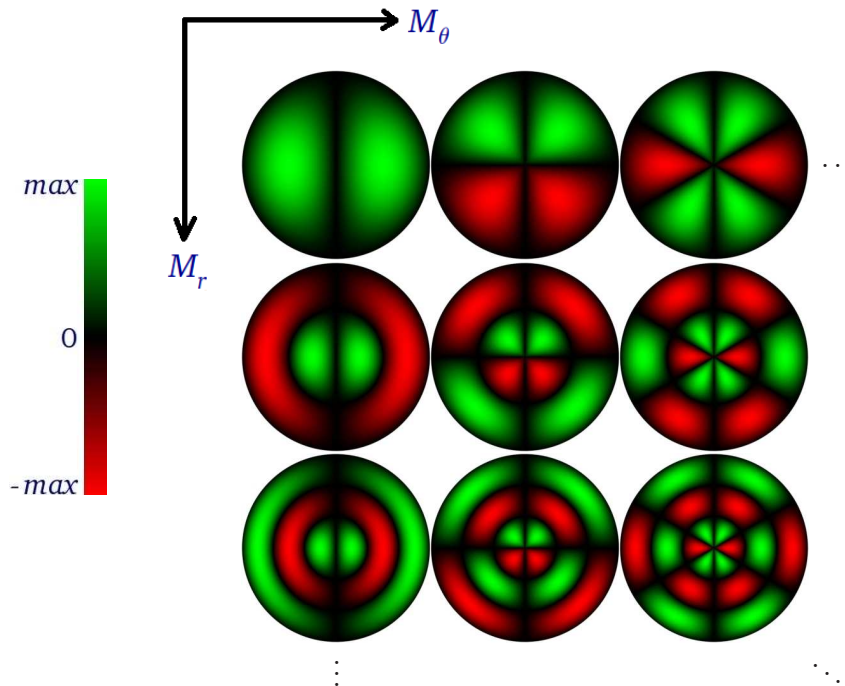


Figure 3.3.: **Initial configuration of basic field χ_0 .** Each one of the nine panels shows the distribution of χ_0 inside of the neutron star for one choice of the pair (M_r, M_θ) according to equation (3.56). The top, left panel visualizes the case $(M_r, M_\theta) = (0, 0)$. Proceeding to the right increases the value of the quantity M_θ , and we have to go down to raise the value of M_r . For each panel, the maximal absolute field value is called max . The values max and $-max$ are represented by the brightest red and green colors, respectively.

represent the values of the twelve basic fields at the iteration step $s = 1, 2, \dots$. Every iteration works in the following manner:

We know the values $\nu_{s-1}, \dots, l_{\phi, s-1}$ and want to evaluate $\nu_s, \dots, l_{\phi, s}$. For that purpose, we compute the eight geometry quantities ν_s, \dots, α_s from the twelve quantities $\nu_{s-1}, \dots, l_{\phi, s-1}$ by inverting the respective Laplacians. Then, we enforce the slicing conditions as explained in Sect. 3.6, and afterwards we apply the gauge condition of Sect. 3.7.

The next step is to compute the four matter quantities $\epsilon_s, \dots, l_{\phi, s}$ using the old values $\epsilon_{s-1}, \dots, l_{\phi, s-1}$ and the newly computed ν_s, \dots, α_s . This method increases the speed of the iteration process. For the total energy density ϵ_s and the pressure p_s , we use equations (2.86) and (2.73), respectively. The basic field $\chi_{0, s}$ is computed by inverting its Laplacian. However, the fixed point iteration has the tendency to gradually either decrease the field values $\chi_{0, s}$ until they vanish everywhere or to increase them indefinitely. We prevent this by rescaling the stream function $\psi = r \sin \theta \chi_0$ at every iteration step in such a way that the maximum value of $|\psi|$ stays constant. Eventually, for the last field $l_{\phi, s}$, we use equation (2.60).

3.8.3. Removal of lower modes

Let us consider the function $f(\psi)$ of equation (2.71), which specifies how the matter in the neutron star circulates. In this investigation, we consider only the case

$$f(\psi) = k\psi^n \quad (3.57)$$

3. Numerics

with some constant k and

$$n = 0, 1$$

(n is no tensor index and thus $n \in \{r, \theta\}$ does not hold here) as done in [Eriguchi *et al.* \(1986\)](#). For the choice

$$f(\psi) = k\psi$$

there are different meridional circulation modes ψ_m , with $m = 0, 1, 2, \dots$ (no tensor index). However, although our solution method tends towards them during the fixed point iteration, it eventually always converges to the fundamental mode ψ_0 . Hence, in order to obtain higher modes, we project the lower modes away. For that purpose, we assume that we have already evaluated the first $n - 1$ modes, i.e. we know ψ_m for $m = 0, 1, \dots, n - 1$. Then, the fixed point iteration spews out the n -th mode by replacing

$$\psi \rightarrow \psi - \sum_{m=1}^{n-1} c_m \psi_m \quad (3.58)$$

at every iteration step, with adequately chosen coefficients c_m . If an orthogonality relation

$$\int_0^\infty dr \int_0^\pi d\theta r^2 \sin \theta W_m(r, \theta) \psi_m \psi_{m'} = \delta_{mm'}$$

exists, the coefficients c_m are given by

$$c_m = \frac{\int_0^\infty dr \int_0^\pi d\theta r^2 \sin \theta W_m(r, \theta) \psi \psi_m}{\int_0^\infty dr \int_0^\pi d\theta r^2 \sin \theta W_m(r, \theta) \psi_m \psi_m}$$

However, we neither know whether an orthogonality relation exists nor do we know the weight functions $W_m(r, \theta)$. After some experimenting, we found that the choice

$$W_m(r, \theta) = \epsilon + p \quad (3.59)$$

is sufficient to achieve a convergence to higher modes. This does not necessarily mean that (3.59) is the correct weight function, but it must be very close to it.¹

In addition to the replacement (3.58), we perform two additional steps. The pressure distribution of the solutions investigated in this thesis is always equatorially symmetric. However, in our treatment, equatorial symmetry is not obeyed exactly due to the limited numerical accuracy. Therefore, its asymmetry may increase during the fixed point iteration, and eventually we obtain an undesired meridional circulation mode. In order to avoid this, we symmetrize the pressure distribution at every iteration step. A similar method is performed for the basic field χ_0 , which is either equatorially symmetric or equatorially antisymmetric, depending on the considered mode.

¹Numerical tests have shown that the weight factor $W_m(r, \theta) = \epsilon \sqrt{h} / (r^2 \sin \theta)$, with $h = \det h_{ab}$, covers a much wider range of rest mass densities properly than the choice $W_m(r, \theta) = \epsilon + p$. However, for the densities considered in this thesis, the choice (3.59) has turned out to be sufficient, and therefore all results of the thesis were computed with the weight factor (3.59).

4. GRNS

The theory and numerics discussed in the previous chapters are implemented in a code, called GRNS (=‘Generally Rotating Neutron Star’). We chose this name, because the code generalizes the RNS code of N. Stergioulas from a mere azimuthal fluid motion to a general one. The GRNS code is programmed in an object oriented manner in C++ under Linux, without parallelization. In this chapter, we will have a closer look at the GRNS code. We will not explain details of the implementation but focus on how neutron star models can be computed by using the OpenGL user interface of the GRNS code. The source code is available from the author on request.

4.1. Neutron star parameters

To use the GRNS code, one has to first specify the parameters of the neutron star by explicitly setting the parameters in the source code. For that purpose, the user has to edit a file called ‘Control.h’, which is one of several header files in the GRNS code, containing the most important control parameters. In order to specify a neutron star model, one sets the following parameters:

```
CENTER_P
POLYTROPE_GAMMA
POLYTROPE_K
F(PSI)
MAXIMUM_PSI
```

The parameter `CENTER_P` gives the central pressure p_c of the neutron star, measured in erg/cm^3 . The dimensionless parameter `POLYTROPE_GAMMA` is the polytropic exponent Γ . The choice of this exponent determines the dimension of the parameter `POLYTROPE_K`, which is the polytropic constant K and has the dimension $(\text{erg}/\text{cm}^3)^{1-\Gamma}$. The macro `F(PSI)` specifies the function $f(\psi)$ of equation (3.57). As the maximum absolute value of the stream function ψ_{\max} is kept fixed at the value `MAXIMUM_PSI` in erg/s during the iteration, it does not matter how the constant k is chosen in equation (3.57). Therefore, we use either

$$F(\text{PSI}) = 1$$

or

$$F(\text{PSI}) = \text{PSI}$$

Having set all five neutron star parameters, the code must be recompiled.

4.2. Start screen

Running the GRNS-code executable, after a short initialization phase, the start screen appears and the fixed point iteration is launched to compute the fundamental meridional circulation mode. As soon as this mode is calculated at sufficiently high accuracy, the iteration stops automatically. Then, the start screen looks as shown in Fig. 4.1.

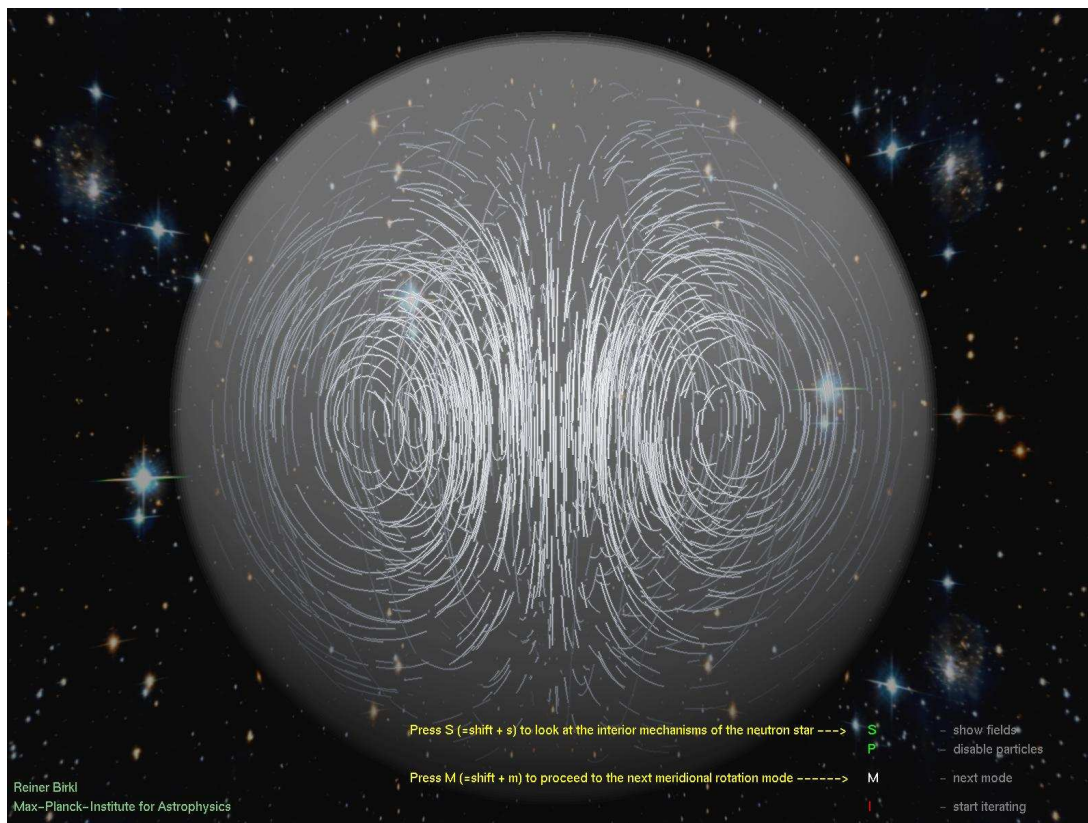


Figure 4.1.: **Start screen of GRNS.** The (3-dimensional) translucent sphere in the start screen represents the neutron star, and the white curves indicate the motion of the fluid inside the star. The start screen is not a still picture but visualized in OpenGL. Therefore, the white curves are permanently moving when watched by the user. The background of the start screen is a picture from Hubble ([Hubble](#)).

Moving the mouse while the left or right mouse buttons are pressed, the neutron star can be shifted around in the OpenGL window. Using instead the middle mouse button, the neutron star can be rotated. At the bottom right corner of the start screen, four ‘keys’ S, P, M and I are displayed. Besides the Escape key to leave the program, these four keys allow the user to interact with GRNS. The key P can be used to disable and enable the visualization of the white curves shown in Fig. 4.1. As soon as the key M is pressed, the next higher meridional circulation mode is computed. For that purpose, an appropriate initial configuration is loaded and afterwards the fixed point iteration is started. The fixed point iteration is shown in real-time. This means that the start screen is updated after every iteration step. The iteration can be stopped and restarted by pressing the key I. As soon as the respective higher meridional circulation mode is obtained, the iteration stops automatically. The result is shown in Fig. 4.2.



Figure 4.2.: **First higher meridional circulation mode.** Pressing the key M in Fig. 4.1 and waiting until the fixed point iteration stops automatically, leads to the first higher meridional circulation mode. The fluid moves from the poles to the center and then along the equator to the surface to get back to the poles.

Pressing again the key M, we get to the next highest mode, and so on. However, we have to wait always until the iteration stops automatically before pressing the key M, because otherwise the higher modes are not computed accurately enough. So, the start screen can be used to compute all meridional circulation modes.

4.3. Overview screen

Pressing the key S leads us to the overview screen, which shows many more details than the start screen (Fig. 4.3). Similarly to the start screen, the overview screen is an OpenGL window and displayed in real-time. That way, it is possible to trace the changes caused by the fixed point iteration for each physical field used by the GRNS code. The advantage of this approach is that it simplifies debugging. In addition to that, it is immediately visible if the fixed point iteration does not converge. This was very helpful in finding the appropriate Poisson equation for the 2-shift M^m (see Sect. 3.2.4).

Let us have a closer look at the bottom left corner of the overview screen (see Fig. 4.3). All quantities of the GRNS code are represented in dimensionless units. Setting the stream function ψ to unity, the quantity $f(1)$ of the overview screen gives the value of the function $f(\psi)$ of equation (3.57) in the internal dimensionless units. If the value $f(1)$ displayed in the overview screen converges to a finite, non-zero value during the fixed point iteration, the GRNS code was able to find the appropriate value of the constant k of equation (3.57) automatically (solutions with $f(1) = 0$ are pathological ones).

The bottom left corner also shows a measure of convergence, defined in the following manner. Let us consider an arbitrary scalar field $F(r, \theta)$ whose value at the grid point (r_i, θ_j) is called $F_{s,i,j}$ at the iteration step $s = 1, 2, \dots$. Then, the **convergence indicator**

4. GRNS

C_s shown in the GRNS code at the iteration step s is defined as

$$C_s = 100 \frac{\sum_{i=i_{\min}}^{i_{\max}} \sum_{j=j_{\min}}^{j_{\max}} |F_{s,i,j} - F_{s-1,i,j}|}{\sum_{i=i_{\min}}^{i_{\max}} \sum_{j=j_{\min}}^{j_{\max}} |F_{s,i,j}|} \quad (4.1)$$

So, when the scalar field does not change anymore, the convergence indicator becomes $C_s = 0$. The value displayed at the bottom left corner of the overview screen (Fig. 4.3) is the maximum of the convergence indicator C_s of all twelve basic fields (3.1). That way, the displayed value is most sensitive to the basic field which converges least.

4.4. Field screen

The disadvantage of the overview screen is that the field panels are very small. This problem is solved by pressing the key A, which magnifies the currently selected field in the field screen. When the GRNS code is started, the field ν is selected by default. Fig. 4.4 shows this scalar field magnified in the field screen. Pressing the page up and page down keys, the user can change the currently selected field. Fig. 4.5 displays the 3-shift N^a in the field screen.

4.5. Additional features

Several additional features are implemented in the user interface of the GRNS code. Pressing the key F5 automatically makes a screenshot. The key F6 can be used to start and stop capturing the visualized OpenGL frames, which are converted into a movie when the GRNS code is left by the user. In addition to that, it is possible to display the numerical grid and also the ghost zone. It was very helpful during the debugging phase to see the field values in the ghost zone in real-time.

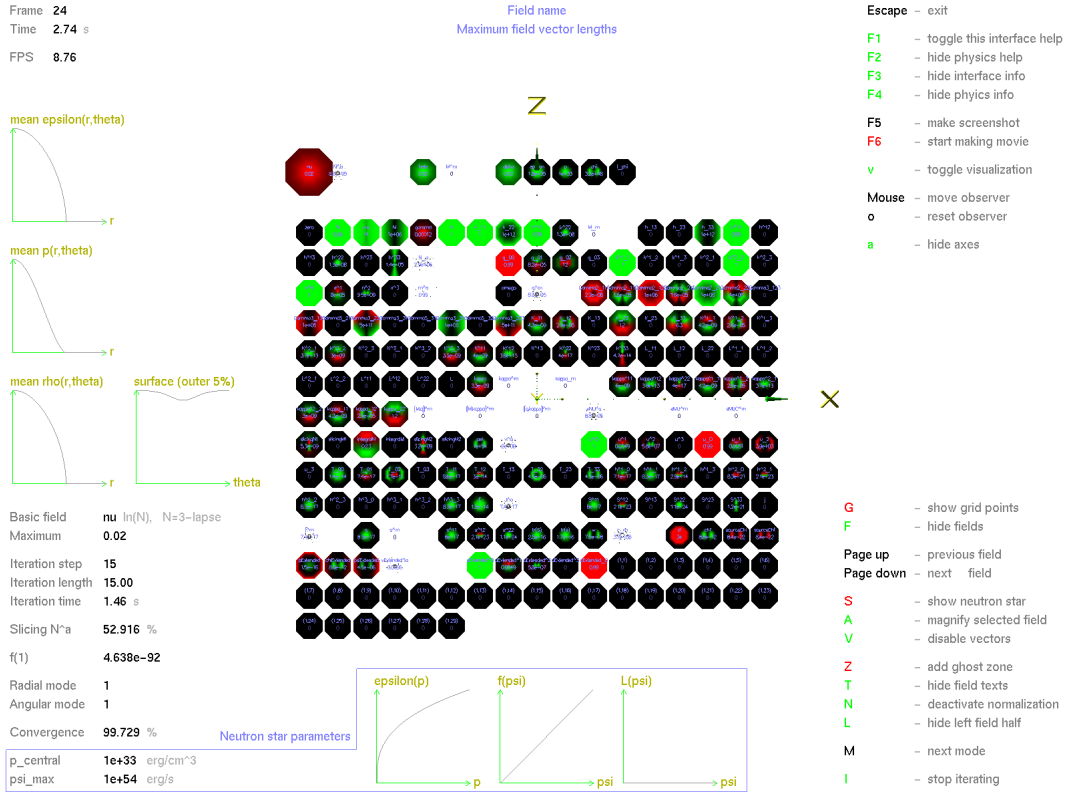


Figure 4.3.: **Overview screen of GRNS.** The overview screen shows all physical fields used in the GRNS code simultaneously. Due to the limited space, the fields are visualized in a very low resolution as the tiny objects in the middle of the screen. The top row shows the basic fields (3.1), the first being the scalar field ν . Scalar fields or components of quantities with more than one index are drawn as discs, whose color coding is the same one as in Fig. 3.3. The next three columns in the top row (between the field ν and the first green disc appearing in that row) contain the components of the 3-lapse N^a . However, even though it is possible to visualize them as three separate scalar fields by pressing the key V, the above frame shows N^a in the vector visualization mode (barely visible and causing white gaps). In that mode, the three components of N^a are visualized as vectors. Below the basic fields, 227 ancillary fields are displayed, which can be discerned by the blue text shown above the fields (barely visible). The blue text at the top of the screen gives the field name and the length of the longest field vector (scalars are considered as 1-vectors). The top left corner shows the current OpenGL frame, the user time and the visualization speed (frames per second). Similar to the start screen and all other OpenGL screens, the overview screen is interactive and changes during the fixed point iteration in real-time. The panels at the right show possible ways to interact with the overview screen (not explained in detail here). The blue box at the bottom of the screen displays the neutron star parameters (including the function $L(\psi)$ of equation (2.60), which is set equal to zero in all models investigated in this thesis). The remaining numbers in the lower left part of the frame give information about the status of the fixed point iteration and the currently selected field. In the above example, the basic field ν is selected and therefore the disc belonging to it is somewhat larger than all other ones. Eventually, the small plots on the left display angularly averaged radial profiles and the deformation of the stellar surface.

4. GRNS

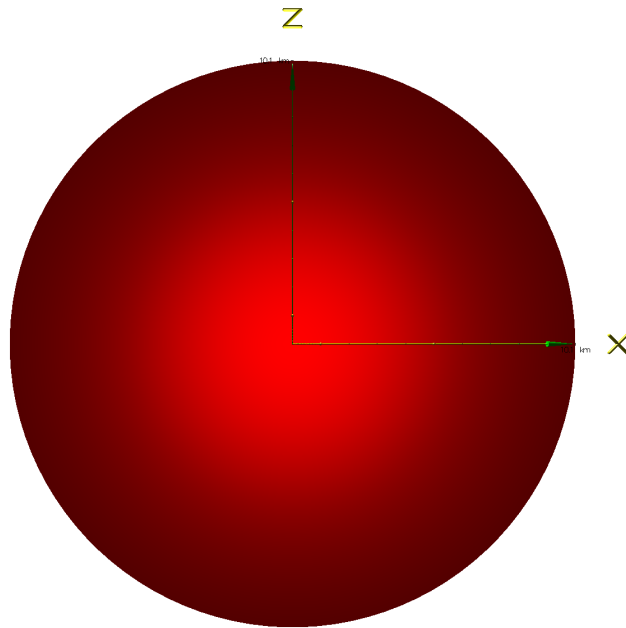


Figure 4.4.: **Field screen of GRNS with scalar field.** The plot shows the scalar field ν in the field screen of the GRNS code for the fundamental meridional circulation mode. The color encoding is the same one as in Fig. 3.3.

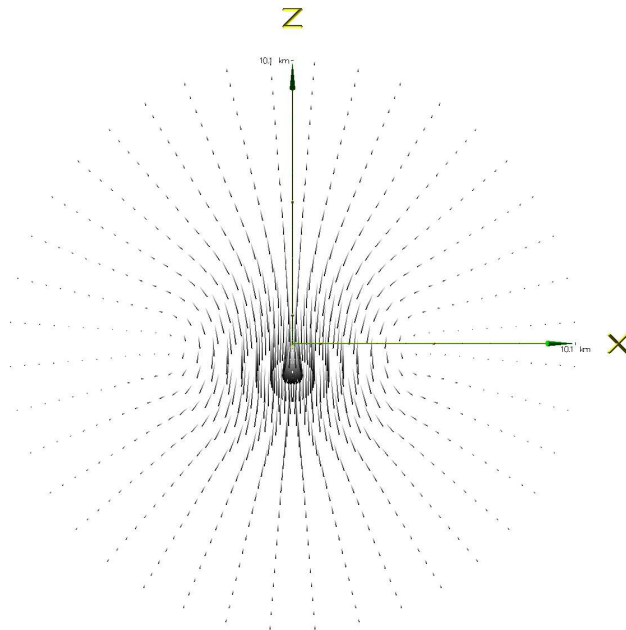


Figure 4.5.: **Field screen of GRNS with 3-vector field.** The plot shows the 3-shift N^a in the field screen of the GRNS code for the fundamental meridional circulation mode. The vectors are represented by the short lines, which are darkest at the head of the vectors. A strongly reduced resolution is used in the above plot to increase the visibility of the individual vectors.

5. Tests

We use the four parameters

```
RESOLUTION
POLYNOMIALS
CENTIMETER
GRID_RADIUS
```

in the file ‘Control.h’ to perform convergence and consistency tests. The following sections explain each parameter and give the result of the corresponding test. Each such test is based on the following settings:

$$\begin{aligned} p_c &= 10^{33} \frac{\text{erg}}{\text{cm}^3} \\ \Gamma &= 3 \\ \rho_c &= 2 \cdot 10^{14} \frac{\text{g}}{\text{cm}^3} \\ f(\psi) &= \psi \\ \psi_{\max} &= 10^{54} \frac{\text{erg}}{\text{s}} \end{aligned} \tag{5.1}$$

These are the parameters discussed in Sect. 4.1, where the polytropic constant K is set by the central rest mass density ρ_c , which obeys $p_c = K\rho_c^\Gamma$ due to equation (2.85). As already mentioned in the caption of Fig. 4.3, we choose $L(\psi) = 0$ such that the Lagrangian angular momentum component l_ϕ vanishes according to equation (2.60). We will explain this choice in more detail in Chapter 6.

5.1. Resolution

The resolution of the numerical grid is set by the two parameters RS and THETAS in the file ‘Control.h’, which give the number of radial and angular grid lines, respectively. In principle, both quantities can take any value above unity. However, there are certain constraints (explained in ‘Control.h’) which have to be obeyed to make the OpenGL visualization work properly. In this investigation, we consider three different resolutions, which can be selected by setting the parameter RESOLUTION to one of the values shown in Tab. 5.1. By default, the low resolution 0 is selected in the GRNS code. The advantage of this choice is that the OpenGL visualization operates fluently on a typical desktop machine. For the results shown in the Chapter 6, we use the medium resolution 1. The high resolution 2 is used only to test the convergence of the GRNS code as shown in Fig. 5.1.

In that figure, we see that for the fundamental mode the GRNS code converges for all three resolutions of Tab. 5.1, i.e. the convergence indicator C_s approaches zero during the fixed point iteration. For higher modes, the convergence indicator drops initially,

RESOLUTION	RS	THETAS
0	59	52
1	150	156
2	501	507

Table 5.1.: **Standard grid resolutions.** The GRNS code possesses three standard resolutions for the numerical grid, discerned by the parameter RESOLUTION. For each resolution, the table shows the number of radial and angular grid lines, given by the two parameters RS and THETAS.

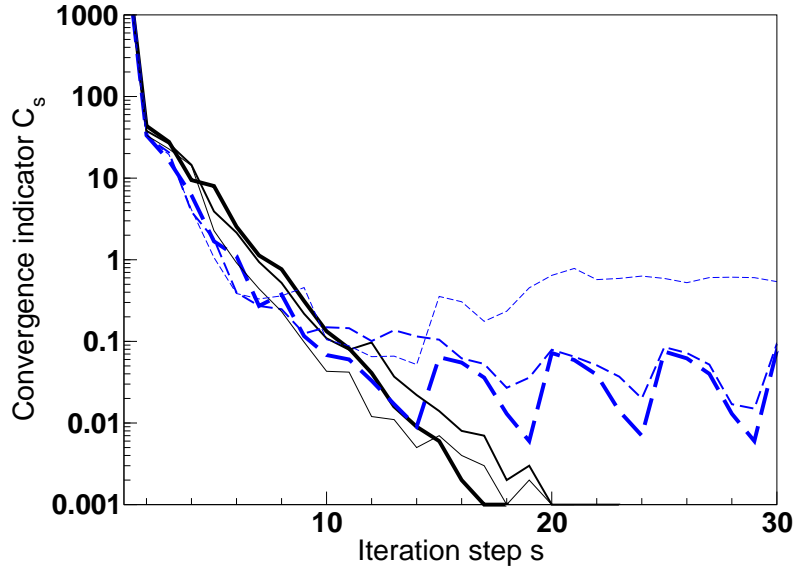


Figure 5.1.: **Resolution-dependent convergence behavior.** The figure shows the dependence of the convergence indicator C_s defined in equation (4.1) on the number of the iteration step s . The three solid lines refer to the three resolutions of Tab. 5.1, the thickness decreasing with the resolution (highest resolution corresponding to thinnest line). The corresponding blue, dashed lines refer to the first higher mode, respectively.

but then starts to fluctuate never reaching the value zero. Improving the weight given in equation (3.59) might improve this behavior.

5.2. Polynomials

In Chapter 3, we several times encountered sums like

$$\sum_{l=\dots}^{\infty} \dots$$

The parameter POLYNOMIALS in the file ‘Control.h’ specifies how many terms of such sums are actually computed, i.e. we replace

$$\sum_{l=\dots}^{\infty} \rightarrow \sum_{l=\dots}^{\text{POLYNOMIALS}}$$

in the GRNS code. Fig. 5.2 shows the result of convergence tests for the three values POLYNOMIALS = 3, 10, 50. The default value is

$$\text{POLYNOMIALS} = 10$$

which is also used for the results of Chapter 6. The convergence behavior visible in Fig. 5.2 is similar to that encountered in Fig. 5.1. The higher modes drop again initially, but eventually begin to fluctuate. The drop is weakest for POLYNOMIALS = 3, because in that case the number of terms taken into account in the sums is at the verge of being sufficient to produce reasonable results.

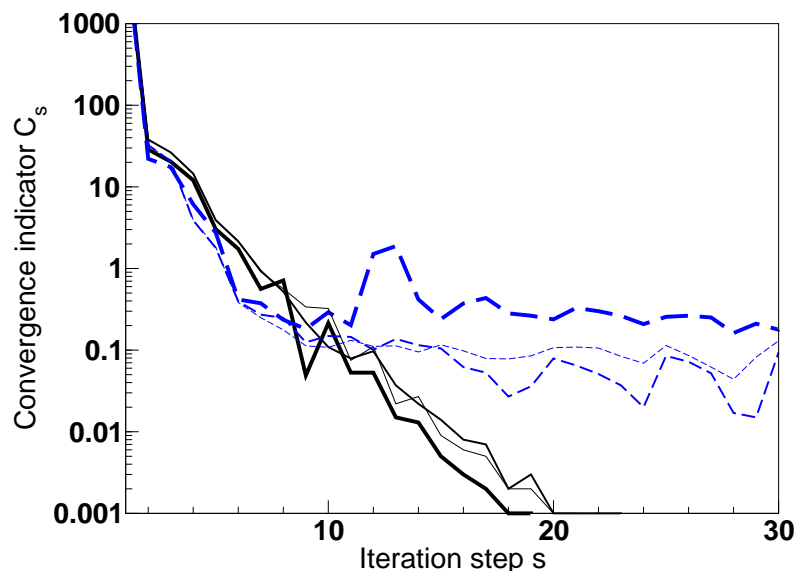


Figure 5.2.: **Polynomials-dependent convergence behavior.** The figure shows the dependence of the convergence indicator C_s defined in equation (4.1) on the number of the iteration step s . The three solid lines refer to the values POLYNOMIALS = 3, 10, 50, where the thickness decreases with the number chosen for that parameter (highest parameter value corresponding to thinnest line). The corresponding blue, dashed lines refer to the first higher mode, respectively.

5.3. Centimeter

As mentioned in equation (2.1), we use geometrized units such that

$$c = 1$$

5. Tests

to express seconds in terms of centimeters and

$$G = 1$$

to do the same for grams. That way, it is possible to write all mathematical quantities used in this investigation in terms of centimeters. However, in a numerical implementation, abstract objects like centimeters cannot be used directly. Instead, we have to map them to numbers. For that purpose, we set

$$1 \text{ cm} = \text{CENTIMETER}$$

where the parameter `CENTIMETER` is a numerical value. The default choice is

$$\text{CENTIMETER} = 1$$

To check the consistency of the GRNS code, we have investigated the choices `CENTIMETER = 10-10` and `CENTIMETER = 1010` without having encountered any problems.

5.4. Grid radius

The last test concerns the parameter `GRID_RADIUS`, which gives the radial size of the numerical grid in terms of centimeters. The default value is

$$\text{GRID_RADIUS} = 10^6$$

which corresponds to a radius of 10 kilometers. We have considered the value `GRID_RADIUS = 6 · 105`, for which the default neutron star of the GRNS code is still fully inside the numerical grid. And, also the value `GRID_RADIUS = 2 · 106` was investigated. In that case the neutron star is small compared to the numerical grid such that effectively the grid resolution is small. This has reduced the quality of the convergence behavior somewhat. However, for all checked values of `GRID_RADIUS` we have not encountered any severe problems.

6. Results

6.1. Assumptions

To close this investigation, we use the GRNS code to actually compute neutron star models. For that purpose, we consider the settings (5.1) and choose the medium resolution of Tab. 5.1:

$$\text{RESOLUTION} = 1$$

In addition to that, we limit ourselves to

$$L(\psi) = 0 \tag{6.1}$$

(see equation (2.60)) in all computations below such that the Lagrangian angular momentum l_ϕ vanishes. Consequently, there will be no azimuthal fluid motion but only a meridional one. We have analyzed other cases than (6.1), too. However, we have not found solutions except for $L(\psi) = \text{const}$. In those cases, the modulus of the azimuthal fluid velocity rises strongly when approaching the symmetry axis. Moreover, this kind of fluid motion has shown a tendency to increase with increasing resolution. Therefore, we are unable to determine whether the solutions found for $L(\psi) = \text{const}$ are truly physical ones. Hence, we restrict ourselves to the case (6.1).

This does not imply that the GRNS code is limited to a purely meridional fluid motion. In principle, it can deal with a mixture of stationary meridional and azimuthal flow. However, in case of objects with spherical topology, nature allows only either a purely azimuthal fluid motion, as already investigated by N. Stergioulas in his RNS code, or only meridional circulation. Possible ways to achieve a mixture of both flows requires a different topology, namely a toroidal one, or the inclusion of the electromagnetic field. A first step towards the latter direction is discussed in Appendix J. However, any further investigation in this direction would go beyond the scope of this thesis.

6.2. Case $f(\psi) = \psi$

6.2.1. Fundamental mode

Having no azimuthal fluid motion, we will present a **meridional circulation mode analysis** as performed in [Eriguchi *et al.* \(1986\)](#), working in the following manner: We choose

$$f(\psi) = \psi$$

and compute the fundamental meridional circulation mode. For that purpose, we start the GRNS code with the initial configuration $(M_r, M_\theta) = (0, 0)$ (see equation (3.56) and the top, left panel of Fig. 3.3) and let it perform 40 fixed point iterations. We use this number of iterations for the higher modes, too. The basic fields describing the fundamental mode are shown in Figs. 6.1, 6.2 (left panel) and 6.3 (upper, left panel).

6. Results

We do not display the 2-shift M^m , because it turns out to be zero everywhere. This is the case for all models computed in this investigation. Moreover, the relative difference between the basic geometry fields α and β is smaller than 10^{-5} , again for all modes. Therefore, we plot only one of the two fields in Fig. 6.1, namely the field α .

Let us have a closer look at Fig. 6.1. The radial size of the numerical grid is 10 kilometers. In that entire region, the basic geometry field ν is negative and the field α positive. Both fields do not vanish on the boundary of the numerical grid, because this happens infinitely far away from the neutron star. Moreover, despite the radial coordinate size being exactly 10 kilometers, the curvature of space has the consequence that the radial physical size

$$r_p(\theta) = \int_0^{r_{\max}} e^{\alpha(r,\theta)} dr$$

of the numerical grid is about 10.1 kilometers. The neutron star itself has only a radius of about 5.7 kilometers, as shown by the lower two panels of Fig. 6.1. These two panels show the total energy density ϵ and the pressure p . Both fields drop to zero at the surface of the neutron star, which is the outermost contour in the two panels. Even though the surface appears to be spherical, the upper panel of Fig. 6.8 shows that the neutron star is somewhat prolate (fraction between polar and equatorial radial coordinate of surface is ≈ 1.004).

The four panels of Fig. 6.1 are nearly identical to the TOV-solution used to start the fixed point iteration (not plotted). Therefore, we continue with the left panel of Fig. 6.2, which shows the 3-shift N^a . In contrast to the TOV-solution, where the 3-shift vector vanishes, there is a significant dragging of spacetime for the fundamental meridional circulation mode. The 3-shift vector N^a is longest at the center of the neutron star and drops to zero at an infinite distance. Moreover, we realize that the vectors in the left panel of Fig. 6.2 roughly follow the contours of the upper, left panel of Fig. 6.3, which shows the basic field χ_0 . The field χ_0 specifies the fluid motion. The fluid moves along the contours of the field χ_0 in a counter-clockwise manner, similar to the 3-shift N^a .

Our fundamental meridional circulation mode is similar to that shown in Fig. 1b of [Eriguchi *et al.* \(1986\)](#). However, it is important to be aware that the upper, left panel of Fig. 6.3 shows the basic field χ_0 , whereas [Eriguchi *et al.* \(1986\)](#) plot the stream function $\psi = r \sin \theta \chi_0$.

6.2.2. Higher modes

Having found the fundamental meridional circulation mode, we are now able to compute the higher modes successively. For that purpose we increase the value of M_θ one by one, i.e. we consider $M_r = 0$ and $M_\theta = \{1, 2, \dots\}$. The initial configurations resulting from equation (3.56) are used to compute the higher modes, respectively. For each mode, the already computed modes provide the quantities ψ_m , applied in equation (3.58) to project lower modes away. The computed modes are shown in Figs. 6.3, 6.4, 6.5 and 6.6, respectively. Each of these modes can be compared to a certain value of the pair (M_r, M_θ) by counting the number of vortices. So, we obtain modes, which belong to $M_r > 0$ even though we have chosen $M_r = 0$ for all initial configurations. In addition to that, we do not obtain the modes in an ordered manner but somewhat randomly. Both effects are a result of the nonlinearity of the field equations. We could also choose, e.g., $M_\theta = 0$ for all initial configurations and select $M_r = \{1, 2, \dots\}$. That way, we would get the same meridional circulation modes, but in a different order. In addition to that, it was necessary to modify some of the modes to compare them with Fig. 3.3 by inverting

the sign of the fields χ_0 and N^a .

Let us have a closer look at Figs. 6.3, 6.4, 6.5 and 6.6, respectively. The upper and lower right panels of Fig. 6.3 are similar to Figs. 1d and 1e of [Eriguchi *et al.* \(1986\)](#). In a likewise manner, we compare the upper, left panel of Fig. 6.5 with Fig. 1c of [Eriguchi *et al.* \(1986\)](#). So, we are able to qualitatively reproduce the results of [Eriguchi *et al.* \(1986\)](#). We have not only computed the four modes of [Eriguchi *et al.* \(1986\)](#) but in total twelve meridional circulation modes.

For the mode shown in the upper, left panel of Fig. 6.5, the right panel of Fig. 6.2 shows the corresponding 3-shift N^a . Obviously, the 3-shift is strongly influenced by the shape of the contours of the field χ_0 . This behavior is valid for all modes. Eventually, we return to Fig. 6.8. There, the lower panel shows the neutron star surface, which contains an additional kink in the equatorial plane compared to the fundamental mode (upper panel). This kink is a result of the inner green vortex of the upper, left panel of Fig. 6.5. This behavior continues on to the other modes, where several kinks can appear on the neutron star surface.

6.3. Case $f(\psi) = 1$

Eventually, we investigate the case

$$f(\psi) = 1 \tag{6.2}$$

for equation (3.57). The resulting basic geometry field χ_0 is shown in Fig. 6.7, which has a shape similar to Fig. 1a of [Eriguchi *et al.* \(1986\)](#). There appears to be only one single mode for (6.2), because the GRNS code fails to compute higher modes. All in all, we have been able to qualitatively reproduce the results of [Eriguchi *et al.* \(1986\)](#) for spherical topology.

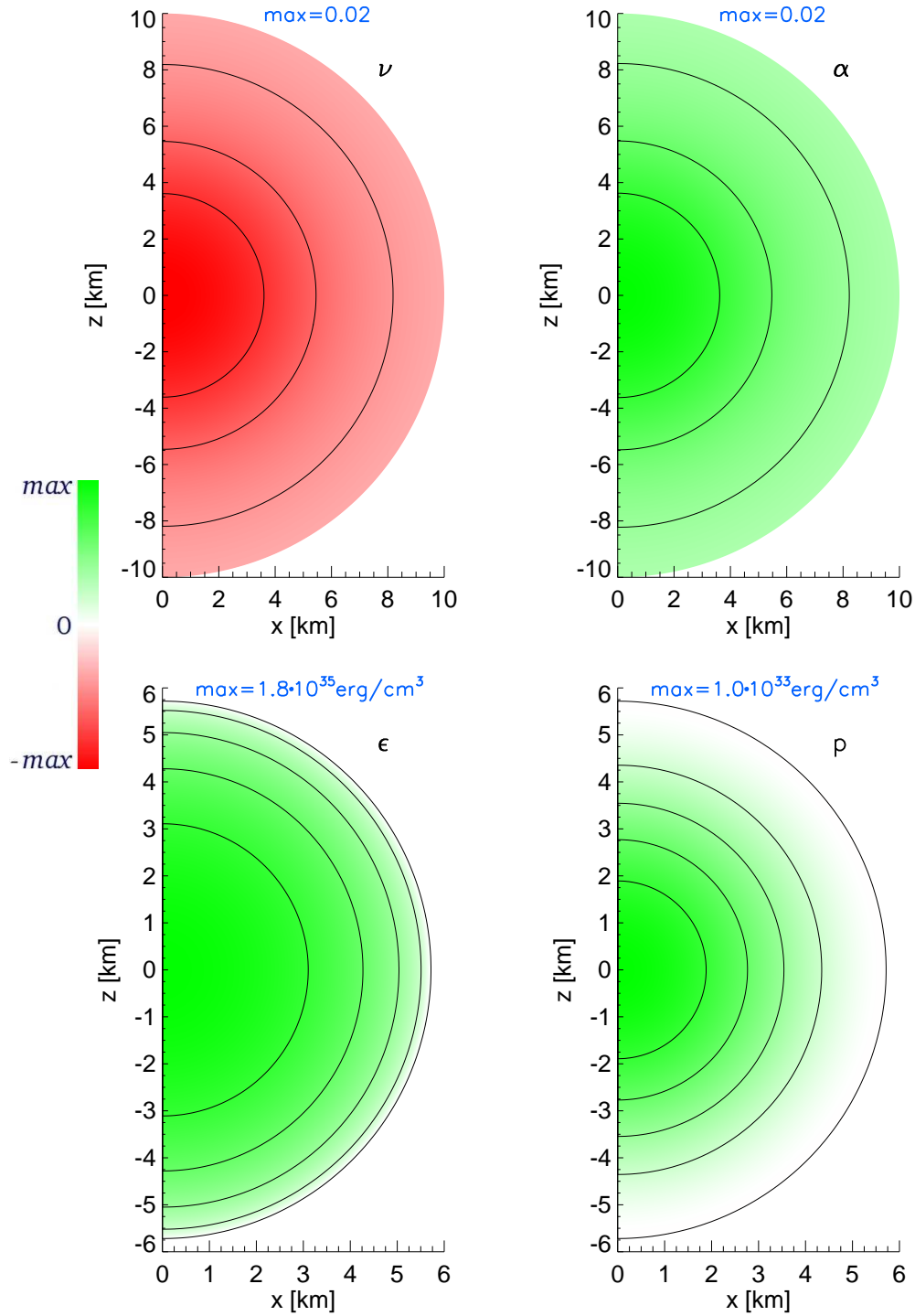


Figure 6.1.: **Basic fields of the fundamental meridional circulation mode.** The upper two panels show the basic geometry fields ν and α of the fundamental meridional circulation mode, and the lower two ones are the corresponding total energy density ϵ and the pressure p . The color coding is similar to the one used in the GRNS code as shown in Fig. 3.3, except that black has been replaced by white. The contours are spaced equidistantly, the distance being a fifth of the maximal absolute field value max , which is shown at the top of each plot (in blue).

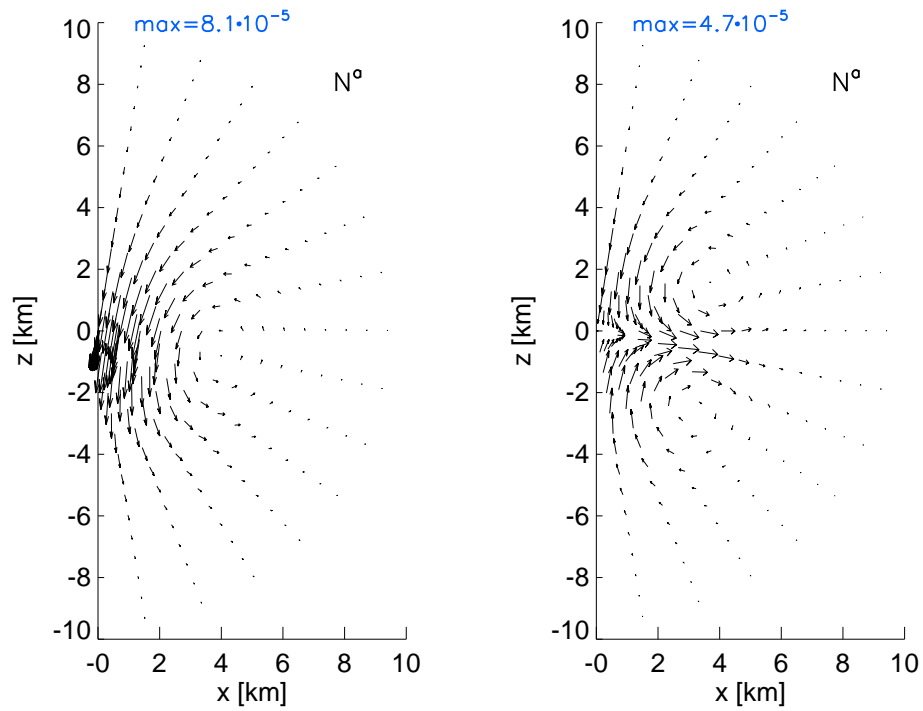


Figure 6.2.: **3-shift N^a for two meridional circulation modes.** The two panels show the 3-shift N^a in the (x, z) -plane for the first two meridional circulation modes spewed out by the GRNS code, i.e. the modes of Figs. 4.1 and 4.2 (=upper two panels of Fig. 6.3). The 3-shift component N^ϕ is zero, and therefore the displayed vectors lie entirely in the meridional (x, z) -plane. The length *max* of the longest displayed vector is given at the top of each panel, respectively (in blue). To increase the visibility, vectors are shown only for a fraction of the actually used grid points.

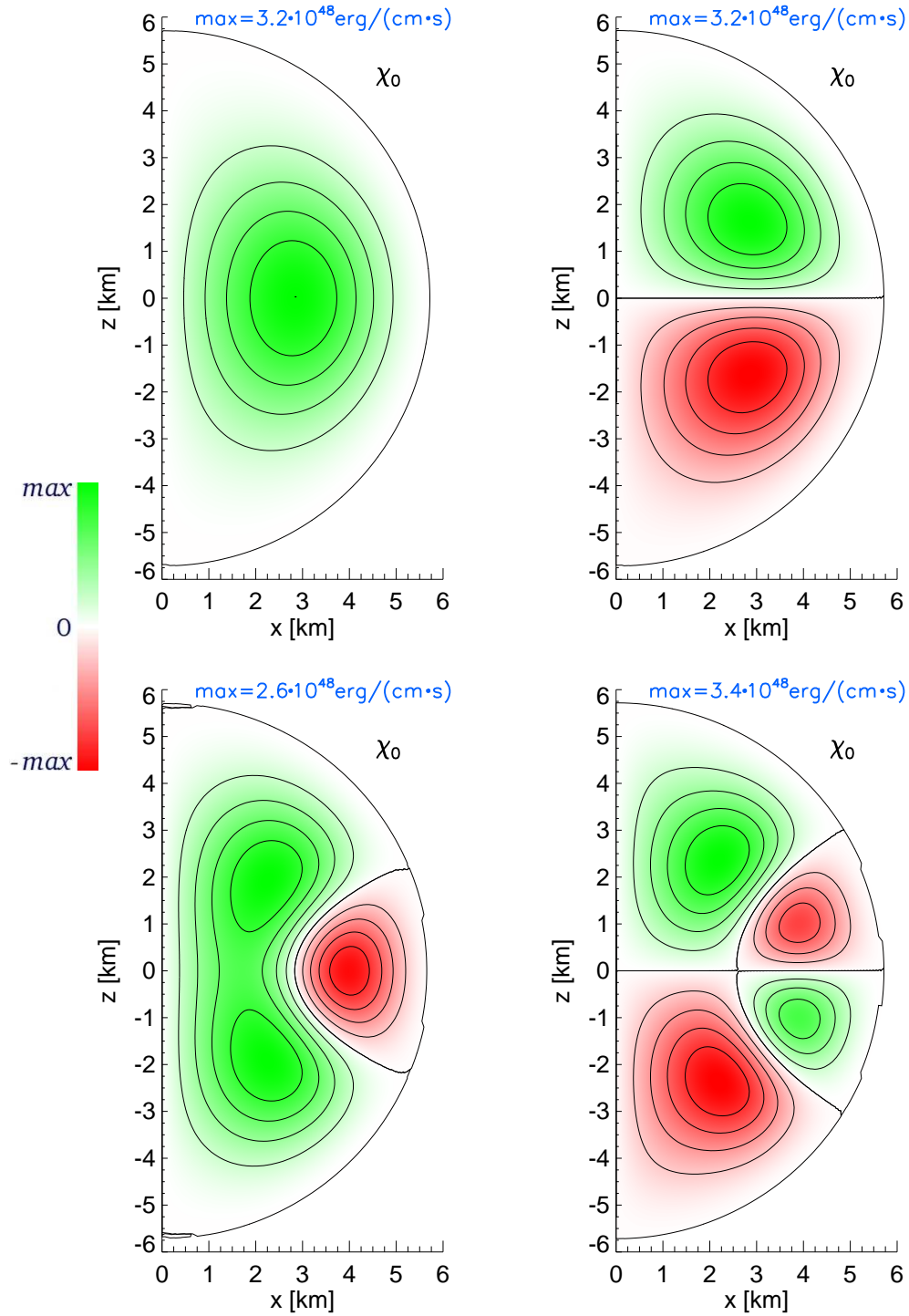


Figure 6.3.: **Basic field χ_0 for different meridional circulation modes belonging to $M_r = 0$.** The four panels show the basic field χ_0 for the first four meridional circulation modes belonging to the initial configurations $M_r = 0$ and $M_\theta = \{0, 1, 2, 3\}$ as given in equation (3.56). The color coding is the same one as in Fig. 6.1. The outermost contour corresponds to the neutron star surface. In the lower two panels, this contour exhibits some kinks which are a result of the finite grid resolution. The upper two panels correspond to the two panels shown in Fig. 6.2.

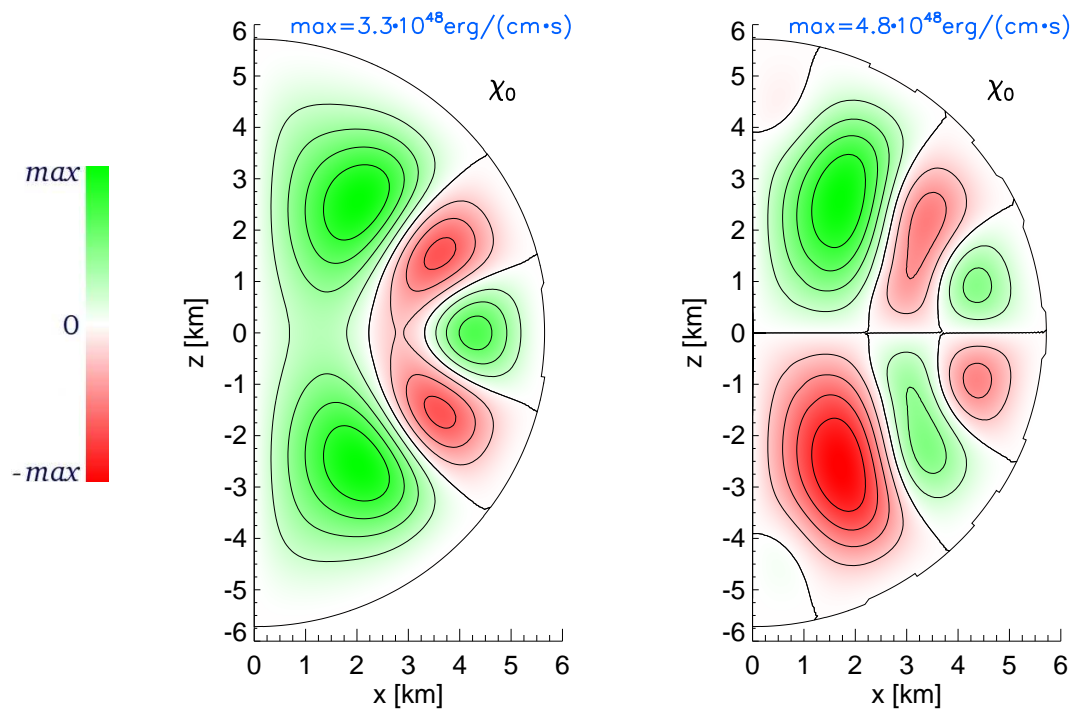


Figure 6.4.: Basic field χ_0 for different meridional circulation modes belonging to $M_r = 0$. Continuation of Fig. 6.3 for $M_\theta = \{4, 5\}$.

6. Results

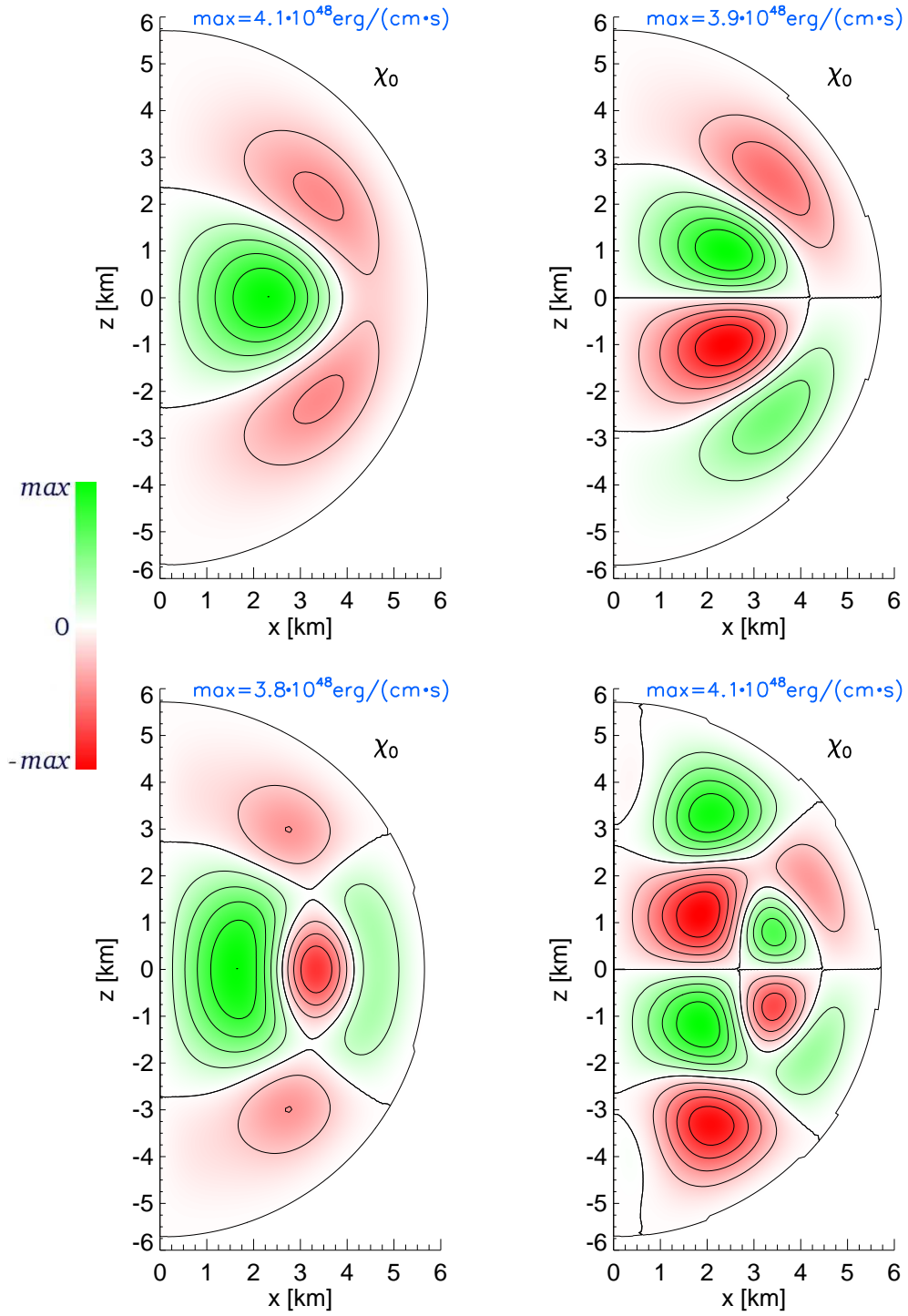


Figure 6.5.: **Basic field χ_0 for different meridional circulation modes belonging to $M_r = 1$.** The panels show the four meridional circulation modes for which $M_r = 1$ and $M_\theta = \{0, 1, 2, 3\}$. The color coding is the same one as in Fig. 6.3.

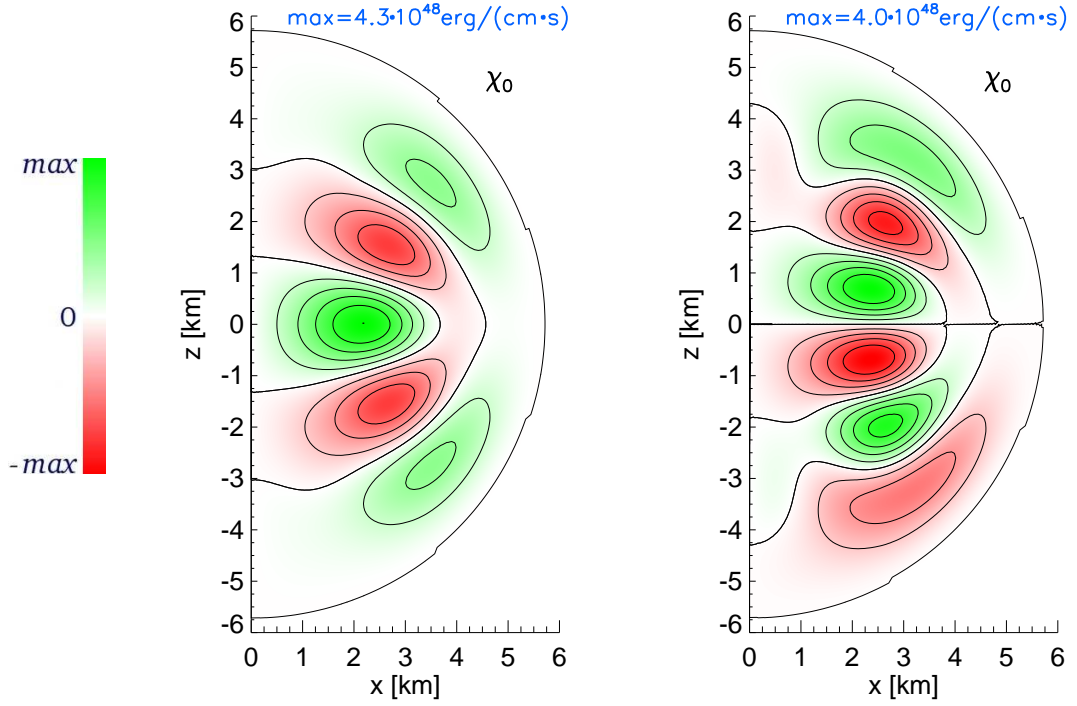


Figure 6.6.: **Basic field χ_0 for different meridional circulation modes belonging to $M_r = 2$.** The panels show the two meridional circulation modes for which $M_r = 2$ and $M_\theta = \{0, 1\}$. The color coding is the same one as in Fig. 6.3.

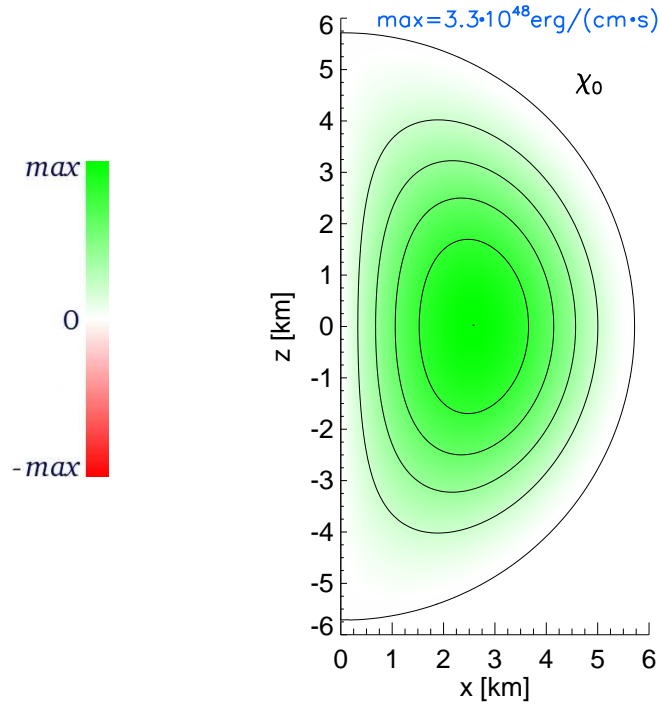


Figure 6.7.: **Basic field χ_0 for the case $f(\psi) = 1$.** The color coding is the same one as in Fig. 6.3.

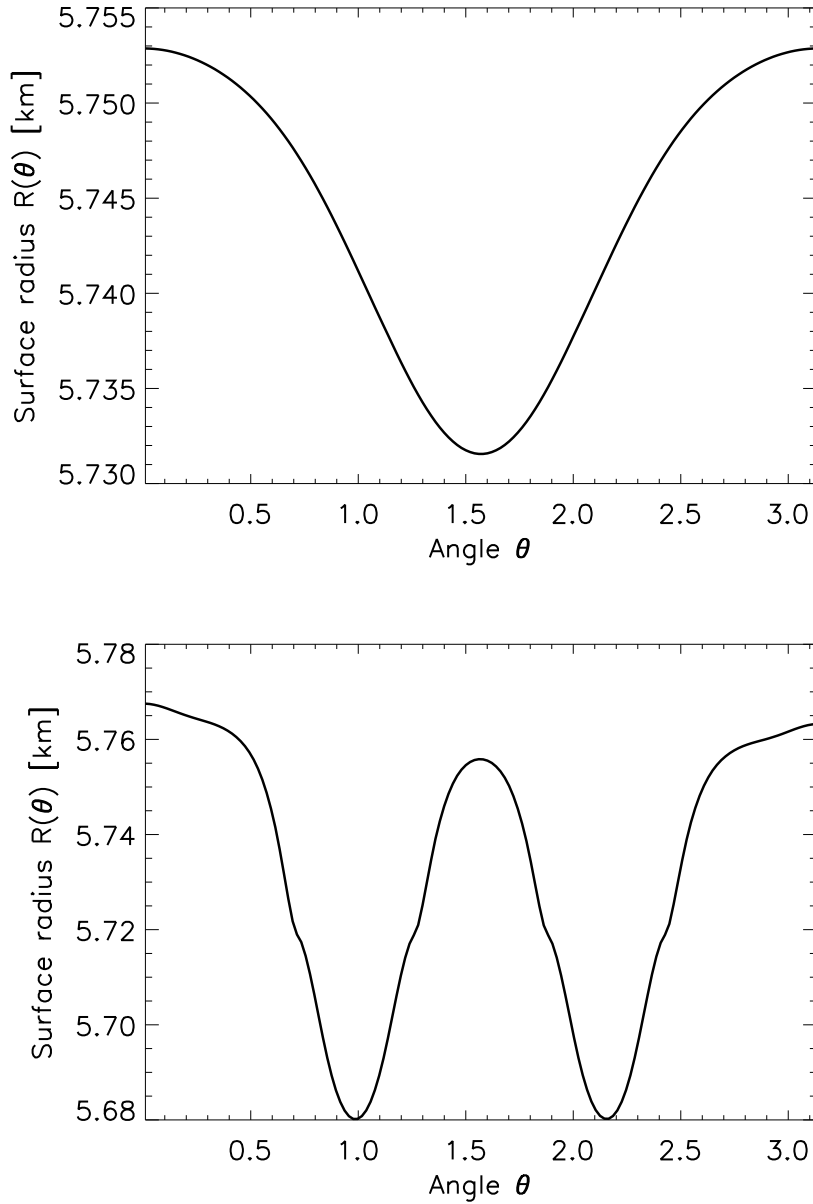


Figure 6.8.: **Surface radius.** The two plots show the surface radius $R(\theta)$ for the fundamental meridional circulation mode $(M_r, M_\theta) = (0, 0)$ (upper, left plot of Fig. 6.3) and the mode $(M_r, M_\theta) = (1, 1)$ (upper, right plot of Fig. 6.5). The surface deformations in the lower plot are responsible for the two dents visible in the outermost contour of the upper, right plot of Fig. 6.5.

7. Conclusions

We have computed the first stationary, axisymmetric neutron star models with meridional circulation in the framework of general relativity. For that purpose, we have constructed the GRNS code, a new code, which uses a fixed point iteration method starting from a Tolman-Oppenheimer-Volkoff-like initial configuration, similarly to the RNS code of N. Stergioulas.

We took the method of Komatsu *et al.* (1989), used in the RNS code and applicable only to purely azimuthal fluid motions, and generalized it to include also meridional ones, based on the theoretical considerations of Gourgoulhon & Bonazzola (1993). This was possible, because we were able to rewrite the metric equations of Gourgoulhon & Bonazzola (1993) as Poisson equations in flat space, and we found Green functions for each of these equations. In contrast to the RNS code, we had to explicitly take slicing conditions into account, and we had to perform additional gauge fixing conditions not investigated in Gourgoulhon & Bonazzola (1993). For the matter equations, we extended the Newtonian stream function method of Eriguchi *et al.* (1986) to general relativity. However, we did not adopt the Newton-Raphson iteration scheme used by these authors but extended the fixed point iteration method to hydrodynamics. The RNS code allowing only a command line interaction, we created an OpenGL user interface for the GRNS code. This interface allows the user to directly control the fixed point iteration method and to oversee the status of all physical fields in real-time. This approach was not only helpful in the debugging phase, it also helped to solve several issues which prevented convergence of the fixed point iteration at first stage.

As the RNS code is restricted to azimuthal fluid motions, our initial goal was to use the GRNS code to compute neutron star models with a mixture of both azimuthal and meridional fluid motions. However, we were unable to find valid such solutions, not even some which obey the angular momentum conditions studied by Randers (1941) and Roxburgh (1974). Therefore, we focused on an investigation of purely meridional circulation modes as done in the Newtonian case by Eriguchi *et al.* (1986). Due to the chosen fixed point iteration method, we were able to compute these modes in a very automatized manner, not requiring manual parameter adjustments as done by Eriguchi *et al.* (1986). However, to find higher modes during the fixed point iteration, we had to develop a method to project lower modes away.

To validate the GRNS code, we performed several convergence and consistency tests. We investigated different resolutions of the used numerical grid and found a sufficient convergence behavior for all modes. For the higher modes, the fixed point iteration ends in a fluctuating state rather early. Such situations are also known from the RNS code and not problematic. In our case, the reason for the fluctuations is possibly an inaccuracy of the method to project lower modes away. Similarly to the RNS code, we have rewritten integrals used for the Green function method as sums containing Legendre polynomials. We conducted convergence tests for different numbers of such polynomials taken into account in the GRNS code.

Eventually, we used the GRNS code to perform a meridional circulation mode analysis

7. Conclusions

similar to [Eriguchi *et al.* \(1986\)](#). We found the same qualitative behavior as these authors in the case of spherical topology. However, we were not able to perform a quantitative comparison, because of the rather low numerical resolution used by [Eriguchi *et al.* \(1986\)](#). Our automatized mode computation allowed us to find a dozen of modes with a sufficient convergence behavior, being decisively more than those found by [Eriguchi *et al.* \(1986\)](#). That way, we were able to identify a two-dimensional classification of the meridional circulation modes, different from the one found by [Eriguchi *et al.* \(1986\)](#).

There are clear perspectives for a future application of the outcomes of this investigation. Perturbing the obtained modes, a dynamical evolution of the neutron star can show the influence of meridional circulations on gravitational waves, for which a direct detection is expected in the near future and which are thus a topic currently of widespread interest in relativistic astrophysics. Another application is investigating the influence of meridional circulations on neutron star oscillations, which can be observed in the electromagnetic spectrum. Both methods offer a way to experimentally determine whether meridional circulations are present in neutron stars. At the current stage we are not able to eventually determine how widespread such circulations are in nature, because in our approach we were unable to evaluate stability criteria of the circulation modes.

At the moment, the GRNS code supports only polytropic equations of state. An extension to barotropes is straightforward and requires only a more general specification of the total energy density function in the code. However, a generalization to baroclinic equations of state is not that easy and would require a completely different approach. This is not even investigated in the Newtonian case, where [Eriguchi *et al.* \(1986\)](#) have thought in that direction but never succeeded. Due to having generalized the stream function method of [Eriguchi *et al.* \(1986\)](#) and not having applied the approach of [Komatsu *et al.* \(1989\)](#) for the hydrodynamical part of the field equations, the GRNS code is not able to reproduce the models of the RNS code. In principle, it is possible to extend the GRNS code to these models even with the stream function method. For that purpose, a constraint on the Lagrangian angular momentum has to be solved. We have not proceeded in that direction, because this case has already been investigated extensively with the RNS code.

In the near future, several other ways to go beyond the scope of this investigation will be important. Originally intended only for spherical topologies, N. Stergioulas has extended the RNS code to toroidal ones, which are also investigated by [Eriguchi *et al.* \(1986\)](#) in their meridional circulation mode analysis. A similar generalization for the GRNS code will overcome the angular momentum issue found by [Randers \(1941\)](#) and [Roxburgh \(1974\)](#) and might thus allow for a mixture of azimuthal and meridional fluid motions. Another step in that direction is the inclusion of a magnetic field. We have already made a few thoughts in that direction and our theoretical calculations done in that context show the principle way to go. We have found that the field equation for the Lagrangian angular momentum is strongly affected by the magnetic field. Hence, it could be possible that magnetic fields allow a mixture of both fluid motion types even for spherical topologies.

A. Christoffel symbols of the first kind

A.1. 2-surfaces $\Sigma_{t\phi}$

The Christoffel symbols of the first kind on the 2-surfaces $\Sigma_{t\phi}$ of constant time t and constant angle ϕ are given by equation (2.31) as

$${}^2\Gamma_{mno} = \frac{1}{2} (\partial_n k_{mo} + \partial_o k_{nm} - \partial_m k_{no})$$

with the 2-metric k_{mn} . Due to the symmetry ${}^2\Gamma_{mno} = {}^2\Gamma_{mon}$, the only relevant components are

$$\begin{aligned} {}^2\Gamma_{rrr} &= \frac{1}{2} (\partial_r k_{rr} + \partial_r k_{rr} - \partial_r k_{rr}) \\ {}^2\Gamma_{rr\theta} &= \frac{1}{2} (\partial_r k_{r\theta} + \partial_\theta k_{rr} - \partial_r k_{r\theta}) \\ {}^2\Gamma_{r\theta\theta} &= \frac{1}{2} (\partial_\theta k_{r\theta} + \partial_\theta k_{\theta r} - \partial_r k_{\theta\theta}) \\ {}^2\Gamma_{\theta rr} &= \frac{1}{2} (\partial_r k_{\theta r} + \partial_r k_{r\theta} - \partial_\theta k_{rr}) \\ {}^2\Gamma_{\theta r\theta} &= \frac{1}{2} (\partial_r k_{\theta\theta} + \partial_\theta k_{r\theta} - \partial_\theta k_{r\theta}) \\ {}^2\Gamma_{\theta\theta\theta} &= \frac{1}{2} (\partial_\theta k_{\theta\theta} + \partial_\theta k_{\theta\theta} - \partial_\theta k_{\theta\theta}) \end{aligned}$$

Using the choice (2.19) for the meridional coordinates, they simplify to

${}^2\Gamma_{rrr}$	$=$	$\frac{1}{2}\partial_r k_{rr}$
${}^2\Gamma_{rr\theta}$	$=$	$\frac{1}{2}\partial_\theta k_{rr}$
${}^2\Gamma_{\theta r\theta}$	$=$	$\frac{1}{2}\partial_r k_{\theta\theta}$
${}^2\Gamma_{\theta\theta\theta}$	$=$	$\frac{1}{2}\partial_\theta k_{\theta\theta}$
${}^2\Gamma_{r\theta\theta}$	$=$	$-{}^2\Gamma_{\theta r\theta}$
${}^2\Gamma_{\theta rr}$	$=$	$-{}^2\Gamma_{rr\theta}$

A. Christoffel symbols of the first kind

A.2. 3-surfaces Σ_t

The Christoffel symbols of the first kind on the 3-surfaces Σ_t of constant time t are defined by equation (2.30) as

$${}^3\Gamma_{abc} = \frac{1}{2}(\partial_b h_{ac} + \partial_c h_{ba} - \partial_a h_{bc})$$

with the 3-metric h_{ab} . These Christoffel symbols do not only have the symmetry ${}^3\Gamma_{abc} = {}^3\Gamma_{acb}$, they also obey ${}^3\Gamma_{mno} = {}^2\Gamma_{mno}$. Therefore, we have to consider only the components

$$\begin{aligned} {}^3\Gamma_{rr\phi} &= \frac{1}{2}(\partial_r h_{r\phi} + \partial_\phi h_{rr} - \partial_r h_{r\phi}) \\ {}^3\Gamma_{r\theta\phi} &= \frac{1}{2}(\partial_\theta h_{r\phi} + \partial_\phi h_{\theta r} - \partial_r h_{\theta\phi}) \\ {}^3\Gamma_{r\phi\phi} &= \frac{1}{2}(\partial_\phi h_{r\phi} + \partial_\phi h_{\phi r} - \partial_r h_{\phi\phi}) \\ {}^3\Gamma_{\theta r\phi} &= \frac{1}{2}(\partial_r h_{\theta\phi} + \partial_\phi h_{r\theta} - \partial_\theta h_{r\phi}) \\ {}^3\Gamma_{\theta\theta\phi} &= \frac{1}{2}(\partial_\theta h_{\theta\phi} + \partial_\phi h_{\theta\theta} - \partial_\theta h_{\theta\phi}) \\ {}^3\Gamma_{\theta\phi\phi} &= \frac{1}{2}(\partial_\phi h_{\theta\phi} + \partial_\phi h_{\phi\theta} - \partial_\theta h_{\phi\phi}) \\ {}^3\Gamma_{\phi rr} &= \frac{1}{2}(\partial_r h_{\phi r} + \partial_r h_{r\phi} - \partial_\phi h_{rr}) \\ {}^3\Gamma_{\phi r\theta} &= \frac{1}{2}(\partial_r h_{\phi\theta} + \partial_\theta h_{r\phi} - \partial_\phi h_{r\theta}) \\ {}^3\Gamma_{\phi r\phi} &= \frac{1}{2}(\partial_r h_{\phi\phi} + \partial_\phi h_{r\phi} - \partial_\phi h_{r\phi}) \\ {}^3\Gamma_{\phi\theta\theta} &= \frac{1}{2}(\partial_\theta h_{\phi\theta} + \partial_\theta h_{\theta\phi} - \partial_\phi h_{\theta\theta}) \\ {}^3\Gamma_{\phi\theta\phi} &= \frac{1}{2}(\partial_\theta h_{\phi\phi} + \partial_\phi h_{\theta\phi} - \partial_\phi h_{\theta\phi}) \\ {}^3\Gamma_{\phi\phi\phi} &= \frac{1}{2}(\partial_\phi h_{\phi\phi} + \partial_\phi h_{\phi\phi} - \partial_\phi h_{\phi\phi}) \end{aligned}$$

Considering axisymmetry, we can simplify them to

$${}^3\Gamma_{r\theta\phi} = \frac{1}{2}(\partial_\theta h_{r\phi} - \partial_r h_{\theta\phi})$$

$${}^3\Gamma_{\phi r\theta} = \frac{1}{2}(\partial_\theta h_{r\phi} + \partial_r h_{\theta\phi})$$

$${}^3\Gamma_{r\phi\phi} = -\frac{1}{2}\partial_r h_{\phi\phi}$$

$${}^3\Gamma_{\theta\phi\phi} = -\frac{1}{2}\partial_\theta h_{\phi\phi}$$

$${}^3\Gamma_{\phi rr} = \partial_r h_{r\phi}$$

$${}^3\Gamma_{\phi\theta\theta} = \partial_\theta h_{\theta\phi}$$

$${}^3\Gamma_{\theta r\phi} = -{}^3\Gamma_{r\theta\phi}$$

$${}^3\Gamma_{\phi r\phi} = -{}^3\Gamma_{r\phi\phi}$$

$${}^3\Gamma_{\phi\theta\phi} = -{}^3\Gamma_{\theta\phi\phi}$$

A. Christoffel symbols of the first kind

B. Derivation of correct 3-lapse equation

In our thesis, we have to use equation (B3) of Gourgoulhon & Bonazzola (1993) to compute the 3-lapse N . Unfortunately, there is a mistake in that equation. Therefore, we will rederive it, here. For that purpose, we will frequently refer to the equations in Gourgoulhon & Bonazzola (1993). Such references are denoted by (GB...), i.e., for example, equation (B3) of Gourgoulhon & Bonazzola (1993) will be referenced merely as (GBB3). In addition to that, we recall our index convention $\alpha, \beta, \dots, \omega \in \{t, r, \theta, \phi\}$, $a, b, \dots, l \in \{r, \theta, \phi\}$ and $m, n, \dots, q \in \{r, \theta\}$, which differs from the one of Gourgoulhon & Bonazzola (1993), slightly. Note that this Appendix is a self-contained part, i.e., we do not refer to quantities defined in the rest of this thesis, because then the reader only requires the paper of Gourgoulhon & Bonazzola (1993) to reproduce the computations.

We start with equation (GB2a)

$$\nu = \ln N$$

which leads to

$$\frac{1}{N}N_{,m} = \nu_{,m} \quad (\text{B.1})$$

Hence,

$$\frac{1}{N}N_{,mn} = \frac{1}{N}(N\nu_{,m})_{,n} = \nu_{,mn} + \nu_{,m}\nu_{,n} \quad (\text{B.2})$$

Likewise, equation (GBB2e)

$$\mu = \ln M$$

results in

$$\frac{1}{M}M_{,m} = \mu_{,m} \quad (\text{B.3})$$

Next, equation (GB3.7) tells us that the 2-metric is

$$k_{mn} = A^2 \begin{pmatrix} 1 & 0 \\ 0 & r^2 \end{pmatrix} \quad (\text{B.4})$$

such that

$$k^{mn} = \frac{1}{A^2} \begin{pmatrix} 1 & 0 \\ 0 & \frac{1}{r^2} \end{pmatrix} \quad (\text{B.5})$$

In the following computation, the above relations are used. This computation takes place on the hypersurfaces Σ_t of constant time t . Therefore, we use only spatial indices a, b, \dots , and the 3-metric h_{ab} has to be used for raising and lowering tensor indices. In addition to that, we are aware that this metric commutes with the 3-covariant derivative $[\]$ as defined in (GB2.5). Then, we obtain

$$\begin{aligned} \frac{1}{N}N^{|a}{}_{|a} &= \frac{1}{N}h^{ab}N_{|ab} \\ &= \frac{1}{N}\left(h^{ab}N_{|a}\right)_{|b} \end{aligned}$$

B. Derivation of correct 3-lapse equation

$$\begin{aligned}
&\stackrel{\text{(GB2.5)}}{=} \frac{1}{N} \left(h^{ab} h_a^\gamma N_{,\gamma} \right)_{|b} \\
&\stackrel{\text{stationarity}}{=} \frac{1}{N} \left(h^{ab} h_a^c N_{,c} \right)_{|b} \\
&= \frac{1}{N} \left(h^{ab} N_{,a} \right)_{|b} \\
&= \frac{1}{N} h^{ab} N_{,a|b} \\
&= \frac{1}{N} h^{ab} \left(N_{,ab} - {}^3 \Gamma_{ab}^c N_{,c} \right) \\
&\stackrel{\text{axisymmetry}}{=} \frac{1}{N} \left(h^{mn} N_{,mn} - h^{ab} \Gamma_{ab}^m N_{,m} \right) \\
&\stackrel{\text{(GB2.20), (B.2)}}{=} \left(k^{mn} + m^m m^n \right) \left(\nu_{,mn} + \nu_{,m} \nu_{,n} \right) \\
&\quad - \frac{N_{,m}}{2N} h^{ab} h^{cm} \left(h_{cb,a} + h_{ac,b} - h_{ab,c} \right) \\
&\stackrel{\text{(B.1)}}{=} k^{mn} \nu_{,mn} + \left(k^{mn} + m^m m^n \right) \nu_{,m} \nu_{,n} + m^m m^n \nu_{,mn} \\
&\quad + \nu_{,m} h^{ab} h^{cm} \left(\frac{1}{2} h_{ab,c} - h_{ac,b} \right) \\
&\stackrel{\text{(B.5), axisymmetry}}{=} \frac{1}{A^2} \left(\nu_{,rr} + \frac{\nu_{,\theta\theta}}{r^2} \right) + \left[\frac{1}{A^2} + (m^r)^2 \right] (\nu_{,r})^2 \\
&\quad + \left[\frac{1}{(rA)^2} + (m^\theta)^2 \right] (\nu_{,\theta})^2 \\
&\quad + (m^r)^2 \nu_{,rr} + 2m^r m^\theta \nu_{,r\theta} + (m^\theta)^2 \nu_{,\theta\theta} \\
&\quad + \nu_{,m} \left(\frac{1}{2} h^{ab} h^{mn} h_{ab,n} - h^{am} h^{bn} h_{ab,n} \right) \\
&\quad + 2m^r m^\theta \nu_{,r} \nu_{,\theta} \tag{B.6}
\end{aligned}$$

The first three lines after the last equality sign appear on the left hand side of equation (GBB3), too. Therefore, we focus on the last two lines, where the first one can be rewritten to

$$\begin{aligned}
&\nu_{,m} \left(\frac{1}{2} h^{ab} h^{mn} h_{ab,n} - h^{am} h^{bn} h_{ab,n} \right) \\
&= \nu_{,m} \left(\frac{1}{2} h^{op} h^{mn} h_{op,n} + h^{o3} h^{mn} h_{o3,n} + \frac{1}{2} h^{33} h^{mn} h_{33,n} \right. \\
&\quad \left. - h^{om} h^{pn} h_{op,n} - h^{om} h^{3n} h_{o3,n} - h^{3m} h^{on} h_{3o,n} - h^{3m} h^{3n} h_{33,n} \right) \\
&\stackrel{\text{(GB2.20), (GB2.25), (GB2.24)}}{=} \nu_{,m} \left[\frac{1}{2} (k^{op} + m^o m^p) (k^{mn} + m^m m^n) k_{op,n} - \frac{m^o}{M} (k^{mn} + m^m m^n) M_{o,n} \right. \\
&\quad + \frac{1}{2M^2} (k^{mn} + m^m m^n) (M^2 + M_o M^o)_{,n} \\
&\quad - (k^{om} + m^o m^m) (k^{pn} + m^p m^n) k_{op,n} \\
&\quad \left. + (k^{om} + m^o m^m) \frac{m^n}{M} M_{o,n} + \frac{m^m}{M} (k^{on} + m^o m^n) M_{o,n} \right]
\end{aligned}$$

$$\begin{aligned}
& \left[-\frac{m^m m^n}{M^2} (M^2 + M_o M^o)_{,n} \right] \\
= & \nu_{,m} \left[\frac{1}{2} k^{op} (k^{mn} + m^m m^n) k_{op,n} + \frac{1}{2} m^o m^p k^{mn} k_{op,n} \right. \\
& + \frac{1}{2} m^o m^p m^m m^n k_{op,n} - k^{om} (k^{pn} + m^p m^n) k_{op,n} - m^o m^m k^{pn} k_{op,n} \\
& - m^o m^m m^p m^n k_{op,n} \\
& + (-m^o k^{mn} + k^{om} m^n + m^m k^{on} + m^m m^n m^o) \frac{M_{o,n}}{M} \\
& \left. + \frac{1}{2M^2} k^{mn} (M^2 + M_o M^o)_{,n} - \frac{m^m m^n}{2M^2} (M^2 + M_o M^o)_{,n} \right] \\
\stackrel{(GB2.24)}{=} & \nu_{,m} \left[\frac{1}{2} k^{op} (k^{mn} + m^m m^n) k_{op,n} + \frac{1}{2} m^o m^p k^{mn} k_{op,n} \right. \\
& - \frac{1}{2} m^m m^n m^o m^p k_{op,n} - k^{om} (k^{pn} + m^p m^n) k_{op,n} - m^o m^m k^{pn} k_{op,n} \\
& + \left(-\frac{1}{2} m^o k^{mn} + k^{om} m^n + m^m k^{on} + \frac{1}{2} m^m m^n m^o \right) \frac{(k_{op} M^p)_{,n}}{M} \\
& + k^{mn} \frac{M_{,n}}{M} + \frac{1}{2M^2} k^{mn} M_o M^o_{,n} \\
& \left. - m^m m^n \frac{M_{,n}}{M} - \frac{1}{2M^2} m^m m^n M_o M^o_{,n} \right] \\
\stackrel{(GB2.20), (B.3)}{=} & \nu_{,m} \left[\frac{1}{2} k^{op} (k^{mn} + m^m m^n) k_{op,n} + \frac{1}{2} m^o m^p k^{mn} k_{op,n} \right. \\
& - \frac{1}{2} m^m m^n m^o m^p k_{op,n} - k^{om} (k^{pn} + m^p m^n) k_{op,n} - m^o m^m k^{pn} k_{op,n} \\
& + \left(-\frac{1}{2} m^o k^{mn} + k^{om} m^n + m^m k^{on} + \frac{1}{2} m^m m^n m^o \right) k_{op,n} m^p \\
& + \left(-\frac{1}{2} m^o k^{mn} + k^{om} m^n + m^m k^{on} + \frac{1}{2} m^m m^n m^o \right) k_{op} \frac{M^p_{,n}}{M} \\
& + k^{mn} \mu_{,n} + \frac{1}{2M^2} k^{mn} k_{op} M^p M^o_{,n} \\
& \left. - m^m m^n \frac{M_{,n}}{M} - \frac{1}{2M^2} m^m m^n k_{op} M^p M^o_{,n} \right] \\
= & \nu_{,m} \left[\frac{1}{2} k^{op} (k^{mn} + m^m m^n) k_{op,n} - k^{om} k^{pn} k_{op,n} \right. \\
& \left. + (k^{om} m^n + m^m k^{on}) k_{op} \frac{M^p_{,n}}{M} + k^{mn} \mu_{,n} - m^m m^n \frac{M_{,n}}{M} \right] \\
\stackrel{(GB2.24)}{=} & \nu_{,m} \left[\frac{1}{2} k^{op} (k^{mn} + m^m m^n) k_{op,n} - k^{om} k^{pn} k_{op,n} \right. \\
& + (\delta_o^m m^n + m^m \delta_o^n) m^o_{,n} - (\delta_o^m m^n + m^m \delta_o^n) M^o \left(\frac{1}{M} \right)_{,n} \\
& \left. + k^{mn} \mu_{,n} - m^m m^n \frac{M_{,n}}{M} \right] \\
\stackrel{(GB2.24)}{=} & \nu_{,m} \left[\frac{1}{2} k^{op} (k^{mn} + m^m m^n) k_{op,n} - k^{om} k^{pn} k_{op,n} \right.
\end{aligned}$$

B. Derivation of correct 3-lapse equation

$$\begin{aligned}
& \left. + m^n m^m{}_{,n} + m^m m^n{}_{,n} + m^n m^m \frac{M_{,n}}{M} + k^{mn} \mu_{,n} \right] \\
\stackrel{\text{(GB2.24)}}{=} & k^{mn} \nu_{,m} \mu_{,n} + m^n m^r{}_{,n} \nu_{,r} + m^n m^\theta{}_{,n} \nu_{,\theta} \\
& + \nu_{,m} \left(\frac{1}{2} k^{op} k^{mn} k_{op,n} - k^{om} k^{pn} k_{op,n} \right) \\
& + m^m \nu_{,m} \left[\left(\frac{M^n}{M} \right)_{,n} - M^n \left(\frac{1}{M} \right)_{,n} + \frac{1}{2} k^{op} m^n (k_{op,n} + k_{no,p} - k_{no,p}) \right] \\
\stackrel{\text{(GB2.24)}, \text{(B.5)}}{=} & \frac{1}{A^2} \left(\mu_{,r} \nu_{,r} + \frac{\mu_{,\theta} \nu_{,\theta}}{r^2} \right) + \left(m^r m^r{}_{,r} + m^\theta m^r{}_{,\theta} \right) \nu_{,r} \\
& + \left(m^r m^\theta{}_{,r} + m^\theta m^\theta{}_{,\theta} \right) \nu_{,\theta} + \nu_{,m} \left(\frac{1}{2} k^{op} k^{mn} - k^{om} k^{pn} \right) k_{op,n} \\
& + m^m \nu_{,m} \left(\frac{M^n}{M} + k^{op} \frac{M^n}{M} \Gamma_{pno} \right) \tag{B.7}
\end{aligned}$$

Here, the first three terms in round brackets can be found on the left hand side of equation (GBB3). The term in the subsequent round bracket simplifies to

$$\begin{aligned}
& \nu_{,m} \left(\frac{1}{2} k^{op} k^{mn} - k^{om} k^{pn} \right) k_{op,n} \\
\stackrel{\text{(B.4)}, \text{(B.5)}}{=} & \nu_{,m} \left(\frac{1}{2A^2} k^{mn} - k^{rm} k^{rn} \right) (A^2)_{,n} + \nu_{,m} \left[\frac{1}{2(rA)^2} k^{mn} - k^{\theta m} k^{\theta n} \right] (r^2 A^2)_{,n} \\
\stackrel{\text{(B.5)}}{=} & \nu_{,m} \frac{1}{A^2} k^{mn} (A^2)_{,n} - \nu_{,r} \frac{1}{A^4} (A^2)_{,r} \\
& + \nu_{,m} \frac{1}{2r^2} k^{mn} (r^2)_{,n} - \nu_{,\theta} \frac{1}{(rA)^4} (r^2 A^2)_{,\theta} \\
= & \nu_{,m} \frac{1}{2r^2} k^{mn} (r^2)_{,n} \\
= & \frac{\nu_{,r}}{rA^2}
\end{aligned}$$

In addition to that, the last line in equation (B.7) can be rewritten to

$$\begin{aligned}
& m^m \nu_{,m} \left(\frac{M^n}{M} + k^{op} \frac{M^n}{M} \Gamma_{pno} \right) \\
\stackrel{\text{(GB2.24)}, \text{(B.1)}}{=} & \frac{M^m}{NM} N_{,m} \frac{1}{M} \left(k_n^o M^n{}_{,o} + k^{\alpha\beta} M^\gamma \Gamma_{\alpha\beta\gamma} \right) \\
\stackrel{\text{(GB2.22)}, \text{stationarity, axisymmetry}}{=} & \frac{M^\alpha}{NM} N_{,\alpha} \frac{1}{M} k_\gamma^\delta \left(M^\gamma{}_{,\delta} + \Gamma_{\delta\epsilon}^\gamma M^\epsilon \right) \\
= & \frac{M^\alpha}{NM} k_\alpha^\beta N_{;\beta} \frac{1}{M} k_\gamma^\delta M^\gamma{}_{;\delta} \\
\stackrel{\text{(GB2.21)}}{=} & \frac{M^\alpha}{NM} N_{||\alpha} \frac{1}{M} M^\beta{}_{||\beta} \\
\stackrel{\text{(GB2.36)}, \text{stationarity, axisymmetry}}{=} & -L \frac{M^m}{NM} N_{||m} \\
\stackrel{\text{(GB3.10)}}{=} & -\frac{L^2}{2}
\end{aligned}$$

Hence, equation (B.7) becomes

$$\begin{aligned}
& \nu_{,m} \left(\frac{1}{2} h^{ab} h^{mn} h_{ab,n} - h^{am} h^{bn} h_{ab,n} \right) \\
&= \frac{1}{A^2} \left[\left(\frac{1}{r} + \mu_{,r} \right) \nu_{,r} + \frac{\mu_{,\theta} \nu_{,\theta}}{r^2} \right] \\
& \quad + \left(m^r m^r_{,r} + m^\theta m^r_{,\theta} \right) \nu_{,r} + \left(m^r m^\theta_{,r} + m^\theta m^\theta_{,\theta} \right) \nu_{,\theta} - \frac{L^2}{2}
\end{aligned}$$

We insert this result in equation (B.6) and arrive at

$$\begin{aligned}
& \frac{1}{N} N^{|a}{}_a \\
&= \frac{1}{A^2} \left[\nu_{,rr} + \left(\frac{1}{r} + \mu_{,r} \right) \nu_{,r} + \frac{\nu_{,\theta\theta}}{r^2} + \frac{\mu_{,\theta} \nu_{,\theta}}{r^2} \right] + \left[\frac{1}{A^2} + (m^r)^2 \right] (\nu_{,r})^2 \\
& \quad + \left[\frac{1}{(rA)^2} + (m^\theta)^2 \right] (\nu_{,\theta})^2 + (m^r)^2 \nu_{,rr} + 2m^r m^\theta \nu_{,r\theta} + (m^\theta)^2 \nu_{,\theta\theta} \\
& \quad + \left(m^r m^r_{,r} + m^\theta m^r_{,\theta} \right) \nu_{,r} + \left(m^r m^\theta_{,r} + m^\theta m^\theta_{,\theta} \right) \nu_{,\theta} - \frac{L^2}{2} + 2m^r m^\theta \nu_{,r} \nu_{,\theta}
\end{aligned}$$

Making use of equation (GB3.11)

$$N^{|a}{}_a = N \left[4\pi (E + S^a{}_a) + K_{ab} K^{ab} \right]$$

we finally obtain equation (C.1), listed in Appendix C. Comparing equation (C.1) with (GBB3), we realize that the term $2m^r m^\theta \nu_{,r} \nu_{,\theta}$ is missing on the left hand side of equation (GBB3).

There are mistakes in the equations (GBB4a) and (GBB4b), too. However, we do not prove this here, because just like [Gourgoulhon & Bonazzola \(1993\)](#) we used a Mathematica program. The correct versions of equations (GBB4a) and (GBB4b) are given in Appendix C, again.

B. Derivation of correct 3-lapse equation

C. Geometry equations

In the following, we list the corrected equations (B3-B7) of [Gourgoulhon & Bonazzola \(1993\)](#). These equations are required to compute the metric $g_{\alpha\beta}$.

C.1. Equation for ν

The equation for the geometry field $\nu = \ln N$ is given by equation (B3) in the paper of [Gourgoulhon & Bonazzola \(1993\)](#). The correct version of this equation is

$$\begin{aligned}
& \frac{1}{A^2} \left[\nu_{,rr} + \left(\frac{1}{r} + \mu_{,r} \right) \nu_{,r} + \frac{\nu_{,\theta\theta}}{r^2} + \frac{\mu_{,\theta} \nu_{,\theta}}{r^2} \right] + \left[\frac{1}{A^2} + (m^r)^2 \right] (\nu_{,r})^2 \\
& + \left[\frac{1}{(rA)^2} + (m^\theta)^2 \right] (\nu_{,\theta})^2 + (m^r)^2 \nu_{,rr} + 2m^r m^\theta \nu_{,r\theta} + (m^\theta)^2 \nu_{,\theta\theta} \\
& + \left(m^r m^r_{,r} + m^\theta m^r_{,\theta} \right) \nu_{,r} + \left(m^r m^\theta_{,r} + m^\theta m^\theta_{,\theta} \right) \nu_{,\theta} + 2m^r m^\theta \nu_{,r\nu,\theta} \\
& = 4\pi (E + S_a^a) + K_{ab} K^{ab} + \frac{L^2}{2}
\end{aligned} \tag{C.1}$$

C.2. Equations for N^a

There are three equations for the three components of the 3-shift N^a . The first of these equations is

$$\begin{aligned}
& \left[\frac{1}{A^2} + (m^r)^2 \right] \left\{ N^r_{,rr} + \left(\frac{1}{r} + \mu_{,r} \right) N^r_{,r} - \left[\frac{1}{r^2} + (\mu_{,r})^2 \right] N^r \right\} \\
& + \left[\frac{1}{(rA)^2} + (m^\theta)^2 \right] N^r_{,\theta\theta} + \left[\frac{1}{(rA)^2} - (m^\theta)^2 \right] \mu_{,\theta} N^r_{,\theta} - \frac{2}{r} \left[\frac{1}{A^2} + (m^r)^2 \right] N^{\theta}_{,\theta} \\
& - \left\{ \left[\frac{1}{A^2} - (m^r)^2 \right] \frac{M_{,r\theta}}{M} + \left[\frac{1}{A^2} + (m^r)^2 \right] \mu_{,r} \mu_{,\theta} \right\} N^\theta + 2m^r m^\theta N^r_{,r\theta} \\
& + N^r_{,r} \left\{ 2 \left[\frac{1}{A^2} + (m^r)^2 \right] \alpha_{,r} + m^r m^\theta (2\alpha_{,\theta} - \mu_{,\theta}) + m^r \frac{M_{,\theta}}{M} + m^\theta \frac{M^r_{,\theta}}{M} \right\} \\
& + N^r_{,\theta} \left\{ 2 \left[\frac{1}{(rA)^2} + 2(m^\theta)^2 \right] \alpha_{,\theta} + m^r m^\theta \left(\mu_{,r} + 4\alpha_{,r} + \frac{1}{r} \right) - \frac{m^r M^r_{,\theta}}{r^2 M} \right. \\
& \quad \left. + \frac{m^\theta}{M} \left(M^r_{,r} + 2M^\theta_{,\theta} \right) \right\} + 2N^r_{,r} \left[\frac{\alpha_{,\theta}}{A^2} + (m^r)^2 \mu_{,\theta} - m^r \frac{M^r_{,\theta}}{M} \right] \\
& + N^{\theta}_{,\theta} \left\{ -2 \left[\frac{1}{A^2} + (m^r)^2 \right] \alpha_{,r} + 2m^r m^\theta (\mu_{,\theta} - \alpha_{,\theta}) - 2m^r \frac{M_{,\theta}}{M} \right\}
\end{aligned}$$

C. Geometry equations

$$\begin{aligned}
& + \frac{m^\theta}{M} \left(r^2 M^\theta_{,r} - M^r_{,\theta} \right) \Big\} + N^\varphi_{,\theta} \left\{ \frac{2M^r}{(rA)^2} (\mu_{,\theta} - \alpha_{,\theta}) \right. \\
& + 2 \frac{M^\theta}{A^2} \left[\alpha_{,r} - \mu_{,r} + \frac{1}{r} + \frac{(Am^r)^2}{r} \right] + 2m^r m^\theta (M^\theta_{,\theta} - M^r_{,r}) \\
& - \frac{1}{r^2} \left[\frac{1}{A^2} - (m^r)^2 + (rm^\theta)^2 \right] M^r_{,\theta} + \left[\frac{1}{A^2} + (m^r)^2 - (rm^\theta)^2 \right] M^\theta_{,r} \Big\} \\
& + N^r \left\{ 2 \left[\frac{1}{A^2} + 2(m^r)^2 \right] \alpha_{,r} \left(\mu_{,r} - \frac{1}{r} \right) - \left[\frac{1}{A^2} - (m^r)^2 \right] \frac{M_{,rr}}{M} \right. \\
& + m^r m^\theta \left(-\mu_{,r} \mu_{,\theta} + 4\alpha_{,\theta} \mu_{,r} - 2 \frac{\alpha_{,\theta}}{r} - 2\alpha_{,r} \alpha_{,\theta} + \frac{M_{,r\theta}}{M} - 2 \frac{A_{,r\theta}}{A} \right) \\
& + 2(m^r)^2 \left[\frac{\mu_{,r}}{r} - (\alpha_{,r})^2 - \frac{A_{,rr}}{A} \right] + \frac{m^r}{M} \left[2M^r_{,r} \left(\mu_{,r} - 4\alpha_{,r} - \frac{1}{r} \right) \right. \\
& \quad \left. - M^\theta_{,r} (\mu_{,\theta} + 2\alpha_{,\theta}) + 2M^\theta_{,\theta} \left(\mu_{,r} - \alpha_{,r} - \frac{1}{r} \right) - 2M^r_{,rr} - M^\theta_{,r\theta} \right] \\
& + \frac{m^\theta}{M} [M^r_{,r} (\mu_{,\theta} - 4\alpha_{,\theta}) - M^r_{,r\theta}] \\
& \left. - \frac{1}{M^2} \left[2(M^r_{,r})^2 + M^r_{,r} M^\theta_{,\theta} + r^2 (M^\theta_{,r})^2 \right] \right\} \\
& + N^\theta \left\{ \frac{2}{A^2} \alpha_{,\theta} \mu_{,r} + m^r m^\theta \left[4\alpha_{,\theta} \mu_{,\theta} - 2(\alpha_{,\theta})^2 - (\mu_{,\theta})^2 + \frac{M_{,\theta\theta}}{M} - 2 \frac{A_{,\theta\theta}}{A} \right] \right. \\
& + 2(m^r)^2 \left(\frac{\mu_{,\theta}}{r} - \frac{\alpha_{,\theta}}{r} - \alpha_{,r} \alpha_{,\theta} + 2\mu_{,\theta} \alpha_{,r} - \frac{A_{,r\theta}}{A} \right) \\
& + \frac{m^r}{M} \left[2M^r_{,r} (\mu_{,\theta} - \alpha_{,\theta}) - 2M^r_{,\theta} \left(3\alpha_{,r} + \frac{1}{r} \right) + M^\theta_{,\theta} (\mu_{,\theta} - 4\alpha_{,\theta}) \right. \\
& \quad \left. - M^\theta_{,\theta\theta} - 2M^r_{,r\theta} \right] + \frac{m^\theta}{M} [M^r_{,\theta} (\mu_{,\theta} - 4\alpha_{,\theta}) - M^r_{,\theta\theta}] \\
& \left. - \frac{1}{M^2} \left(M^r_{,\theta} M^\theta_{,\theta} + 2M^r_{,r} M^r_{,\theta} + r^2 M^\theta_{,r} M^\theta_{,\theta} \right) \right\} \\
& = -16\pi N J^r - 2K^{rr} N_{,r} - 2K^{r\theta} N_{,\theta} \tag{C.2}
\end{aligned}$$

This is the corrected version of equation (B4a) of [Gourgoulhon & Bonazzola \(1993\)](#). For that purpose, in the last but two line, the term $M^r_{,\theta\theta}/M$ was replaced by $M^r_{,\theta\theta}$. A similar correction was necessary in equation (B4b)

$$\begin{aligned}
& \left[\frac{1}{A^2} + (m^r)^2 \right] N^\theta_{,rr} + \left[\frac{1}{A^2} \left(\frac{3}{r} + \mu_{,r} \right) + (m^r)^2 \left(\frac{3}{r} - \mu_{,r} \right) \right] N^\theta_{,r} \\
& + \left[\frac{1}{(rA)^2} + (m^\theta)^2 \right] \left(N^\theta_{,\theta\theta} + \mu_{,\theta} N^\theta_{,\theta} \right) - N^\theta \left\{ \left[\frac{1}{(rA)^2} + (m^\theta)^2 \right] (\mu_{,\theta})^2 \right. \\
& \quad \left. + \left[\frac{1}{(rA)^2} - (m^\theta)^2 \right] \frac{M_{,\theta\theta}}{M} \right\} + \frac{2N^r_{,\theta}}{r^3 A^2} + 2m^r m^\theta N^\theta_{,r\theta} \\
& + N^r_{,r} \left\{ -2 \left[\frac{1}{(rA)^2} + (m^\theta)^2 \right] \alpha_{,\theta} + 2m^r m^\theta (\mu_{,r} - \alpha_{,r}) \right. \\
& \quad \left. + \frac{1}{M} \left[m^r \left(\frac{M^r_{,\theta}}{r^2} - M^\theta_{,r} \right) - 2m^\theta M^r_{,r} \right] \right\} + N^r_{,\theta} \left[\frac{2}{(rA)^2} \alpha_{,r} \right.
\end{aligned}$$

$$\begin{aligned}
 & + 2 \left(m^\theta \right)^2 \mu_{,r} - 2m^\theta \frac{M^{\theta,r}}{M} \Big] + N^{\theta,r} \left\{ 2 \left[\frac{1}{A^2} + 2(m^r)^2 \right] \alpha_{,r} \right. \\
 & \left. + m^r m^\theta (\mu_{,\theta} + 4\alpha_{,\theta}) + \frac{1}{M} \left[m^r (2M^r_{,r} + M^\theta_{,\theta}) - m^\theta r^2 M^{\theta,r} \right] \right\} \\
 + N^{\theta,\theta} & \left\{ 2 \left[\frac{1}{(rA)^2} + (m^\theta)^2 \right] \alpha_{,\theta} + m^r m^\theta \left(2\alpha_{,r} - \mu_{,r} + \frac{1}{r} \right) \right. \\
 & \left. + \frac{1}{M} \left(m^r M^{\theta,r} + m^\theta M^r_{,r} \right) \right\} + N^{\varphi,r} \left\{ \frac{2M^r}{(rA)^2} (\alpha_{,\theta} - \mu_{,\theta}) \right. \\
 & \left. + 2\frac{M^\theta}{A^2} \left[\mu_{,r} - \alpha_{,r} - \frac{1}{r} - \frac{(Am^r)^2}{r} \right] + 2m^r m^\theta (M^r_{,r} - M^\theta_{,\theta}) \right. \\
 & \left. + \frac{1}{r^2} \left[\frac{1}{A^2} - (m^r)^2 + (rm^\theta)^2 \right] M^r_{,\theta} - \left[\frac{1}{A^2} + (m^r)^2 - (rm^\theta)^2 \right] M^{\theta,r} \right\} \\
 + N^r & \left\{ \left[\frac{2}{r^3 A^2} - \left(\frac{1}{(rA)^2} + (m^\theta)^2 \right) \mu_{,r} \right] \mu_{,\theta} - \left[\frac{1}{(rA)^2} - (m^\theta)^2 \right] \frac{M_{,r\theta}}{M} \right. \\
 & \left. + \frac{2}{r} \left[\frac{1}{(rA)^2} - (m^\theta)^2 \right] \alpha_{,\theta} + \frac{2}{(rA)^2} \alpha_{,r} \mu_{,\theta} + m^r m^\theta \left[2\frac{\mu_{,r}}{r} - 4\frac{\alpha_{,r}}{r} - \frac{1}{r^2} \right. \right. \\
 & \left. \left. + 4\alpha_{,r} \mu_{,r} - 2(\alpha_{,r})^2 - (\mu_{,r})^2 + \frac{M_{,rr}}{M} - 2\frac{A_{,rr}}{A} \right] \right. \\
 & \left. + 2(m^\theta)^2 \left[(2\mu_{,r} - \alpha_{,r}) \alpha_{,\theta} - \frac{A_{,r\theta}}{A} \right] + \frac{m^r}{M} \left[\left(\mu_{,r} - 4\alpha_{,r} - \frac{3}{r} \right) M^{\theta,r} \right. \right. \\
 & \left. \left. - M^{\theta,rr} \right] + \frac{m^\theta}{M} \left[M^r_{,r} \left(\mu_{,r} - 4\alpha_{,r} - \frac{1}{r} \right) - 6M^{\theta,r} \alpha_{,\theta} \right. \right. \\
 & \left. \left. - 2M^{\theta,\theta} \left(-\mu_{,r} + \alpha_{,r} + \frac{1}{r} \right) - M^r_{,rr} - 2M^{\theta,r\theta} \right] \right. \\
 & \left. - \frac{1}{M^2} \left(\frac{1}{r^2} M^r_{,r} M^r_{,\theta} + M^r_{,r} M^{\theta,r} + 2M^{\theta,r} M^{\theta,\theta} \right) \right\} \\
 + N^\theta & \left\{ 2 \left[\frac{1}{(rA)^2} + 2(m^\theta)^2 \right] \alpha_{,\theta} \mu_{,\theta} + m^r m^\theta \left[2\frac{\mu_{,\theta}}{r} - 2\frac{\alpha_{,\theta}}{r} - \mu_{,r} \mu_{,\theta} + 4\alpha_{,r} \mu_{,\theta} \right. \right. \\
 & \left. \left. - 2\alpha_{,r} \alpha_{,\theta} + \frac{M_{,r\theta}}{M} - 2\frac{A_{,r\theta}}{A} \right] - 2(m^\theta)^2 \left[(\alpha_{,\theta})^2 + \frac{A_{,\theta\theta}}{A} \right] \right. \\
 & \left. + \frac{m^r}{M} \left[M^{\theta,\theta} \left(\mu_{,r} - 4\alpha_{,r} - \frac{3}{r} \right) - M^{\theta,r\theta} \right] + \frac{m^\theta}{M} \left[2M^r_{,r} (\mu_{,\theta} - \alpha_{,\theta}) \right. \right. \\
 & \left. \left. - M^r_{,\theta} \left(\mu_{,r} + 2\alpha_{,r} + \frac{1}{r} \right) + 2M^{\theta,\theta} (\mu_{,\theta} - 4\alpha_{,\theta}) - M^r_{,r\theta} - 2M^{\theta,\theta\theta} \right] \right. \\
 & \left. - \frac{1}{M^2} \left[\left(\frac{M^r_{,\theta}}{r} \right)^2 + 2(M^{\theta,\theta})^2 + M^r_{,r} M^{\theta,\theta} \right] \right\} \\
 = & -16\pi N J^\theta - 2K^{\theta r} N_{,r} - 2K^{\theta\theta} N_{,\theta} \tag{C.3}
 \end{aligned}$$

where in the last but two line the expression $-M^r_{,r\theta}/M - 2M^{\theta,\theta\theta}/M - 2A_{,\theta\theta}/A$ has been replaced by $-M^r_{,r\theta} - 2M^{\theta,\theta\theta}$. The third equation (B4c) does not require any corrections:

$$\left[\frac{1}{A^2} + (m^r)^2 \right] N^{\varphi,rr} + \left\{ \frac{1}{r} \left[\frac{1}{A^2} + (m^r)^2 \right] + \left[\frac{3}{A^2} - (m^r)^2 \right] \mu_{,r} \right\} N^{\varphi,r}$$

C. Geometry equations

$$\begin{aligned}
& + \left[\frac{1}{(rA)^2} + (m^\theta)^2 \right] N^\varphi_{,\theta\theta} + \left[\frac{3}{(rA)^2} - (m^\theta)^2 \right] \mu_{,\theta} N^\varphi_{,\theta} + 2m^r m^\theta N^\varphi_{,r\theta} \\
& + 2\frac{N^r}{M} \left[m^r (\mu_{,r} - \alpha_{,r}) - m^\theta \alpha_{,\theta} - \frac{M^r_{,r}}{M} \right] + \frac{N^r_{,\theta}}{M} \left[2m^\theta \mu_{,r} \right. \\
& \quad \left. - \frac{1}{M} \left(M^\theta_{,r} + \frac{M^r_{,\theta}}{r^2} \right) \right] + \frac{N^\theta_{,r}}{M} \left[2m^r \mu_{,\theta} - \frac{1}{M} \left(r^2 M^\theta_{,r} + M^r_{,\theta} \right) \right] \\
& + 2\frac{N^\theta}{M} \left[m^\theta (\mu_{,\theta} - \alpha_{,\theta}) - m^r \left(\alpha_{,r} + \frac{1}{r} \right) - \frac{M^\theta_{,\theta}}{M} \right] + N^\varphi_{,r} \left[-m^r m^\theta \mu_{,\theta} \right. \\
& \quad \left. + 4m^r \left(m^r \alpha_{,r} + m^\theta \alpha_{,\theta} \right) + \frac{m^r}{M} \left(4M^r_{,r} + M^\theta_{,\theta} \right) \right. \\
& \quad \left. + \frac{m^\theta}{M} \left(2M^r_{,\theta} + r^2 M^\theta_{,r} \right) \right] + N^\varphi_{,\theta} \left[-m^r m^\theta \mu_{,r} + 4m^\theta \left(m^r \alpha_{,r} + m^\theta \alpha_{,\theta} \right) \right. \\
& \quad \left. + \frac{3}{r} m^r m^\theta + \frac{m^r}{M} \left(\frac{M^r_{,\theta}}{r^2} + 2M^\theta_{,r} \right) + \frac{m^\theta}{M} \left(M^r_{,r} + 4M^\theta_{,\theta} \right) \right] \\
& + \frac{N^r}{M} \left\{ m^r \left[2\frac{\mu_{,r}}{r} - 4\frac{\alpha_{,r}}{r} - \frac{1}{r^2} - (\mu_{,r})^2 - 2(\alpha_{,r})^2 + 4\alpha_{,r}\mu_{,r} + \frac{M_{,rr}}{M} - 2\frac{A_{,rr}}{A} \right] \right. \\
& \quad \left. + m^\theta \left(-\mu_{,r}\mu_{,\theta} + 4\alpha_{,\theta}\mu_{,r} - 2\frac{\alpha_{,\theta}}{r} - 2\alpha_{,r}\alpha_{,\theta} + \frac{M_{,r\theta}}{M} - 2\frac{A_{,r\theta}}{A} \right) \right. \\
& \quad \left. + \frac{1}{M} \left[M^r_{,r} \left(\mu_{,r} - 4\alpha_{,r} - \frac{1}{r} \right) - M^\theta_{,r} (\mu_{,\theta} + 2\alpha_{,\theta}) \right. \right. \\
& \quad \left. \left. + 2M^\theta_{,\theta} \left(\mu_{,r} - \alpha_{,r} - \frac{1}{r} \right) - M^r_{,rr} - M^\theta_{,r\theta} \right] \right\} \\
& + \frac{N^\theta}{M} \left\{ m^r \left[-\mu_{,r}\mu_{,\theta} + \left(4\alpha_{,r} + \frac{2}{r} \right) \mu_{,\theta} - 2\frac{\alpha_{,\theta}}{r} - 2\alpha_{,r}\alpha_{,\theta} + \frac{M_{,r\theta}}{M} - 2\frac{A_{,r\theta}}{A} \right] \right. \\
& \quad \left. + m^\theta \left[-(\mu_{,\theta})^2 - 2(\alpha_{,\theta})^2 + 4\alpha_{,\theta}\mu_{,\theta} + \frac{M_{,\theta\theta}}{M} - 2\frac{A_{,\theta\theta}}{A} \right] \right. \\
& \quad \left. + \frac{1}{M} \left[2M^r_{,r} (\mu_{,\theta} - \alpha_{,\theta}) - M^r_{,\theta} \left(\mu_{,r} + 2\alpha_{,r} + \frac{1}{r} \right) \right. \right. \\
& \quad \left. \left. + M^\theta_{,\theta} (\mu_{,\theta} - 4\alpha_{,\theta}) - M^r_{,r\theta} - M^\theta_{,\theta\theta} \right] \right\} \\
& = -16\pi N J^\varphi - 2K^{\varphi r} N_{,r} - 2K^{\varphi\theta} N_{,\theta}
\end{aligned} \tag{C.4}$$

C.3. Equation for β

The equation for the basic geometry field $\beta = \ln(M/r \sin \theta)$ is

$$\begin{aligned}
& \frac{1}{A^2} \left[(MN)_{,rr} + \frac{1}{r} (MN)_{,r} + \frac{1}{r^2} (MN)_{,\theta\theta} \right] \\
& = 8\pi MN s_m^m - 2\kappa_r [M, q]^r - 2\kappa_\theta [M, q]^\theta - M \left(q^r + \omega \frac{M^r}{M} \right) \kappa_{,r} \\
& \quad - M \left(q^\theta + \omega \frac{M^\theta}{M} \right) \kappa_{,\theta} + MN (\kappa_{mn} \kappa^{mn} + \kappa^2 - L_{mn} L^{mn})
\end{aligned} \tag{C.5}$$

C.4. Equations for M^m

For the two components of the 2-shift M^m , there are the two equations

$$\begin{aligned}
& \frac{1}{A^2} \left[M^r_{,rr} + \left(\frac{1}{r} + 2\alpha_{,r} \right) M^r_{,r} + \frac{M^r_{,\theta\theta}}{r^2} + \frac{2}{r^2} \alpha_{,\theta} M^r_{,\theta} - \left(\frac{1}{r^2} + 2\frac{\alpha_{,r}}{r} \right) M^r \right. \\
& \quad \left. + 2\alpha_{,\theta} M^\theta_{,r} - 2 \left(\frac{1}{r} + \alpha_{,r} \right) M^\theta_{,\theta} \right] \\
= & 16\pi M s^r - 2L^{rr} N \left(\frac{M}{N} \right)_{,r} - 2L^{r\theta} N \left(\frac{M}{N} \right)_{,\theta} + \frac{L}{NA^2} (MN)_{,r} \\
& + 2\frac{M}{N} [q, \kappa]^r + 2\frac{\omega}{N} [M, \kappa]^r + 2 \left(\frac{\kappa}{A^2} - \kappa^{rr} \right) \frac{M^2}{N} \left(\frac{\omega}{M} \right)_{,r} - 2\kappa^{r\theta} \frac{M^2}{N} \left(\frac{\omega}{M} \right)_{,\theta} \\
& - 2M \left(2\kappa^r_{,r} \kappa^r + 2\kappa^r_{,\theta} \kappa^\theta - \kappa \kappa^r \right) \tag{C.6}
\end{aligned}$$

and

$$\begin{aligned}
& \frac{1}{A^2} \left[M^\theta_{,rr} + \left(\frac{3}{r} + 2\alpha_{,r} \right) M^\theta_{,r} + \frac{M^\theta_{,\theta\theta}}{r^2} + \frac{2}{r^2} \alpha_{,\theta} M^\theta_{,\theta} - \frac{2}{r^2} \alpha_{,\theta} M^r_{,r} \right. \\
& \quad \left. + \frac{2}{r^2} \left(\frac{1}{r} + \alpha_{,r} \right) M^r_{,\theta} + \frac{2}{r^3} \alpha_{,\theta} M^r \right] \\
= & 16\pi M s^\theta - 2L^{\theta r} N \left(\frac{M}{N} \right)_{,r} - 2L^{\theta\theta} N \left(\frac{M}{N} \right)_{,\theta} + \frac{L}{r^2 NA^2} (MN)_{,\theta} \\
& + 2\frac{M}{N} [q, \kappa]^\theta + 2\frac{\omega}{N} [M, \kappa]^\theta - 2\kappa^{\theta r} \frac{M^2}{N} \left(\frac{\omega}{M} \right)_{,r} + \left[\frac{\kappa}{(rA)^2} - \kappa^{\theta\theta} \right] \frac{M^2}{N} \left(\frac{\omega}{M} \right)_{,\theta} \\
& - 2M \left(2\kappa^\theta_{,r} \kappa^r + 2\kappa^\theta_{,\theta} \kappa^\theta - \kappa \kappa^\theta \right) \tag{C.7}
\end{aligned}$$

C.5. Equation for α

The last geometry equation gives the basic geometry field $\alpha = \ln A$:

$$\begin{aligned}
& \frac{1}{A^2} \left[(\alpha + \nu)_{,rr} + \frac{1}{r} (\alpha + \nu)_{,r} + \frac{1}{r^2} (\alpha + \nu)_{,\theta\theta} \right] \\
= & 8\pi s - \frac{1}{A^2} \left[(\nu_{,r})^2 + \frac{1}{r^2} (\nu_{,\theta})^2 \right] + \frac{1}{N} \left(q^r + \omega \frac{M^r}{M} \right) \kappa_{,r} + \frac{1}{N} \left(q^\theta + \omega \frac{M^\theta}{M} \right) \kappa_{,\theta} \\
& + \frac{2}{MN} \kappa_r [M, q]^r + \frac{2}{MN} \kappa_\theta [M, q]^\theta + 3\kappa_m \kappa^{mn} + \frac{1}{2} (\kappa_{mn} \kappa^{mn} + \kappa^2 + L_{mn} L^{mn}) \tag{C.8}
\end{aligned}$$

C. Geometry equations

D. Determinants

In the following, we will prove two important relations between the three determinants $g = \det g_{\alpha\beta}$, $h = \det h_{ab}$ and $k = \det k_{mn}$ of the 4-metric $g_{\alpha\beta}$, the 3-metric h_{ab} and the 2-metric k_{mn} , respectively. For that purpose, we make use of equation (7.8) of [D'Inverno \(1992\)](#) for the 4-metric $g_{\alpha\beta}$:

$$\partial_\alpha g = g g^{\beta\gamma} \partial_\alpha g_{\beta\gamma}$$

In a similar manner, there are the equations

$$\partial_a h = h h^{bc} \partial_a h_{bc}$$

and

$$\partial_m k = h h^{bc} \partial_a h_{bc}$$

for the 3-metric h_{ab} and the 2-metric k_{mn} , respectively. Then, the decompositions (2.11) and (2.12) of the 4-metric $g_{\alpha\beta}$ lead to

$$\begin{aligned} \partial_a \ln(-g) &= \frac{\partial_a g}{g} \\ &= g^{\beta\gamma} \partial_a g_{\beta\gamma} \\ &= g^{tt} \partial_a g_{tt} + 2g^{tb} \partial_a g_{tb} + g^{bc} \partial_a g_{bc} \\ &= -\frac{1}{N^2} \partial_a \left(h^{bc} N_b N_c - N^2 \right) + 2 \frac{N^b}{N^2} \partial_a N_b + \left(h^{bc} - \frac{N^b N^c}{N^2} \right) \partial_a h_{bc} \\ &= 2 \frac{\partial_a N}{N} + \frac{\partial_a h}{h} - \frac{1}{N^2} \left(N_b N^d h_{cd} \partial_a h^{bc} + N^b N_d h^{cd} \partial_a h_{bc} \right) \\ &= 2 \partial_a \ln N + \partial_a \ln h - \frac{N_b N^d}{N^2} \left(h_{cd} \partial_a h^{bc} + h^{bc} \partial_a h_{cd} \right) \end{aligned}$$

The expression in the round bracket vanishes, because

$$h_{bc} \partial_a h^{cd} + h^{cd} \partial_a h_{bc} = \partial_a \left(h_{cd} h^{bc} \right) = \partial_a \delta_d^b = 0$$

So, we arrive at the first of the two relations to be proven:

$$\boxed{\partial_a \ln(-g) = \partial_a (2\nu + \ln h)} \quad (\text{D.1})$$

For the second relation, we use the decompositions (2.17) and (2.18) of the 3-metric h_{ab} such that

$$\begin{aligned} \partial_m \ln h &= \frac{\partial_m h}{h} \\ &= h^{ab} \partial_m h_{ab} \\ &= \left(k^{no} + \frac{M^n M^o}{M^2} \right) \partial_m k_{no} - 2 \frac{M^n}{M^2} \partial_m M_n + \frac{1}{M^2} \partial_m \left(M^2 + k^{no} M_n M_o \right) \end{aligned}$$

D. Determinants

$$\begin{aligned}
&= 2\frac{\partial_m M}{M} + \frac{\partial_m k}{k} + \frac{1}{M^2} (M_n M^p k_{op} \partial_m k^{no} + M^n M_p k^{op} \partial_m k_{no}) \\
&= 2\partial_m \ln M + \partial_m \ln k + \frac{M_n M^p}{M^2} (k_{op} \partial_m k^{no} + k^{no} \partial_m k_{op})
\end{aligned}$$

The expression in the round brackets is again zero, since

$$k_{op} \partial_m k^{no} + k^{no} \partial_m k_{op} = \partial_m (k^{no} k_{op}) = \partial_m \delta_p^n = 0$$

Then, we get

$$\boxed{\partial_m \ln h = \partial_m (2\mu + \ln k)} \tag{D.2}$$

Both relations (D.1) and (D.2) are an immediate result of the equations

$$\sqrt{-g} = N\sqrt{h}$$

and

$$\sqrt{h} = M\sqrt{k}$$

presented, but not proven in [Gourgoulhon & Bonazzola \(1993\)](#).

E. Polytropic equation of state

The polytropic equation of state is

$$p = K\rho^\Gamma \quad (\text{E.1})$$

with the pressure p , the polytropic constant K , the rest mass density ρ and the polytropic exponent Γ . In this section, we will derive a relation between the rest mass density ρ and the total energy density ϵ (=rest energy density+thermal energy density) such that we can express the total energy density ϵ merely in terms of the pressure p . For that purpose, we use the first law of thermodynamics, written as

$$d\epsilon = \rho T ds + h d\rho$$

with the temperature T , the specific entropy s and the relativistic enthalpy

$$h = \frac{\epsilon + p}{\rho}$$

Following [Friedman & Stergioulas](#), we ignore entropy gradients such that we can assume a uniform entropy distribution. Therefore, $ds = 0$, and the first law of thermodynamics becomes

$$d\epsilon = \frac{\epsilon + p}{\rho} d\rho$$

or

$$d\left(\frac{\epsilon}{\rho}\right) = \frac{p}{\rho^2} d\rho = K\rho^{\Gamma-2} d\rho$$

Then, we demand

$$\lim_{p \rightarrow 0} \frac{\epsilon}{\rho} = 1$$

such that

$$\frac{\epsilon}{\rho} = 1 + \int_0^\rho d\rho K\rho^{\Gamma-2} = 1 + K \frac{\rho^{\Gamma-1}}{\Gamma-1}$$

Thus, we find the following relation between the total energy density ϵ and the rest mass density ρ :

$$\epsilon = \rho + K \frac{\rho^\Gamma}{\Gamma-1}$$

Applying equation (E.1), we eventually arrive at

$$\boxed{\epsilon = \frac{p}{\Gamma-1} + \left(\frac{p}{K}\right)^{\frac{1}{\Gamma}}} \quad (\text{E.2})$$

This relation expresses the total energy density ϵ in terms of the pressure p .

E. Polytropic equation of state

F. Sources of 3-shift Poisson equation

In this appendix, we present the sources S_N^a of the Poisson equation (3.9) for the 3-shift N^a . The three components of the 3-vector S_N^a are the r -component

$$\begin{aligned}
& S_N^r \\
= & A^2 \left\{ -16\pi N J^r - 2K^{rr} N_{,r} - 2K^{r\theta} N_{,\theta} - 2m^r m^\theta N^r_{,r\theta} \right. \\
& - N^r_{,r} \left\{ 2 \left[\frac{1}{A^2} + (m^r)^2 \right] \alpha_{,r} + m^r m^\theta (2\alpha_{,\theta} - \mu_{,\theta}) + m^r \frac{M^\theta_{,\theta}}{M} + m^\theta \frac{M^r_{,\theta}}{M} \right\} \\
& - N^r_{,\theta} \left\{ 2 \left[\frac{1}{(rA)^2} + 2(m^\theta)^2 \right] \alpha_{,\theta} + m^r m^\theta \left(\mu_{,r} + 4\alpha_{,r} + \frac{1}{r} \right) - \frac{m^r M^r_{,\theta}}{r^2 M} \right. \\
& \left. + \frac{m^\theta}{M} \left(M^r_{,r} + 2M^\theta_{,\theta} \right) \right\} - 2N^\theta_{,r} \left[\frac{\alpha_{,\theta}}{A^2} + (m^r)^2 \mu_{,\theta} - m^r \frac{M^r_{,\theta}}{M} \right] \\
& - N^\theta_{,\theta} \left\{ -2 \left[\frac{1}{A^2} + (m^r)^2 \right] \alpha_{,r} + 2m^r m^\theta (\mu_{,\theta} - \alpha_{,\theta}) - 2m^r \frac{M^\theta_{,\theta}}{M} \right. \\
& \left. + \frac{m^\theta}{M} \left(r^2 M^\theta_{,r} - M^r_{,\theta} \right) \right\} - N^\varphi_{,\theta} \left\{ \frac{2M^r}{(rA)^2} (\mu_{,\theta} - \alpha_{,\theta}) \right. \\
& \left. + 2 \frac{M^\theta}{A^2} \left[\alpha_{,r} - \mu_{,r} + \frac{1}{r} + \frac{(Am^r)^2}{r} \right] + 2m^r m^\theta (M^\theta_{,\theta} - M^r_{,r}) \right. \\
& \left. - \frac{1}{r^2} \left[\frac{1}{A^2} - (m^r)^2 + (rm^\theta)^2 \right] M^r_{,\theta} + \left[\frac{1}{A^2} + (m^r)^2 - (rm^\theta)^2 \right] M^\theta_{,r} \right\} \\
& - N^r \left\{ 2 \left[\frac{1}{A^2} + 2(m^r)^2 \right] \alpha_{,r} \left(\mu_{,r} - \frac{1}{r} \right) - \left[\frac{1}{A^2} - (m^r)^2 \right] \frac{M_{,rr}}{M} \right. \\
& \left. + m^r m^\theta \left(-\mu_{,r} \mu_{,\theta} + 4\alpha_{,\theta} \mu_{,r} - 2 \frac{\alpha_{,\theta}}{r} - 2\alpha_{,r} \alpha_{,\theta} + \frac{M_{,r\theta}}{M} - 2 \frac{A_{,r\theta}}{A} \right) \right. \\
& \left. + 2(m^r)^2 \left[\frac{\mu_{,r}}{r} - (\alpha_{,r})^2 - \frac{A_{,rr}}{A} \right] + \frac{m^r}{M} \left[2M^r_{,r} \left(\mu_{,r} - 4\alpha_{,r} - \frac{1}{r} \right) \right. \right. \\
& \left. \left. - M^\theta_{,r} (\mu_{,\theta} + 2\alpha_{,\theta}) + 2M^\theta_{,\theta} \left(\mu_{,r} - \alpha_{,r} - \frac{1}{r} \right) - 2M^r_{,rr} - M^\theta_{,r\theta} \right] \right. \\
& \left. + \frac{m^\theta}{M} [M^r_{,r} (\mu_{,\theta} - 4\alpha_{,\theta}) - M^r_{,r\theta}] \right. \\
& \left. - \frac{1}{M^2} \left[2(M^r_{,r})^2 + M^r_{,r} M^\theta_{,\theta} + r^2 (M^\theta_{,r})^2 \right] \right\} \\
& - N^\theta \left\{ \frac{2}{A^2} \alpha_{,\theta} \mu_{,r} + m^r m^\theta \left[4\alpha_{,\theta} \mu_{,\theta} - 2(\alpha_{,\theta})^2 - (\mu_{,\theta})^2 + \frac{M_{,\theta\theta}}{M} - 2 \frac{A_{,\theta\theta}}{A} \right] \right. \\
& \left. + 2(m^r)^2 \left(\frac{\mu_{,\theta}}{r} - \frac{\alpha_{,\theta}}{r} - \alpha_{,r} \alpha_{,\theta} + 2\mu_{,\theta} \alpha_{,r} - \frac{A_{,r\theta}}{A} \right) \right\}
\end{aligned}$$

F. Sources of 3-shift Poisson equation

$$\begin{aligned}
& + \frac{m^r}{M} \left[2M^r_{,r} (\mu_{,\theta} - \alpha_{,\theta}) - 2M^r_{,\theta} \left(3\alpha_{,r} + \frac{1}{r} \right) + M^{\theta}_{,\theta} (\mu_{,\theta} - 4\alpha_{,\theta}) \right. \\
& - M^{\theta}_{,\theta\theta} - 2M^r_{,r\theta} \left. \right] + \frac{m^\theta}{M} \left[M^r_{,\theta} (\mu_{,\theta} - 4\alpha_{,\theta}) - M^r_{,\theta\theta} \right] \\
& - \frac{1}{M^2} \left(M^r_{,\theta} M^{\theta}_{,\theta} + 2M^r_{,r} M^r_{,\theta} + r^2 M^{\theta}_{,r} M^{\theta}_{,\theta} \right) \left. \right\} \\
& - (m^r)^2 \left\{ N^r_{,rr} + \left(\frac{1}{r} + \mu_{,r} \right) N^r_{,r} - \left[\frac{1}{r^2} + (\mu_{,r})^2 \right] N^r \right\} \\
& - \left(m^\theta \right)^2 N^r_{,\theta\theta} + \left(m^\theta \right)^2 \mu_{,\theta} N^r_{,\theta} + \frac{2}{r} (m^r)^2 N^{\theta}_{,\theta} - (m^r)^2 \beta_{,r\theta} N^{\theta} \left. \right\} \\
& - \beta_{,r} N^r_{,r} + \left[\frac{2}{r} \beta_{,r} + (\beta_{,r})^2 \right] N^r - \frac{1}{r^2} \beta_{,\theta} N^r_{,\theta} \\
& + \left(\frac{2}{r} \beta_{,\theta} + 2 \cot \theta \beta_{,r} + \beta_{,r\theta} + 2\beta_{,r} \beta_{,\theta} \right) N^{\theta}
\end{aligned}$$

the θ -component

$$\begin{aligned}
& S_N^\theta \\
= & A^2 \left\{ -16\pi N J^\theta - 2K^{\theta r} N_{,r} - 2K^{\theta\theta} N_{,\theta} - 2m^r m^\theta N^{\theta}_{,r\theta} \right. \\
& - N^r_{,r} \left\{ -2 \left[\frac{1}{(rA)^2} + (m^\theta)^2 \right] \alpha_{,\theta} + 2m^r m^\theta (\mu_{,r} - \alpha_{,r}) \right. \\
& \quad \left. + \frac{1}{M} \left[m^r \left(\frac{M^r_{,\theta}}{r^2} - M^{\theta}_{,r} \right) - 2m^\theta M^r_{,r} \right] \right\} \\
& - N^r_{,\theta} \left[\frac{2}{(rA)^2} \alpha_{,r} + 2 (m^\theta)^2 \mu_{,r} - 2m^\theta \frac{M^{\theta}_{,r}}{M} \right] \\
& - N^{\theta}_{,r} \left\{ 2 \left[\frac{1}{A^2} + 2(m^r)^2 \right] \alpha_{,r} + m^r m^\theta (\mu_{,\theta} + 4\alpha_{,\theta}) \right. \\
& \quad \left. + \frac{1}{M} \left[m^r (2M^r_{,r} + M^{\theta}_{,\theta}) - m^\theta r^2 M^{\theta}_{,r} \right] \right\} \\
& - N^{\theta}_{,\theta} \left\{ 2 \left[\frac{1}{(rA)^2} + (m^\theta)^2 \right] \alpha_{,\theta} + m^r m^\theta \left(2\alpha_{,r} - \mu_{,r} + \frac{1}{r} \right) \right. \\
& \quad \left. + \frac{1}{M} (m^r M^{\theta}_{,r} + m^\theta M^r_{,r}) \right\} - N^{\varphi}_{,r} \left\{ \frac{2M^r}{(rA)^2} (\alpha_{,\theta} - \mu_{,\theta}) \right. \\
& \quad \left. + 2 \frac{M^\theta}{A^2} \left[\mu_{,r} - \alpha_{,r} - \frac{1}{r} - \frac{(Am^r)^2}{r} \right] + 2m^r m^\theta (M^r_{,r} - M^{\theta}_{,\theta}) \right. \\
& \quad \left. + \frac{1}{r^2} \left[\frac{1}{A^2} - (m^r)^2 + (rm^\theta)^2 \right] M^r_{,\theta} - \left[\frac{1}{A^2} + (m^r)^2 - (rm^\theta)^2 \right] M^{\theta}_{,r} \right\} \\
& - N^r \left\{ - (m^\theta)^2 \mu_{,r} \mu_{,\theta} + (m^\theta)^2 \frac{M_{,r\theta}}{M} - \frac{1}{(rA)^2} (2 \cot \theta \beta_{,r} + \beta_{,r\theta} + 2\beta_{,r} \beta_{,\theta}) \right. \\
& \quad \left. + \frac{2}{r} \left[\frac{1}{(rA)^2} - (m^\theta)^2 \right] \alpha_{,\theta} + \frac{2}{(rA)^2} \alpha_{,r} \mu_{,\theta} + m^r m^\theta \left[2 \frac{\mu_{,r}}{r} - 4 \frac{\alpha_{,r}}{r} - \frac{1}{r^2} \right. \right. \\
& \quad \left. \left. + 4\alpha_{,r} \mu_{,r} - 2(\alpha_{,r})^2 - (\mu_{,r})^2 + \frac{M_{,rr}}{M} - 2 \frac{A_{,rr}}{A} \right] \right\}
\end{aligned}$$

$$\begin{aligned}
& +2 \left(m^\theta\right)^2 \left[\left(2\mu_{,r} - \alpha_{,r}\right) \alpha_{,\theta} - \frac{A_{,r\theta}}{A} \right] + \frac{m^r}{M} \left[\left(\mu_{,r} - 4\alpha_{,r} - \frac{3}{r}\right) M^\theta_{,r} \right. \\
& \quad \left. - M^\theta_{,rr} \right] + \frac{m^\theta}{M} \left[M^r_{,r} \left(\mu_{,r} - 4\alpha_{,r} - \frac{1}{r}\right) - 6M^\theta_{,r} \alpha_{,\theta} \right. \\
& \quad \left. - 2M^\theta_{,\theta} \left(-\mu_{,r} + \alpha_{,r} + \frac{1}{r}\right) - M^r_{,rr} - 2M^\theta_{,r\theta} \right] \\
& \quad \left. - \frac{1}{M^2} \left(\frac{1}{r^2} M^r_{,r} M^r_{,\theta} + M^r_{,r} M^\theta_{,r} + 2M^\theta_{,r} M^\theta_{,\theta} \right) \right\} \\
& - N^\theta \left\{ 2 \left[\frac{1}{(rA)^2} + 2 \left(m^\theta\right)^2 \right] \alpha_{,\theta} \mu_{,\theta} + m^r m^\theta \left[2 \frac{\mu_{,\theta}}{r} - 2 \frac{\alpha_{,\theta}}{r} - \mu_{,r} \mu_{,\theta} + 4\alpha_{,r} \mu_{,\theta} \right. \right. \\
& \quad \left. \left. - 2\alpha_{,r} \alpha_{,\theta} + \frac{M_{,r\theta}}{M} - 2 \frac{A_{,r\theta}}{A} \right] - 2 \left(m^\theta\right)^2 \left[(\alpha_{,\theta})^2 + \frac{A_{,\theta\theta}}{A} \right] \right. \\
& \quad \left. + \frac{m^r}{M} \left[M^\theta_{,\theta} \left(\mu_{,r} - 4\alpha_{,r} - \frac{3}{r}\right) - M^\theta_{,r\theta} \right] + \frac{m^\theta}{M} \left[2M^r_{,r} (\mu_{,\theta} - \alpha_{,\theta}) \right. \right. \\
& \quad \left. \left. - M^r_{,\theta} \left(\mu_{,r} + 2\alpha_{,r} + \frac{1}{r}\right) + 2M^\theta_{,\theta} (\mu_{,\theta} - 4\alpha_{,\theta}) - M^r_{,r\theta} - 2M^\theta_{,\theta\theta} \right] \right. \\
& \quad \left. - \frac{1}{M^2} \left[\left(\frac{M^r_{,\theta}}{r}\right)^2 + 2 \left(M^\theta_{,\theta}\right)^2 + M^r_{,r} M^\theta_{,\theta} \right] \right\} \\
& - (m^r)^2 N^\theta_{,rr} - \frac{1}{A^2} \beta_{,r} N^\theta_{,r} - (m^r)^2 \left(\frac{3}{r} - \mu_{,r}\right) N^\theta_{,r} \\
& - \left(m^\theta\right)^2 \left(N^\theta_{,\theta\theta} + \mu_{,\theta} N^\theta_{,\theta}\right) + \left(m^\theta\right)^2 \left(\cot^2 \theta + 1 - \beta_{,\theta\theta}\right) N^\theta \left. \right\} \\
& - \frac{1}{r^2} \beta_{,\theta} N^\theta_{,\theta} + N^\theta \frac{1}{r^2} \left[4 \cot \theta \beta_{,\theta} + 2 \left(\beta_{,\theta}\right)^2 + \beta_{,\theta\theta} \right]
\end{aligned}$$

and the ϕ -component

$$\begin{aligned}
& S_N^\phi \\
= & A^2 \left\{ -16\pi N J^\varphi - 2K^{\varphi r} N_{,r} - 2K^{\varphi\theta} N_{,\theta} - 2m^r m^\theta N^{\varphi}_{,r\theta} \right. \\
& \quad - 2 \frac{N^r_{,r}}{M} \left[m^r (\mu_{,r} - \alpha_{,r}) - m^\theta \alpha_{,\theta} - \frac{M^r_{,r}}{M} \right] \\
& \quad - \frac{N^r_{,\theta}}{M} \left[2m^\theta \mu_{,r} - \frac{1}{M} \left(M^\theta_{,r} + \frac{M^r_{,\theta}}{r^2} \right) \right] \\
& \quad - \frac{N^\theta_{,r}}{M} \left[2m^r \mu_{,\theta} - \frac{1}{M} \left(r^2 M^\theta_{,r} + M^r_{,\theta} \right) \right] \\
& \quad - 2 \frac{N^\theta_{,\theta}}{M} \left[m^\theta (\mu_{,\theta} - \alpha_{,\theta}) - m^r \left(\alpha_{,r} + \frac{1}{r} \right) - \frac{M^\theta_{,\theta}}{M} \right] \\
& \quad - N^{\varphi}_{,r} \left[-m^r m^\theta \mu_{,\theta} + 4m^r \left(m^r \alpha_{,r} + m^\theta \alpha_{,\theta} \right) + \frac{m^r}{M} \left(4M^r_{,r} + M^\theta_{,\theta} \right) \right. \\
& \quad \quad \left. + \frac{m^\theta}{M} \left(2M^r_{,\theta} + r^2 M^\theta_{,r} \right) \right] \\
& \quad - N^{\varphi}_{,\theta} \left[-m^r m^\theta \mu_{,r} + 4m^\theta \left(m^r \alpha_{,r} + m^\theta \alpha_{,\theta} \right) + \frac{3}{r} m^r m^\theta \right.
\end{aligned}$$

F. Sources of 3-shift Poisson equation

$$\begin{aligned}
& + \frac{m^r}{M} \left(\frac{M^r{}_{,\theta}}{r^2} + 2M^{\theta}{}_{,r} \right) + \frac{m^\theta}{M} \left(M^r{}_{,r} + 4M^{\theta}{}_{,\theta} \right) \Big] \\
- \frac{N^r}{M} & \left\{ m^r \left[2\frac{\mu_{,r}}{r} - 4\frac{\alpha_{,r}}{r} - \frac{1}{r^2} - (\mu_{,r})^2 - 2(\alpha_{,r})^2 + 4\alpha_{,r}\mu_{,r} + \frac{M_{,rr}}{M} - 2\frac{A_{,rr}}{A} \right] \right. \\
& + m^\theta \left(-\mu_{,r}\mu_{,\theta} + 4\alpha_{,\theta}\mu_{,r} - 2\frac{\alpha_{,\theta}}{r} - 2\alpha_{,r}\alpha_{,\theta} + \frac{M_{,r\theta}}{M} - 2\frac{A_{,r\theta}}{A} \right) \\
& + \frac{1}{M} \left[M^r{}_{,r} \left(\mu_{,r} - 4\alpha_{,r} - \frac{1}{r} \right) - M^{\theta}{}_{,r} (\mu_{,\theta} + 2\alpha_{,\theta}) \right. \\
& \quad \left. + 2M^{\theta}{}_{,\theta} \left(\mu_{,r} - \alpha_{,r} - \frac{1}{r} \right) - M^r{}_{,rr} - M^{\theta}{}_{,r\theta} \right] \Big\} \\
- \frac{N^\theta}{M} & \left\{ m^r \left[-\mu_{,r}\mu_{,\theta} + \left(4\alpha_{,r} + \frac{2}{r} \right) \mu_{,\theta} - 2\frac{\alpha_{,\theta}}{r} - 2\alpha_{,r}\alpha_{,\theta} + \frac{M_{,r\theta}}{M} - 2\frac{A_{,r\theta}}{A} \right] \right. \\
& + m^\theta \left[-(\mu_{,\theta})^2 - 2(\alpha_{,\theta})^2 + 4\alpha_{,\theta}\mu_{,\theta} + \frac{M_{,\theta\theta}}{M} - 2\frac{A_{,\theta\theta}}{A} \right] \\
& + \frac{1}{M} \left[2M^r{}_{,r} (\mu_{,\theta} - \alpha_{,\theta}) - M^r{}_{,\theta} \left(\mu_{,r} + 2\alpha_{,r} + \frac{1}{r} \right) + M^{\theta}{}_{,\theta} (\mu_{,\theta} - 4\alpha_{,\theta}) \right. \\
& \quad \left. - M^r{}_{,r\theta} - M^{\theta}{}_{,\theta\theta} \right] \Big\} \\
& - (m^r)^2 N^{\varphi}{}_{,rr} - \left[\frac{3}{A^2} - (m^r)^2 \right] \beta_{,r} N^{\varphi}{}_{,r} - (m^\theta)^2 N^{\varphi}{}_{,\theta\theta} \\
& - \left[\frac{3}{(rA)^2} - (m^\theta)^2 \right] \beta_{,\theta} N^{\varphi}{}_{,\theta} + (m^\theta)^2 \cot \theta N^{\varphi}{}_{,\theta} \Big\}
\end{aligned}$$

G. Associated Legendre polynomials

Every function $f(\theta, \phi)$ can be expanded in terms of spherical harmonics $Y_{lm}(\theta, \phi)$ as (p. 128f of Jackson 2006)

$$f(\theta, \phi) = \sum_{l=0}^{\infty} \sum_{m=-l}^l f_{lm} Y_{lm}(\theta, \phi)$$

with the coefficients

$$f_{lm} = \int d\Omega f(\theta, \phi) Y_{lm}^*(\theta, \phi)$$

Assuming

$$f(\theta, \phi) = f(\theta) \cos \phi$$

equation (3.36) tells us

$$f_{lm} = \sqrt{\frac{(2l+1)(l-m)!}{4\pi(l+m)!}} \int_0^\pi d\theta f(\theta) P_l^m(\cos \theta) \sin \theta \int_0^{2\pi} d\phi e^{-im\phi} \cos \phi$$

We evaluate the second integral with the help of equations (3.45) and (3.46) such that

$$f_{lm} = \pi \delta_{|m|}^1 \sqrt{\frac{(2l+1)(l-m)!}{4\pi(l+m)!}} \int_0^\pi d\theta f(\theta) P_l^m(\cos \theta) \sin \theta$$

Then, equation (3.40) gives

$$\begin{aligned} f_{l,-1} &= \pi \sqrt{\frac{(2l+1)(l+1)!}{4\pi(l-1)!}} \int_0^\pi d\theta f(\theta) P_l^{-1}(\cos \theta) \sin \theta \\ &= -\pi \sqrt{\frac{(2l+1)(l-1)!}{4\pi(l+1)!}} \int_0^\pi d\theta f(\theta) P_l^1(\cos \theta) \sin \theta \\ &= -f_{l,1} \end{aligned}$$

and together with equation (3.36) we find

$$\begin{aligned} Y_{l,-1}(\theta, \phi) &= \sqrt{\frac{(2l+1)(l+1)!}{4\pi(l-1)!}} P_l^{-1}(\cos \theta) e^{-i\phi} \\ &= -\sqrt{\frac{(2l+1)(l-1)!}{4\pi(l+1)!}} P_l^1(\cos \theta) (e^{i\phi})^* \\ &= -Y_{l,1}^*(\theta, \phi) \end{aligned}$$

G. Associated Legendre polynomials

Thus, we arrive at

$$\begin{aligned}
 f(\theta, \phi) &= \sum_{l=1}^{\infty} (f_{l,-1} Y_{l,-1}(\theta, \phi) + f_{l,1} Y_{l,1}(\theta, \phi)) \\
 &= \sum_{l=1}^{\infty} f_{l,1} (Y_{l,-1}^*(\theta, \phi) + Y_{l,1}(\theta, \phi)) \\
 &= 2 \sum_{l=1}^{\infty} f_{l,1} \sqrt{\frac{(2l+1)(l-1)!}{4\pi(l+1)!}} P_l^1(\cos \theta) \cos \phi \\
 &= \sum_{l=1}^{\infty} f_l P_l^1(\cos \theta) \cos \phi
 \end{aligned}$$

with the coefficients

$$f_l = 2 \sqrt{\frac{(2l+1)(l-1)!}{4\pi(l+1)!}} \pi \sqrt{\frac{(2l+1)(l-1)!}{4\pi(l+1)!}} \int_0^\pi d\theta f(\theta) P_l^1(\cos \theta) \sin \theta$$

So, every function $f(\theta)$ can be expanded as

$$f(\theta) = \sum_{l=1}^{\infty} f_l P_l^1(\cos \theta) \quad (\text{G.1})$$

$$f_l = \frac{(2l+1)}{2l(l+1)} \int_0^\pi d\theta f(\theta) P_l^1(\cos \theta) \sin \theta \quad (\text{G.2})$$

H. Slicing conditions in flat space

In the following, we will rewrite the two slicing conditions (3.8) and (3.9) of [Gourgoulhon & Bonazzola \(1993\)](#) in terms of our basic fields in flat space.

H.1. Maximal time slicing

The maximal time slicing condition is given in equation (3.8) of [Gourgoulhon & Bonazzola \(1993\)](#):

$$N^a{}_{|a} = 0 \quad (\text{H.1})$$

Due to equations (2.34) and (2.32), we find

$$N^a{}_{|a} = N^a{}_{,a} + {}^3\Gamma_{ab}^a N^b$$

and

$${}^3\Gamma_{ab}^a N^b = h^{ac} {}^3\Gamma_{cab} N^b = \frac{1}{2} h^{ac} (\partial_a h_{cb} + \partial_b h_{ac} - \partial_c h_{ab}) N^b$$

such that

$$N^a{}_{|a} = N^a{}_{,a} + \frac{1}{2} h^{ac} \partial_b h_{ac} N^b$$

and hence due to axisymmetry

$$N^a{}_{|a} = N^m{}_{,m} + \frac{1}{2} h^{ab} \partial_n h_{ab} N^n \quad (\text{H.2})$$

Next, we expand

$$h^{ab} \partial_n h_{ab} = h^{mo} \partial_n h_{mo} + h^{\varphi m} \partial_n h_{\varphi m} + h^{m\varphi} \partial_n h_{m\varphi} + h^{\varphi\varphi} \partial_n h_{\varphi\varphi}$$

and use equations (2.17) and (2.18):

$$\begin{aligned} h^{ab} \partial_n h_{ab} &= \left(k^{mo} + \frac{M^m M^o}{M^2} \right) \partial_n k_{mo} - \frac{M^o}{M^2} \partial_n M_o \\ &\quad - \frac{M^m}{M^2} \partial_n M_m + \frac{1}{M^2} \partial_n (M^2 + M_m M^m) \end{aligned} \quad (\text{H.3})$$

Moreover, we apply equation (2.19) and evaluate

$$\begin{aligned} k^{mo} \partial_n k_{mo} N^n &= k^{rr} \partial_r k_{rr} N^r + k^{\theta\theta} \partial_r k_{\theta\theta} N^r + k^{rr} \partial_\theta k_{rr} N^\theta + k^{\theta\theta} \partial_\theta k_{\theta\theta} N^\theta \\ &= \frac{1}{A^2} \left[\partial_r (A^2) N^r + \frac{1}{r^2} \partial_r (r^2 A^2) N^r + \partial_\theta (A^2) N^\theta + \frac{1}{r^2} \partial_\theta (r^2 A^2) N^\theta \right] \\ &= \frac{1}{A^2} \left[2\partial_r (A^2) N^r + \frac{A^2}{r^2} \partial_r (r^2) N^r + 2\partial_\theta (A^2) N^\theta \right] \end{aligned}$$

H. Slicing conditions in flat space

such that equation (2.23) leads to

$$\frac{1}{2}k^{mo}\partial_n k_{mo}N^n = 2\partial_r\alpha N^r + \frac{1}{r}N^r + 2\partial_\theta\alpha N^\theta \quad (\text{H.4})$$

On the other hand, we recall that the 2-metric k_{mn} has to be used to raise and lower indices of the 2-shift M^m , and compute

$$\begin{aligned} & \frac{M^m M^o}{M^2}\partial_n k_{mo} - \frac{M^o}{M^2}\partial_n M_o - \frac{M^m}{M^2}\partial_n M_m + \frac{1}{M^2}\partial_n (M_m M^m) \\ = & \frac{M^m M^o}{M^2}\partial_n k_{mo} - 2\frac{M^m}{M^2}\partial_n M_m + \frac{1}{M^2}M^m\partial_n M_m + \frac{1}{M^2}M_m\partial_n M^m \\ = & \frac{M^m M^o}{M^2}\partial_n k_{mo} - \frac{M^m}{M^2}\partial_n (k_{mo}M^o) + \frac{1}{M^2}M_m\partial_n M^m \\ = & 0 \end{aligned}$$

Thus, using equations (2.29), (H.3) and (H.4) in the result (H.2), we find

$$N^a|_a = N^m{}_{,m} + N^m\partial_m\mu + \frac{1}{r}N^r + 2\partial_m\alpha N^m$$

For the second term on the right hand side, we use equation (3.5) such that

$$N^m\partial_m\mu = N^m\partial_m[\ln(r\sin\theta) + \beta] = N^m\partial_m\beta + \frac{1}{r}N^r + \cot\theta N^\theta$$

and hence the slicing condition (H.1) becomes

$$N^m{}_{,m} + \frac{2}{r}N^r + \cot\theta N^\theta + (2\alpha + \beta)_{,m}N^m = 0$$

This result can be put into a more compact form. For that purpose, we compute

$$\begin{aligned} 0 &= e^{2\alpha+\beta} \left[N^m{}_{,m} + \frac{2}{r}N^r + \cot\theta N^\theta + (2\alpha + \beta)_{,m}N^m \right] \\ &= e^{2\alpha+\beta} \left(N^m{}_{,m} + \frac{2}{r}N^r + \cot\theta N^\theta \right) + e^{2\alpha+\beta}{}_{,m}N^m \\ &= \left(e^{2\alpha+\beta}N^m \right)_{,m} + e^{2\alpha+\beta} \left(\frac{2}{r}N^r + \cot\theta N^\theta \right) \end{aligned}$$

and use the flat space 3-divergence (2.48):

$$\boxed{{}^3\text{div} \left(e^{2\alpha+\beta} \vec{N} \right) = 0} \quad (\text{H.5})$$

H.2. Conformally minimal azimuthal slicing

Equation (3.9) of Gourgoulhon & Bonazzola (1993) contains the conformally minimal azimuthal slicing condition:

$$(N^2 M^m)_{||m} = 0 \quad (\text{H.6})$$

Similarly to Sect. H.1, we will now reword this condition in terms of our basic fields in flat space. For that purpose, we start with the Leibniz rule, which gives

$$\frac{1}{N^2} (N^2 M^m)_{||m} = 2 \frac{N_{||m}}{N} M^m + M^m_{||m}$$

Then, equation (2.35) leads to

$$\frac{1}{N^2} (N^2 M^m)_{||m} = 2 \frac{N_{,m}}{N} M^m + M^m_{,m} + {}^2\Gamma_{mn}^m M^n$$

Due to equation (2.33), the Christoffel symbol becomes

$${}^2\Gamma_{mn}^m = k^{mo} {}^2\Gamma_{omn} = \frac{1}{2} k^{mo} (\partial_m k_{on} + \partial_n k_{mo} - \partial_o k_{mn})$$

such that

$$\frac{1}{N^2} (N^2 M^m)_{||m} = 2 \frac{N_{,m}}{N} M^m + M^m_{,m} + \frac{1}{2} k^{mo} \partial_n k_{mo} M^n \quad (\text{H.7})$$

Next, replacing $N^m \rightarrow M^m$ in equation (H.4) leads to

$$\frac{1}{2} k^{mo} \partial_n k_{mo} M^n = 2 \partial_r \alpha M^r + \frac{1}{r} M^r + 2 \partial_\theta \alpha M^\theta$$

Hence, equation (2.21) allows us to write equation (H.7) as

$$\frac{1}{N^2} (N^2 M^m)_{||m} = 2 \nu_{,m} M^m + M^m_{,m} + 2 \alpha_{,m} M^m + \frac{1}{r} M^r$$

such that the slicing condition (H.6) becomes

$$M^m_{,m} + \frac{1}{r} M^r + 2 (\alpha + \nu)_{,m} M^m = 0$$

In order to write this result in a more compact manner, we compute

$$\begin{aligned} 0 &= e^{2(\alpha+\nu)} \left[M^m_{,m} + \frac{1}{r} M^r + 2 (\alpha + \nu)_{,m} M^m \right] \\ &= e^{2(\alpha+\nu)} \left(M^m_{,m} + \frac{1}{r} M^r \right) + e^{2(\alpha+\nu)}_{,m} M^m \\ &= \left(e^{2(\alpha+\nu)} M^m \right)_{,m} + e^{2(\alpha+\nu)} \frac{1}{r} M^r \end{aligned}$$

and apply the flat space 2-divergence (3.17):

$$\boxed{{}^2\text{div} \left(e^{2(\alpha+\nu)} \vec{M} \right) = 0} \quad (\text{H.8})$$

H. Slicing conditions in flat space

I. Tolman-Oppenheimer-Volkoff solution

In this investigation, we have assumed stationarity and axisymmetry. Tightening axisymmetry to spherical symmetry allows us to rewrite Einstein's field equation (2.5) to the Tolman-Oppenheimer-Volkoff (TOV) equation

$$\frac{dp}{dr'} = -\frac{\epsilon M(r')}{r'^2} \left(1 + \frac{p}{\epsilon}\right) \left(1 + \frac{4\pi r'^3 p}{M(r')}\right) \left(1 - \frac{2M(r')}{r'}\right)^{-1} \quad (\text{I.1})$$

with the TOV-mass

$$M(r') = 4\pi \int_0^{r'} dx x^2 \epsilon(x)$$

(see [Fließbach 2006](#)). The radial coordinate appearing in the TOV-equation differs from the one used in the rest of this thesis, and therefore it is denoted as r' instead of r . Assuming a central pressure $p(r' = 0)$, the TOV-equation can be integrated. This leads to a pressure profile $p(r')$ and thus to a total energy density profile $\epsilon(r')$. The velocities $v^a(r')$ have to vanish everywhere, because the TOV-equation describes static solutions. Hence, merely the geometry fields remain to be evaluated. However, we have to be careful. The reason is that equation (I.1) is computed from the metric

$$ds^2 = -b(r') dt^2 + a(r') dr'^2 + r'^2 d\Omega^2 \quad (\text{I.2})$$

with $d\Omega^2 = d\theta^2 + \sin^2 \theta d\phi^2$, in contrast to our metric

$$ds^2 = -e^{2\nu(r)} dt^2 + e^{2\alpha(r)} (dr^2 + r^2 d\theta^2) + e^{2\beta(r)} r^2 \sin^2 \theta d\phi^2$$

Assuming

$$\boxed{\beta = \alpha}$$

we have

$$ds^2 = -e^{2\nu(r)} dt^2 + e^{2\alpha(r)} (dr^2 + r^2 d\Omega^2)$$

Comparing this with the metric (I.2) shows that merely the radial coordinate is different. The correlation between the radial TOV-coordinate r' and our radial coordinate r is obviously

$$\sqrt{a(r')} dr' = e^{\alpha(r)} dr \quad (\text{I.3})$$

and

$$r' = e^{\alpha(r)} r \quad (\text{I.4})$$

The latter equation can also be written as

$$\alpha(r) = \ln \frac{r'}{r}$$

I. Tolman-Oppenheimer-Volkoff solution

such that equations (I.3) and (I.4) lead to

$$d\alpha(r) = \frac{dr'}{r'} - \frac{dr}{r} = \left(\frac{1}{r'} - \frac{\sqrt{a(r')}}{e^{\alpha(r)}r} \right) dr' = \frac{1}{r'} \left(1 - \sqrt{a(r')} \right) dr'$$

Due to equation (39.18) of Fließbach (2006), we hence arrive at

$$\boxed{\frac{d\alpha(r(r'))}{dr'} = \frac{1}{r'} \left(1 - \frac{1}{\sqrt{1 - \frac{2M(r')}{r'}}} \right)}$$

Assuming the boundary condition $\alpha(r(r' = \infty)) = 0$, this equation can be integrated, which leads to a profile $\alpha(r(r'))$. Then, equation (I.4) tells us the relation between the TOV-coordinate r' and our radial coordinate r such that we obtain $\alpha(r) = \alpha(r(r'(r)))$.

Finally, we consider equation (39.23)

$$\frac{\frac{db(r')}{dr'}}{b(r')} = -\frac{2\frac{dp}{dr'}}{\epsilon + p}$$

of Fließbach (2006). Using the TOV-equation (I.1), it can be rewritten to

$$\frac{d}{dr'} \ln b(r') = 2 \frac{M(r') + 4\pi r'^3 p}{r'(r' - 2M(r'))}$$

such that $b(r') = e^{2\nu(r)}$ gives

$$\boxed{\frac{d\nu(r(r'))}{dr'} = \frac{M(r') + 4\pi r'^3 p}{r'(r' - 2M(r'))}}$$

We again assume $\nu(r(r' = \infty)) = 0$. Then, an integration gives a profile $\nu(r(r'))$, which allows us to compute the last remaining geometry field $\nu(r) = \nu(r(r'(r)))$.

J. Outlook to electromagnetism

One of the possible ways to go beyond the scope of this investigation and to generalize it is to take the electromagnetic field into account. In this section, we show a few initial steps in that direction, which will eventually lead to a generalization of equation (2.59).

In order to include the electromagnetic field, we replace the stress-energy tensor (2.4) with

$$T_{\alpha\beta} = T_{\alpha\beta}^{\text{matter}} + T_{\alpha\beta}^{\text{EM}}$$

in which

$$T_{\alpha\beta}^{\text{matter}} = (\epsilon + p)u_\alpha u_\beta + pg_{\alpha\beta}$$

is the original stress-energy tensor (2.4) of the fluid and

$$T_{\alpha\beta}^{\text{EM}} = F_{\alpha\gamma}F_{\beta}{}^\gamma - \frac{1}{4}g_{\alpha\beta}F_{\gamma\delta}F^{\gamma\delta}$$

describes the electromagnetic field. The quantity $F_{\alpha\beta} = \partial_\alpha A_\beta - \partial_\beta A_\alpha$ is the electromagnetic field strength expressed in terms of the electromagnetic 4-vector potential A_α . Then, we evaluate

$$\nabla^\beta T_{\beta\alpha}^{\text{EM}} = \nabla^\beta \left(F_{\alpha\gamma}F_{\beta}{}^\gamma - \frac{1}{4}g_{\alpha\beta}F_{\gamma\delta}F^{\gamma\delta} \right) = F_{\alpha\gamma}\nabla^\beta F_{\beta}{}^\gamma + F^{\beta\gamma} \left(\nabla_\beta F_{\alpha\gamma} - \frac{1}{2}\nabla_\alpha F_{\beta\gamma} \right) \quad (\text{J.1})$$

The second term of the outcome can be reworded to

$$\begin{aligned} & F^{\beta\gamma} \left(\nabla_\beta F_{\alpha\gamma} - \frac{1}{2}\nabla_\alpha F_{\beta\gamma} \right) \\ &= \left(\nabla^\beta A^\gamma - \nabla^\gamma A^\beta \right) \left[\nabla_\beta (\nabla_\alpha A_\gamma - \nabla_\gamma A_\alpha) - \frac{1}{2}\nabla_\alpha (\nabla_\beta A_\gamma - \nabla_\gamma A_\beta) \right] \\ &= \nabla^\beta A^\gamma [\nabla_\beta (\nabla_\alpha A_\gamma - \nabla_\gamma A_\alpha) - \nabla_\gamma (\nabla_\alpha A_\beta - \nabla_\beta A_\alpha) - \nabla_\alpha (\nabla_\beta A_\gamma - \nabla_\gamma A_\beta)] \\ &= \nabla^\beta A^\gamma [(\nabla_\gamma \nabla_\beta - \nabla_\beta \nabla_\gamma) A_\alpha + (\nabla_\alpha \nabla_\gamma - \nabla_\gamma \nabla_\alpha) A_\beta + (\nabla_\beta \nabla_\alpha - \nabla_\alpha \nabla_\beta) A_\gamma] \end{aligned}$$

Using equation (6.40) of [D'Inverno \(1992\)](#), we then find

$$F^{\beta\gamma} \left(\nabla_\beta F_{\alpha\gamma} - \frac{1}{2}\nabla_\alpha F_{\beta\gamma} \right) = \nabla^\beta A^\gamma (R_{\alpha\delta\gamma\beta} + R_{\beta\delta\alpha\gamma} + R_{\gamma\delta\beta\alpha}) A^\delta = 0$$

where in the last step we have used the first Bianchi identity ([D'Inverno 1992](#)). Hence, Maxwell's field equation

$$\nabla_\alpha F^{\alpha\beta} = \rho_q u^\beta$$

in which ρ_q is the charge density, allows us to write equation (J.1) as

$$\nabla^\beta T_{\beta\alpha}^{\text{EM}} = \rho_q F_{\alpha\beta} u^\beta$$

J. Outlook to electromagnetism

Due to this result, it is obvious that equation (2.53) has to be generalized to

$$(\epsilon + p) u^\beta \nabla_\beta u^\alpha = -q^{\alpha\beta} \nabla_\beta p - \rho_q q_\gamma^\alpha F^\gamma_\beta u^\beta$$

and with (see equation (2.42))

$$q_\gamma^\alpha F^\gamma_\beta u^\beta = (\delta_\gamma^\alpha + u^\alpha u_\gamma) F^\gamma_\beta u^\beta = F^\alpha_\beta u^\beta$$

we arrive at

$$\boxed{(\epsilon + p) u^\beta \nabla_\beta u^\alpha = -q^{\alpha\beta} \nabla_\beta p - \rho_q F^\alpha_\beta u^\beta}$$

Then, equation (2.54) becomes

$$0 = (\epsilon + p) \left[u^m \partial_m u_\alpha - \frac{1}{2} (\partial_\gamma g_{\beta\alpha} + \partial_\alpha g_{\gamma\beta} - \partial_\beta g_{\gamma\alpha}) u^\beta u^\gamma \right] + \partial_\alpha p + u_\alpha u^m \partial_m p + \rho_q F_{\alpha\beta} u^\beta$$

We expand

$$F_{\alpha\beta} u^\beta = (\partial_\alpha A_\beta - \partial_\beta A_\alpha) u^\beta$$

and use stationarity together with axisymmetry such that

$$F_{\alpha\beta} u^\beta = \partial_\alpha A_\beta u^\beta - \partial_m A_\alpha u^m$$

That way, we are able to generalize equation (2.55) to

$$\frac{\partial_\alpha p + u_\alpha u^m \partial_m p + \rho_q (\partial_\alpha A_\beta u^\beta - \partial_m A_\alpha u^m)}{\epsilon + p} = \frac{1}{2} \partial_\alpha g_{\gamma\beta} u^\beta u^\gamma - u^m \partial_m u_\alpha \quad (\text{J.2})$$

Setting $\alpha = t$ and taking stationarity into account, we obtain

$$\frac{u_t u^m \partial_m p - \rho_q \partial_m A_t u^m}{\epsilon + p} = -u^m \partial_m u_t$$

such that we generalize equation (2.56) to

$$\boxed{v^m \partial_m p = v^m \left[\frac{\rho_q}{u_t} \partial_m A_t - (\epsilon + p) \partial_m \ln u_t \right]} \quad (\text{J.3})$$

On the other hand, setting $\alpha = a$ in equation (J.2) leads to

$$\frac{\partial_a p}{\epsilon + p} = \frac{1}{2} \partial_a g_{\gamma\beta} u^\beta u^\gamma - u^m \partial_m u_a - \frac{u_a u^m \partial_m p + \rho_q (\partial_a A_\beta u^\beta - \partial_m A_a u^m)}{\epsilon + p}$$

Then, equation (J.3) allows us to reformulate

$$\begin{aligned} \frac{\partial_a p}{\epsilon + p} &= \frac{1}{2} \partial_a g_{\gamma\beta} u^\beta u^\gamma - u^m \partial_m u_a \\ &\quad - \frac{u_a u^t v^m \left[\frac{\rho_q}{u_t} \partial_m A_t - (\epsilon + p) \partial_m \ln u_t \right] + \rho_q (\partial_a A_\beta u^\beta - \partial_m A_a u^m)}{\epsilon + p} \\ &= \frac{1}{2} \partial_a g_{\gamma\beta} u^\beta u^\gamma - u^m \partial_m u_a + u_a u^m \partial_m \ln u_t \end{aligned}$$

$$\begin{aligned}
& \frac{\rho_q \left(\frac{u_a}{u_t} u^m \partial_m A_t + \partial_a A_\beta u^\beta - \partial_m A_a u^m \right)}{\epsilon + p} \\
&= \frac{1}{2} \partial_a g_{\gamma\beta} u^\beta u^\gamma - u_t u^m \partial_m \frac{u_a}{u_t} - \frac{\rho_q \left[u^m \left(\frac{u_a}{u_t} \partial_m A_t - \partial_m A_a \right) + u^\beta \partial_a A_\beta \right]}{\epsilon + p}
\end{aligned}$$

Eventually, we use the Lagrangian angular momentum (2.57) and get

$$\frac{\partial_a p}{\epsilon + p} = u_t u^m \partial_m l_a + \frac{1}{2} \partial_a g_{\gamma\beta} u^\beta u^\gamma + \frac{\rho_q \left[u^m (l_a \partial_m A_t + \partial_m A_a) - u^\beta \partial_a A_\beta \right]}{\epsilon + p}$$

such that for $a = \phi$ stationarity leads to

$$\boxed{v^m \partial_m l_\phi = - \frac{\rho_q v^m (l_\phi \partial_m A_t + \partial_m A_\phi)}{u_t (\epsilon + p)}} \quad (\text{J.4})$$

This result generalizes equation (2.59).

Bibliography

- ARNOWITT, R., DESER, S., & MISNER, C. W., **1962**, *The dynamics of general relativity* (L. Witten, Gravitation: An Introduction to Current research; New York: Wiley)
- BECKER, W., **2009**, *Neutron Stars and Pulsars* (Berlin, Heidelberg: Springer-Verlag)
- CAMENZIND, M., **2007**, *Compact objects in Astrophysics: White Dwarfs, Neutron Stars and Black Holes* (Berlin, Heidelberg: Springer-Verlag)
- DIMMELMEIER, H., **2001**, *General Relativistic Collapse of Rotating Stellar Cores in Axisymmetry* (PhD thesis, Technische Universität München)
- D'INVERNO, R. A., **1992**, *Introducing Einstein's relativity* (New York: Oxford University Press)
- ERIGUCHI, Y. & MÜLLER, E., **1991**, *Structure of rapidly rotating axisymmetric stars. I - A numerical method for stellar structure and meridional circulation*, A&A 248, 435–447
- ERIGUCHI, Y., MÜLLER, E., & HACHISU, I., **1986**, *Meridional flow in a self-gravitating body. I - Mechanical flow in a barotropic star with constant specific angular momentum*, A&A 168, 130–138
- FLIESSBACH, T., **1996**, *Elektrodynamik* (Spektrum Akademischer Verlag)
- FLIESSBACH, T., **2006**, *Allgemeine Relativitätstheorie* (München: Spektrum Akademischer Verlag)
- FONT, J. A. & DAIGNE, F., **2002**, *The runaway instability of thick discs around black holes - I. The constant angular momentum case*, MNRAS 334, 383–400
- FRIEDMAN, J. L. & STERGIIOULAS, N., **to be published**, *Rotating Relativistic Stars* (Private communication)
- GOURGOULHON, E. & BONAZZOLA, S., **1993**, *Noncircular axisymmetric stationary spacetimes*, Phys. Rev. D 48, 2635–2652
- HUBBLE, http://www.phys.ncku.edu.tw/~astrolab/mirrors/apod/image/0803/lh95_hst_big.jpg
- HUBBLESITE, http://hubblesite.org/gallery/album/nebula/supernova_remnant/pr2002024a/large_web/
- IOKA, K. & SASAKI, M., **2004**, *Relativistic Stars with Poloidal and Toroidal Magnetic Fields and Meridional Flow*, ApJ 600, 296–316
- JACKSON, J. D., **2006**, *Klassische Elektrodynamik* (Berlin: Walter de Gruyter)

Bibliography

- KAWALER, S. D., NOVIKOV, I., & SRINIVASAN, G., **1997**, *Stellar Remnants* (Berlin, Heidelberg: Springer-Verlag)
- KOMATSU, H., ERIGUCHI, Y., & HACHISU, I., **1989**, *Rapidly rotating general relativistic stars. I - Numerical method and its application to uniformly rotating polytropes*, MNRAS 237, 355–379
- MICHEL, F. C., **1991**, *Theory of neutron star magnetospheres* (Chicago: University of Chicago Press)
- MISNER, C. W., THORNE, K. S., & WHEELER, J. A., **1973**, *Gravitation* (San Francisco: W.H. Freeman and Co.)
- NOZAWA, T., STERGIOLAS, N., GOURGOULHON, E., & ERIGUCHI, Y., **1998**, *Construction of highly accurate models of rotating neutron stars - comparison of three different numerical schemes*, A&AS 132, 431–454
- RANDERS, G., **1941**, *Large-Scale Motion in Stars*, ApJ 94, 109
- ROXBURGH, I. W., **1974**, *Non-Uniformly Rotating, Self-Gravitating, Compressible Masses with Internal Meridian Circulation*, Ap&SS 27, 425–435
- SHAPIRO, S. L., TEUKOLSKY, S. A., & LIGHTMAN, A. P., **1983**, *Black Holes, White Dwarfs, and Neutron Stars: The Physics of Compact Objects* (Physics Today)
- STERGIOLAS, N. & FRIEDMAN, J. L., **1995**, *Comparing models of rapidly rotating relativistic stars constructed by two numerical methods*, ApJ 444, 306–311
- STRAUMANN, N., **2004**, *General relativity with applications to astrophysics* (Berlin: Springer)

Danksagung

Zum Abschluss dieser Arbeit will ich meinen Dank an diejenigen Menschen ausdrücken, die mich während meiner Doktorarbeit unterstützt haben. Ich danke meinem Doktorvater Ewald Müller dafür, dass er mir ein Thema im Bereich der allgemeinen Relativitätstheorie ermöglicht hat. Die fachlichen Unterredungen mit ihm während der letzten Jahre waren von wesentlicher Bedeutung für das Zustandekommen dieser Arbeit. Ausserdem bin ich ihm für die kritische Durchsicht der Entwürfe dieses Manuskripts dankbar.

Diese Doktorarbeit wurde im Rahmen eines IKYDA-Projekts zwischen dem Max-Planck-Institut für Astrophysik und der Aristoteles Universität Thessaloniki durchgeführt. Dabei danke ich Nick Stergioulas, ohne dem diese Arbeit nicht möglich gewesen wäre. Sein RNS Code war der Ausgangspunkt dieser Doktorarbeit. Er hat mir zu Beginn geduldig dabei geholfen mich in das Thema einzuarbeiten und hat mich bis zum Ende meiner Promotion mit hilfreichen Ratschlägen unterstützt.

Ausserdem danke ich Thomas Janka für die Unterstützung bei der Untersuchung von Gamma-Ray-Bursts. In diesem Zusammenhang will ich weitere momentane und ehemalige Mitglieder meines Arbeitsumfeldes erwähnen, nämlich Andreas Bauswein, Fei Xiang, Lorenz Hudepohl, Markus Kromer, Martin Obergaulinger, Nicolay Hammer, Pablo Cerda-Duran, Paula Jofre Pfeil, Thomas Mädler. Ihnen bin ich für die angenehme Arbeitsatmosphäre und die Zusammenarbeit in verschiedener Form dankbar.

Ich danke auch besonders Bernhard Müller für die Fortführung der mittlerweile ein Jahrzehnt andauernden philosophischen Diskussionen. Die Möglichkeit eines freien Willens in einer volldeterministischen Welt durch wissenschaftliche Klarstellung der sprachlich verwendeten Konstrukte ist dabei wohl der wichtigste Punkt, bei dem wir in näherer Vergangenheit zur Übereinstimmung gekommen sind.

Schließlich will ich zwei Menschen danken, die mir über all die Jahre hinweg unermüdliche Unterstützung zukommen liessen: meinen Eltern.